Luís Carlos Henriques Alves

Cellulose solutions: Dissolution, regeneration, solution structure and molecular interactions

Tese de doutoramento em Química, ramo de especialização em Química Macromolecular, orientada por
Professor Doutor Björn Lindman e Doutor Filipe Antunes e apresentada à
Faculdade de Ciências e Tecnologia da Universidade de Coimbra

Setembro de 2015

· U · C ·

UNIVERSIDADE DE COIMBRA

Cellulose solutions: Dissolution, regeneration, solution structure and molecular interactions

Luís Carlos Henriques Alves

Faculdade de Ciências e Tecnologia, Universidade de Coimbra 2015

Tese apresentada à Universidade de Coimbra para apreciação nas provas de Doutoramento em Química, ramo de Química Macromolecular.

Trabalho desenvolvido no Departamento de Química da Faculdade de
Ciências e Tecnologia da Universidade de Coimbra, sob orientação
científica do Professor Doutor Björn Lindman e
do Doutor Filipe Antunes.

"Education is the most powerful weapon which you can use to change the world. Education is the great engine of personal development. It is through education that the daughter of a peasant can become a doctor, that the son of a mineworker can become the head of the mine, that a child of farm workers can become the president of a great nation."

Nelson Mandela

Acknowledgments/Agradecimentos

Finalmente, agradeço àqueles que me acompanham desde o início da minha vida. Os meus pais, Manuel e Florinda e os meus irmãos, Daniel e Miguel que constituíram e constituem os alicerces de tudo. Obrigado por sempre me proporcionaram todas as condições para crescer física e intelectualmente e transmitirem todos os valores essenciais de um ser Humano.

Contents

Abbreviations

AESO – acrylated epoxidized soybean oil

AFM – atomic force microscopy

AGU – anhydroglucopyranose unit

APG – alkyl-polyglucoside

ATR – attenuated total reflectance

CD – cyclodextrin

CMC – carboxymethyl cellulose

CNCs – cellulose nanocrystals

CP – cross polarization

CP/MAS – cross-polarization/magic angle spinning

CrI – crystallinity index

CVM – continuous variation method

DLS – dynamic light scattering

DMAc – N,N-dimethylacetamide

DMF – N,N-dimethylformamide

DMSO – dimethyl sulfoxide

DNA – deoxyribonucleic acid

DP – direct polarization

D.S. – degree of substitution

EDS – energy-dispersive spectrometry

FTIR – fourier transform infrared spectroscopy

HPMC – hydroxypropyl methylcellulose

ILs – ionic liquids

INEPT – insensitive nuclei enhanced by polarization transfer

LOI – lateral order index

MAS - magic angle spinning

MCC – microcrystalline cellulose

MD – molecular dynamics

NaCMC – Carboxymethyl cellulose sodium salt

NMMO – N-methylmorpholine-N-oxide

NMR – nuclear magnetic resonance

PEG – polyethylene glycol

PCS – photon correlation spectroscopy

PLM – polarized light microscopy

PT ssNMR – polarization transfer solid state nuclear magnetic resonance

SEM – scanning electron microscopy

TBAF – tetrabutylammonium fluoride

TBAH – tetrabutylammonium hydroxide

TBA^+ – tetrabutylammonium ion

TBPH – tetrabutylphosphonium hydroxide

TCI – total crystallinity index

TEM – transmission electron microscopy

TPPM – two pulse phase modulation

UV/VIS – ultraviolet/visible absorption spectroscopy

XRD – X-ray diffraction

Abstract

Massive amounts of biomass are produced every year, including millions of tons of cellulose. This almost inexhaustible resource is thus as a stupendous viable alternative for conventional raw materials to be applied in a wide range of areas. Cellulose finds uses in applications of the major interest nowadays ranging from fiber production (textiles), to packaging and biofuels. Nevertheless, in order to produce most of these end products cellulose needs to be dissolved. Dissolution is a very non-trivial and challenging process; cellulose solvents are of remarkable different nature and thus the understanding of the delicate balance between the different interactions involved becomes difficult but essential.

Nowadays there is a discussion going on in literature on the balance between hydrogen bonding and hydrophobic interactions in controlling the solution behavior of cellulose. The commonly accepted picture considers hydrogen bonding as the critical factor to understand the insolubility of cellulose. A recent view rather highlights the role of hydrophobic interactions in cellulose insolubility.

In this treatise new evidences pointing out to the role of hydrophobic interactions on the solubility and regeneration behavior of cellulose are discussed. Using a set of different techniques and approaches the effect of selected additives on the rate and performance of dissolution of cellulose are explored.

It was found that the influence of amphiphilic additives on the thermal stability and gelation of cellulose dopes in alkali-based solvents are illustrative examples of the amphiphilic character of the cellulose. Further experimental support comes from the enhancement in cellulose dissolution when using an amphiphilic cation instead of an inorganic cation. The quality of the amphiphilic solvent can also be tuned by addition of salts or cyclodextrins. The former is rationalized in terms of polyelectrolyte effect where salt is suggested to screen cellulose charges in strong alkali based systems while the later can be understood by specific cyclodextrin-amphiphilic "host-guest" interactions.

On the other hand acidic solvents reveal great efficiency to dissolve cellulose but chemical degradation occurs to some extent. The understanding of the solution state and the molecular organization is usually complicated. Additionally, the typical extremely low pH in cellulose dopes containing high acid concentrations limits the use of many techniques. In this respect, new methodologies were developed such as PT ssNMR, which has shown to be a very capable technique providing detailed molecular information of cellulose solutions.

Cellulose is partially a crystalline polymer where the amorphous fraction varies according to the raw material source, pre-treatments, etc. In a parallel work, the extraction of cellulose nanocrystals (CNCs) from cellulose derivatives was also evaluated. Surprisingly, the cellulose derivatives were found to be significantly crystalline as indicated by an unusual extraction of CNCs. However, while the microcrystalline cellulose (MCC starting material) and the extracted CNCs share the same crystalline organization (cellulose I polymorph), the cellulose derivatives (starting materials) were found to be of cellulose II type. Data shows that there are specific parts of cellulose that remain insoluble during all the modification process.

The influence of different solvents over the level of dissolution of cellulose samples and the properties of the regenerated materials from these solutions are also discussed. It was found that solvents using amphiphilic cations are able to dissolve cellulose to a state of molecular dispersed solutions or close, contrary to inorganic cations, which are not so effective, leading to a colloidal aggregates solution. This level of dissolution results in a completely different regenerated materials, with different crystallinity indexes. All together these results support the importance of the amphiphilic character of cellulose and suggest that an effective dissolution strategy should strongly consider the role of hydrophobic interactions.

Resumo

Sendo a celulose um recurso praticamente inesgotável, pois são geradas por ano milhares de toneladas de biomassa, esta apresenta-se como uma estupenda alternativa a matérias-primas convencionais num vasto número de aplicações. Produção de fibras têxteis, embalagens inovadoras e biocombustíveis são apenas alguns exemplos de elevado interesse nos dias que correm. Contudo, para se obterem muitos destes produtos finais é necessária a sua dissolução. Esse passo de dissolução da celulose é altamente desafiador e nada trivial; os solventes para a celulose são da mais variada natureza e, deste modo, um bom entendimento sobre o delicado balanço entre as diferentes interações moleculares envolvidas é complicado mas essencial.

Atualmente existe uma intensa discussão na comunidade científica acerca do balanço entre o efeito das ligações de hidrogénio e das interações hidrofóbicas no comportamento da celulose em solução. O conceito de que as ligações de hidrogénio eram o factor fundamental no comportamento da celulose e eram as principais responsáveis pela sua insolubilidade foi dominante durante um longo período de tempo. No entanto, esta problemática foi recentemente revista e chamada a atenção para o papel das interações hidrofóbicas na insolubilidade da celulose.

No presente estudo são descritas algumas evidências que reforçam o papel das interações hidrofóbicas no comportamento da celulose durante o processo de dissolução e regeneração. A partir de um conjunto de considerações e técnicas de caracterização reportam-se os efeitos de aditivos específicos sobre a eficiência e grau de dissolução da celulose.

Verificou-se que a estabilidade térmica das soluções em solventes de base alcalina aumenta na presença de aditivos de polaridade intermédia e que aditivos anfifílicos previnem a gelificação das soluções; estes são exemplos ilustrativos do carater anfifílico da celulose. Outras evidências experimentais que suportam esse argumento provêm do aumento da eficiência de dissolução quando se usam catiões anfifílicos em vez de catiões inorgânicos no sistema de solvente. Observou-se ainda que a qualidade dos solventes anfifílicos pode ser alterada por adição de sais ou ciclodextrinas. A adição de sais pode ser racionalizada em termos de efeito de supressão de cargas dos grupos ionizados em meio fortemente alcalino, enquanto o efeito das ciclodextrinas pode ser entendido como a formação de um complexo ciclodextrinas-entidade anfifílica que diminui a disponibilidade da mesma em solução.

Por outro lado, os solventes ácidos são muito eficazes a dissolver celulose, no entanto a dissolução é muitas vezes acompanhada por degradação química. O entendimento da organização molecular nas soluções de celulose é normalmente complicado. Além disso o pH da solução (extremamente baixo), devido à elevada concentração de ácido em solução, limita a aplicação de um elevado número de

técnicas. Contudo, a ressonância magnética com transferência de protão em estado sólido (PT ssNMR) revelou-se uma técnica muito eficaz, revelando importante informação ao nível molecular das soluções de celulose. Demostrou-se ainda ser uma excelente técnica para detetar, e identificar, possíveis produtos provenientes da degradação da celulose em solução.

Reporta-se também a extração de nanocristais de celulose (CNCs) a partir de uma fonte pouco comum. Surpreendentemente os derivados de celulose mostraram-se significativamente cristalinos, contrariamente ao expectável, possibilitando a extração de CNCs. Porém, enquanto a celulose microcristalina (material de partida) e os nanocristais extraídos partilham o mesmo tipo de organização molecular (polimorfo de celulose I), os derivados de celulose (materiais de partida) apresentam uma organização molecular diferente (polimorfo de celulose II). Os resultados demonstram que existem áreas específicas das cadeias de celulose que permanecem insolúveis durante todo o processo de modificação (que envolve um passo de dissolução). Estes resultados estão de acordo com a ideia de que existe apenas um número muito limitado de solventes capazes de dissolver a celulose a um nível molecular.

A influência do uso de solventes com diferentes características no grau de dissolução das amostras terá certamente implicações nas propriedades dos materiais regenerados. Verificou-se que diferentes níveis de dissolução resultam em materiais regenerados com diferentes morfologias e diferentes cristalinidades. Catiões anfifílicos levam a morfologias mais suaves e materiais regenerados menos cristalinos, o que mais uma vez coloca em realce o carater anfifílico da celulose.

Palavras-chave: Dissolução de celulose, interações hidrofóbicas, ligações de hidrogénio, anfifilicidade, solventes, gelificação, PT ss NMR.

CHAPTER 1

Introduction

General aspects

Consumers, industry and governments are increasingly demanding products from renewable and sustainable resources that are biodegradable, non-petroleum based, carbon neutral and, at the same time, generating low environmental, animal/human health and safety risks [1]. In this context, there is almost not any other raw material that offers such a broad variety of applications such as cellulose, the most biodegradable and abundant biopolymer on earth with an estimated annual synthesis in nature of ca. 10^{11}-10^{12} tons [2]. Cellulose is major component of wood, a widely used construction material, but it is also used in the form of natural textile fibers, such as cotton or flax, or in the form of panels and paper. Native cellulose is also a versatile starting material for subsequent chemical modification for the production of a variety of cellulose derivatives with applications in several areas such as food, printing, cosmetic, detergents, enhanced oil recovery, textile, pharmaceutical and domestic life [3, 4], but also for the production of regenerated cellulose-based threads and films [5]. Cellulose is a particularly stable polysaccharide; its stability, mainly due to the crystallinity presented, turns cellulose resistant to hydrolysis by weak acids and bases and also to the

1

hydrolytic action of enzymes because the glycosidic linkages are not readily accessible from microorganisms and fungi.

Although biopolymers are promising options for many applications, a major concern is in many cases a limited solubility in water (and cellulose is a clear example of it) which makes their processing challenging. The solubility of the materials can be to some extent anticipated just from a structural analysis. However, this not always holds. Proteins, DNA or polysaccharides are made of small and water soluble blocks; and if one takes the example of cellulose, it is composed of repeating anhydroglucose units where each unit contains three hydroxyl groups (see figure 1.1). Despite its notable global hydrophilic character, cellulose is insoluble in water and in most common solvents [6-8]; it is relatively consensual that due to the elevated number of hydroxyl groups present in cellulose it can form a highly ordered network of intermolecular and intramolecular hydrogen bonds. This hydrogen bonding based mechanism, essentially represents the established vision on cellulose recalcitrance to dissolution [9]. Hydrogen bonding is typically pointed to explain cellulose molecular association in other systems, even in aqueous systems. In literature, the double helix association in DNA is sometimes suggested to be caused by hydrogen bonding [10]. However, a recent and more accurate view, of the double helix association shows that its association is mostly driven by hydrophobic interactions between the neighbouring stacks of base-pairs that, in general, cause the association and helix formation [11]. Definitely, hydrogen bonds are expected to occur, but are rather responsible for the structural selectivity of the associated state, while the driving force for association are the hydrophobic interactions. A similar thought can be applied to the cellulose case. Cellulose presents a structural anisotropy (discussed below) and therefore it is unclear why there is a substantial gain in free energy in moving a molecule with hydrogen bond capabilities such as water (that can act both as acceptor and donor in hydrogen bonding) from an aqueous medium to a less polar environment. The idea, that the insolubility of cellulose is only driven by hydrogen bonding, was recently revisited and it has been argued that hydrophobic interactions play an important role on cellulose solubility pattern. This alternative but complementary view is important in order to understand the molecular mechanisms for association in an aqueous media and develop suitable solvents for dissolution [6, 12, 13].

Structure and properties of cellulose

Cellulose is the major component of the cell walls of plants having an undisputed role among the raw materials to be used in a sustainable future. In the cell walls it is typically combined with lignin and hemicelluloses and water [14] but cellulose can also be synthesized by bacteria or tunicates. Cellulose was isolated for the first time by the French chemist Payen in 1838 [15] who extracted it from green plants and reported its elemental composition four years later [8].

Regarding its structure, cellulose is a linear homopolymer composed of D-anhydroglucopyranose units (AGU), which are connected by β(1–4)-glycosidic bonds (figure 1.1) [16].
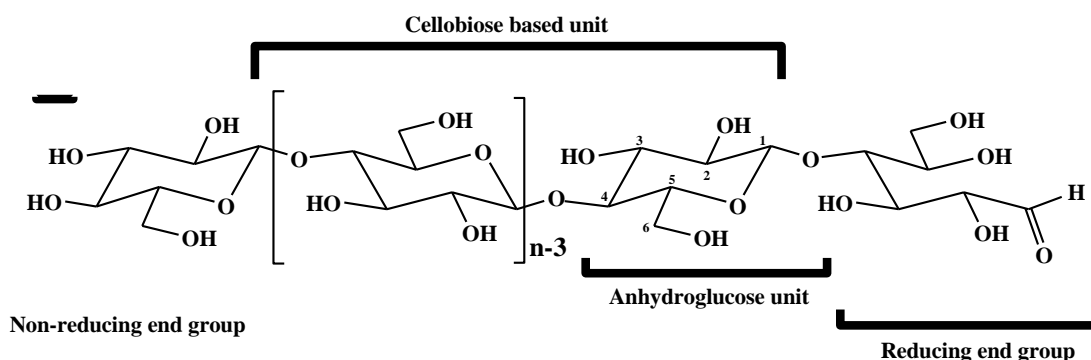
Figure 1.1: Molecular structure of cellulose (n = value of degree of polymerization).

The size of the cellulose molecules can be defined by the average degree of polymerization. The average molecular weight is estimated from the product of the degree of polymerization and the molecular mass of a single AGU. Each AGU has three hydroxyl groups (one primary and two secondary moieties that represent more than 30% by weight), with the exception of the terminal units. These structural features, makes cellulose surface chemistry quite intriguing and opens a broad spectrum of potential reactions, which typically occur in the primary and secondary alcohols [17].

In nature, cellulose is organized in a rather dense and highly hierarchal fashion, from the single AGU up to the micro and macro fibrils, where, as alluded to above, an extended intra- and intermolecular network of hydrogen bonds is responsible by the cohesion between cellulose molecules [18, 19]. The amphiphilic character of cellulose can be derived from its structure; the hydrophilic character is presented in the equatorial

direction of a glucopyranose ring, because all three hydroxyl groups are located on the equatorial positions of the ring. On the other hand, the hydrophobic character is found in the axial direction of the ring, (C-H bonds are located on the axial positions of the ring) [14, 20]. Therefore, it seems clear that cellulose molecules have an intrinsic structural anisotropy (figure 1.2) and due to the intra- and intermolecular hydrogen bonds there is the formation of rather flat ribbons, with sides with markedly different polarity [21-23]; it is expected that all these features considerably influence both the microscopic (e.g. interactions) and macroscopic (e.g. solubility) properties of cellulose. Yamane et al. has proposed that the wetting properties of regenerated cellulose can be attributed to such structural anisotropy [22]. Thus, an efficient solvent should be able to overcome these inter-sheet interactions, in order to efficiently dissolve cellulose [6, 12, 13, 24-26].
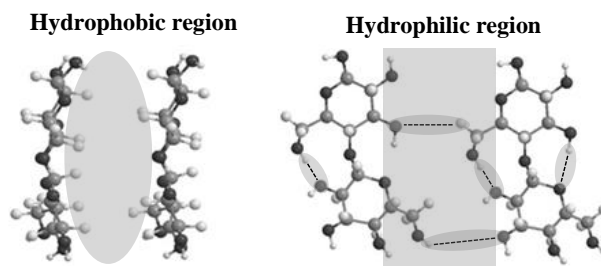
Figure 1.2: Hydrophilic and hydrophobic parts of the cellulose molecule: (left), lateral view of the glucopyranose ring plane showing the hydrogen atoms of C–H bonds on the axial positions of the ring. (right), top view of the glucopyranose ring plane highlighting hypothetic hydrogen bonding between the hydroxyl groups located on the equatorial positions of the ring (adapted from [27]).

Native cellulose is a semi-crystalline polymer and as expected for such class of polymers, cellulose can organize in different forms; in the cell wall of a plant, amorphous regions (low ordered) coexist with crystalline domains (highly ordered) [28]. The degree of crystallinity of the extracted cellulose, usually in the range of 40–60%, is very dependent on the origin and also on the extraction process of the sample [18]. Curiously, the parallel arrangement found in nature (cellulose I polymorph), is not the most stable crystalline form of cellulose; when dissolved and recrystallized, cellulose chains adopt an anti-parallel arrangement, cellulose II polymorph [29, 30], a most stable form. This intriguing process is still unclear. However, it has been postulated that the transition from cellulose I to cellulose II results from the rotation of

the chains in the sheets of a microfibril around their axes, leading only to two variations of the dihedral angle at the glycosidic linkage [28, 31]. This transition can be induced for example by mercerization of the cellulose in alkali solutions [32].

Processing cellulose

Processing cellulose is usually a challenging step during the productive process. Cellulose is not a meltable polymer; the degradation temperature is lower than the melting temperature. Native cellulose, the majority of modified celluloses, as well as regenerated cellulose are not thermoplastic. Only a few cellulose derivatives display thermoplastic behaviour such as cellulose ethers (e.g. methyl cellulose, ethyl cellulose, hydroxyl ethyl cellulose, hydroxylpropyl cellulose, etc.) and cellulose esters such as cellulose alkanoates. Mixed cellulose esters showed limited thermoplastic processability [33].

Recent studies show that the degradation process is influenced by the crystallinity of the cellulose; generally it is initiated in the cellulose amorphous regions and thus, the smaller the size of the crystalline domains the lower the thermal stability of the sample [34]. Cellulose from the same origin can have different thermal stabilities depending on the extraction procedure.

The alternative to melt cellulose is to dissolve it. Although there are many different solvents for cellulose, dissolution is very challenging step. Most of the solvent systems known have a limited capacity of dissolution (i.e. only a few percent of cellulose), are toxic and expensive, thus limiting their industrial uses.

Solvents for cellulose

As mentioned, cellulose is neither meltable nor soluble in usual solvents; water and typical organic solvents fail in this respect [12, 35]. However, this biopolymer is soluble in more striking media, several with no apparent common properties [36]. The huge difficulty in dissolution process can be attributed to the complexity of such a

biopolymeric network, the partial crystalline structure and the extended non covalent interactions among molecules, turning the chemical processing rather difficult.

Cellulose solvents are usually divided in two main groups: derivatizing and non-derivatizing solvents. In figure 1.3 the classification of the more common cellulose solvents is schematized.
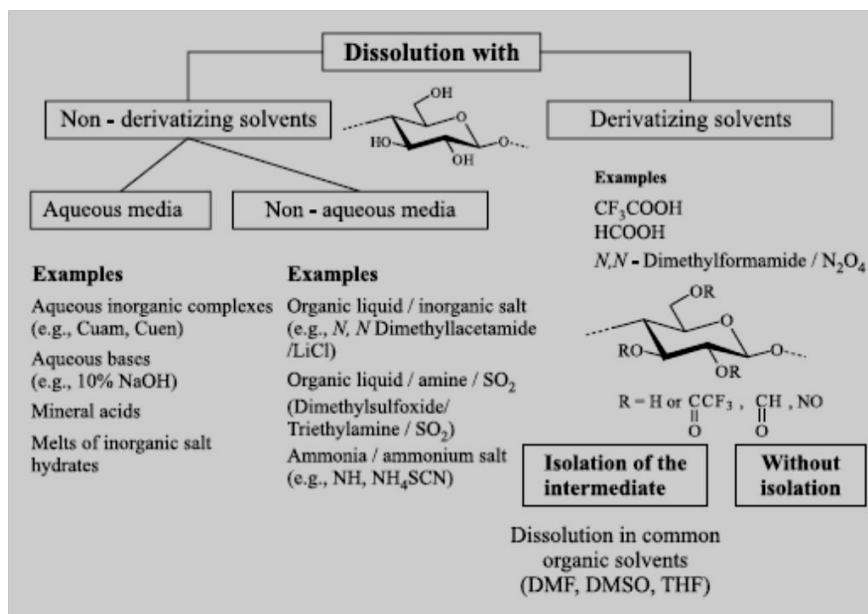
Figure 1.3: Schematic representation of the classification of cellulose solvents [37].

Historically, the first developed was a derivatizing solvent and was described about 150 years ago [17]. As the name suggests, the "derivatizing" solvent group comprises all the systems where cellulose dissolution occurs via the chemical formation of a labile "unstable" ether, ester or acetal intermediate. The viscose process ($NaOH + CS_2$) is the most common derivatizing method used on large scale [28, 38]. An interesting alternative to the viscose process uses urea as a key ingredient to form the cellulose carbamate intermediate which is soluble in an aqueous sodium hydroxide solution, with or without other additives such ZnO [39].

On the other hand, the "non-derivatizing solvent" systems comprise all solvents capable of dissolving cellulose only via physical intermolecular interactions. This class of solvents is particularly relevant for the organic chemistry of cellulose under homogeneous conditions. Historically significant, and of practical relevance also for analytical purposes, is the system introduced by Schweizer in 1857 [40]. Schweizer found that cupper salts and concentrated ammonia effectively dissolve cotton. Similar systems were developed and among the most popular the cuprammonium hydroxide or

simply "cuam" is widely used for degree of polymerization estimation by viscosity determination [41]. In the beginning of 19th century, ethylenediamine was found to be a good alternative to ammonia and also other complexing solvents were designed, such as the cadmium hydroxide in aqueous ethylenediamine, "cadoxen", or nickel oxide in the same aqueous ethylenediamine, "nioxen" [36, 42, 43]. Similar alternative systems have been reported using mainly other transition metals (such as zinc or palladium) combined with an amine or ammonium compound. However, none of these systems have achieved full commercial success [36].

Sobue et al. introduced a new approach and since this work it is known that cellulose is soluble in aqueous NaOH below 268 K within a specific concentration range of NaOH (7–10%) [44]. This system is cheap, potentially non-polluting, uses very common chemicals and relatively easy to handle. However these aqueous alkali systems do not completely disrupt the semicrystalline regions of cellulose and the solubility is limited to cellulose of relatively low degree of polymerization (up to ca. 250). The apparent solubility also depends on the degree of crystallinity and the crystalline arrangement. Pre-treatments such as steam explosion of the dissolving pulp have been successfully used to improve dissolution [45]. Other aqueous systems using bases, such as LiOH [46], or quaternary ammonium hydroxides are also capable of dissolving cellulose [28, 36, 47]. More lately, the aqueous NaOH solutions were doped with additives such as polyethylene glycol, PEG [48], urea [49] and thiourea [50] and reported to enhance dissolution ratio and the stability of the dope.

In 1932 Letters et al. investigated the swelling and dissolution of cellulose in highly concentrated aqueous zinc chloride solution; dissolution was only observed for salt concentrations above 63% (w/w) [51]. Several concentrated aqueous salts solutions were studied, however, only three water/salt systems were described as effective cellulose solvents: $Ca(SCN)_2/H_2O$ [52], $LiSCN/H_2O$ [17] and $ZnCl_2/H_2O$ [53]. Then $Ca(SCN)_2 \cdot 3H_2O$ showed the strong swelling and solvent action on cellulose [54]. Mixtures of NaSCN/KSCN with $Ca(SCN)_2 \cdot 3H_2O$ or dimethyl sulfoxide (DMSO) were also found to be able to dissolve cellulose. The molten system $LiSCN \cdot 2H_2O$ is described as an efficient cellulose solvent [37]. Recently, Leipner et al. reported that $LiClO_4 \cdot 3H_2O$ is a very effective solvent giving transparent cellulose solutions within a few minutes without any pre-treatment or activation [55]. In addition, mixtures of $LiClO_4 \cdot 3H_2O$ with $Mg(ClO_4)_2 \cdot H_2O$ or $MgCl_2.6H_2O$ are also promising solvents [56].

Also non-aqueous systems are apt to dissolve cellulose. Again, the solvent spectrum is large and the number of possible combinations is large. The first developed systems are composed of selected ammonium salts with some simple inorganic compounds, such as SO_2 and NH_3, and can indeed be considered as the origin of two large groups of non-derivatizing non-aqueous solvent systems [36]. The first group generally comprises mixtures of a polar inorganic liquid, SO_2, and an amine (primary, secondary, tertiary aliphatic or secondary alicyclic) [37]. Otherwise, the sulfur component can be modified to $SOCl_2$. Appropriate polar liquids employed are for example N,N-dimethylformamide (DMF), DMSO, N,N-dimethylacetamide (DMAc) or formamide. From the ample diversity of possible mixtures, DMSO/SO_2/diethylamine is one of the most versatile [57].

Among the polar liquids DMSO gained relevance due to the low toxicity presented; relevant mixtures of two-component solvents containing DMSO [37] such as DMSO/methylamine, DMSO/KSCN, DMSO/$CaCl_2$, DMSO/formaldehyde and DMSO/substituted ammonium fluorides, such as tetrabutylammonium fluoride, TBAF (recently reported as a powerful solvent system capable of dissolving cellulose of reasonably high degree of polymerization (650) in a couple of minutes without any pre-treatment at room temperature [58]) were developed. Systems using lithium salts in non-aqueous solutions are also very useful for cellulose analysis and for the preparation of a wide variety of derivatives. In this regard, the DMAc/LiCl mixture, developed by McCormick, should be highlighted [59].

The Lyocell process, whose commercial potential has been demonstrated and is now applied in large scale, is based in the use of N-methylmorpholine-N-oxide (NMMO) as cellulose solvent, which emerged as the best of the amine-oxides in the late 1970's [17]. Solutions with up to 23 wt.% of cellulose can be obtained by dissolving the biopolymer in NMMO aqueous mixtures, and subsequently removing water under vacuum. Nevertheless, two main problems are still associated with the NMMO process; the instability of the solvent which demands major investments in safety technology and the tendency of the regenerated fiber towards fibrillation [60].

Another group of chemical compounds with high potential to dissolve cellulose are ionic liquids (ILs). Systems containing ILs were first employed by Graenacher, in the form of N-alkylpyridinium salts, for the dissolution of cellulose and as media for homogeneous chemical reactions [68]. Their potential was neglected for almost seventy years before the work of Swatloski et al. where several low melting ionic liquids (below

100 °C) were reported as cellulose solvents [61]. This work open a new and exciting field in cellulose research and, since then, a huge variety of ILs has been developed. It is important to note that the number of potential ion combinations available is estimated to provide around 10^{12} ILs [62]. Currently, the most efficient ILs for cellulose dissolution are mainly composed of a salt with halide [63], phosphonate [64], formate [65] or acetate [66] as anion, and imidazolium [67], pyridinium [68], choline [69], or phosphonium [70] as cation. An example of a recently synthesized ionic liquid with huge potential for fiber spinning (i.e. textile applications) is the 1,5-diaza-bicyclo[4.3.0]non-5-enium acetate ([DBNH][OAc]) which is described as a powerful direct cellulose solvent [71]. The development of a process designated as Ioncell-F produces regenerated cellulose fiber with properties comparable (or even superior) to Lyocell [72].

Mechanisms of dissolution

Due to the wide variety of solvents of different nature becomes unclear the understanding of the subtle balance between the different interactions acting during the solubilization process; although numerous and spread opinions, the more consensual vision among the leaders in the field has been that the key factor to dissolve cellulose resides in the solvent ability to break the abovementioned hydrogen bond network (intra- and intermolecular) [50]. The amphiphilic properties of cellulose were recently suggested to play an important role in cellulose solubility pattern and a careful examination of the interactions involved suggests that hydrophobic interactions should not be neglected in the cellulose dissolution process. Actually, hydrophobic interactions have been verified to clearly contribute to the crystal-like structure of cellulose and its stability over a hypothetical solution state; looking on the free energy simulations using oligomers it has been estimated that there is a 2.0 kcal/mol/residue contribution for the hydrophobic stacking while the estimated hydrogen bonding contribution is about eight times lower [14].

Thermodynamically the dissolution of a compound in a solvent is, of course, governed by the free energy of mixing; this law is valid for all mixtures, involving small solutes or large molecules, such as cellulose [18]. A negative variation of the free energy means

that the mixing process will happen spontaneously. However, for the case of polymers, even when the free energy variation is favourable to dissolution, this could not occur, because the process may be too slow on the time scale of observation; strategies to increase the rate of dissolution involves heating and stirring in order to increase the contact between the polymer and the solvent.

Generally the driving force for dissolution, or miscibility, is the entropy of mixing, and not as it is sometimes assumed favourable interactions between solvent and solute [12]. This explains the higher solubility of polyelectrolytes in water when compared with nonionic polymers. Charging up a polymer is always expected to help solubility in many solvent systems, as result of the huge contribution to the translational entropy of mixing promoted by the dissociated counterions. Most likely, this is the reason why cellulose tends to be more soluble/be more penetrated by the aqueous solvent at either high or low pH. Nevertheless, the pK values of the OH groups are such that rather extreme conditions are needed for either deprotonation or protonation; a pKa of 13.5 has been found for the deprotonation of the OH groups of C_2 and C_3 of AGU units of β-cyclodextrin [73].

On the other hand, an acceptable solvent for cellulose must be able to balance the low entropy gain with favourable solvent/polymer interactions. Since cellulose should be regarded as an amphiphilic molecule a good basis for the development of new solvents should focus, not only in eliminating hydrogen bonding but also, on reducing/eliminating hydrophobic interactions among cellulose chains. Both the amorphous and the crystalline regions can be affected by the solvent. However, the crystalline domains, characterized by a lower free energy than the amorphous one, should be more difficult to dissolve due to the reduced accessibility of the solvent caused by the high stability of the solid state [12]. This is particularly relevant since as mentioned above crystalline cellulose domains has an amphipathic-like structure; hydrophobic surfaces consisting of pyranose ring hydrogens and hydrophilic regions arising from the hydroxyl groups directed towards the sides of the ring [12, 23, 74]. In fact, this also follows from the earlier discussion on the effect of additives such as PEG, urea and thiourea on NaOH solutions as these additives are expected to weaken hydrophobic interactions among cellulose molecules (see discussion in the next section).

Consequently, different activation processes are routinely applied to mainly transform the more ordered and less accessible (crystalline) domains of cellulose into disordered

and more accessible regions, in order to facilitate dissolution. It is argued that these alterations of the cellulose structure improve the solvent molecules accessibility to the cellulose chains [28]. The crystallinity effect in dissolution is still controversial despite some clear evidences of its effect. For example, it was showed that sisal pulp (e.g. fibers extracted from the *Agave sisalana* plant) can be easily dissolved than cotton linters in a particular solvent system; the enhanced solubility is attributed to the lower crystallinity index and smaller crystallite size compared to the latter one. After pre-treatment of cotton linter (e.g. mercerization), dissolution was considerably improved and this observation was related to the decrease in both the crystallinity index and average crystal size [75]. Also the high solubility of cellulose derivatives supports the importance of the crystallinity in the solubility pattern of cellulose.

It is also important note that in the majority of the cases, cellulose is not dissolved down to the molecular level but rather forms stable colloidal dispersions where ordered cellulose aggregates of, at least, several hundred chains are present. The structure in solution has been proposed to consist of aggregates of fringed micelle type characterized by a highly ordered cylindrical core of aligned chains, which is insoluble in the solvent, and two spherical coronas surrounding the core ends [76]. Reaching molecularly dispersed systems has been challenging for nearly all known solvent systems. Recently, Cohen et al. reported that ionic liquids are able to dissolve cellulose down to a molecular level [77].

Typically, the cations of ILs are bulky species with amphiphilic properties. Proof of this is that most literature agrees on the formation of aggregates or micelles of ionic liquids in water, similar to a surfactant behavior [78]. Such amphiphilicity should be considered when discussing the mechanism of dissolution of cellulose, as discussed above. Recent molecular dynamics simulations, carried out on cellulose oligomers and 1-ethyl-3-methylimidazolium acetate (C2mimOAc), actually suggest that the cations are in close contact with the cellulose chains via hydrophobic interactions [79]. The same has been concluded when using urea [80].

Role of cellulose interactions in dissolution and regeneration: Amphiphilicity and Hydrophobic Interactions

As discussed above, the dissolution of a polymer is governed by the free energy of mixing [81]. Small oligomers of cellulose as glucose, cellobiose and any other with degree of polymerization slightly higher (<10) are soluble in common solvents, such as water. As the molecular weight increases, the entropic contribution for dissolution decreases [82] and the solubility drops dramatically as the chain length increases [83]. The entropy of mixing for polymers is composed by two terms: a translational term (related with the molecular weight of the polymer) and a second term related to the conformational freedom [12]. Flexible polymers can easily increase their conformational freedom on going into solution; on the other hand, stiff polymers cannot change the conformation and the gain in conformational freedom is very limited. Flexible polymers are, consequently, more soluble than rigid polymers.

Since cellulose is a fairly rigid polymer, its ability to gain configurational entropy in solution is limited, lowering the solubility [84]. Also, native cellulose has a high molecular weight, which inevitably leads to a decrease in the entropic gain in the dissolution process leading to a very low solubility. In addition, the stiffness of the structure and the stacked chains by the hydrophobic regions that allow transverse hydrogen bonds, restrict the entropy of mixing, so that a negative free energy change is not reached. In these circumstances, favourable/unfavourable interactions between polymer and solvent are decisive in determining solubility/insolubility of cellulose in a solvent system.

As alluded to water alone cannot dissolve cellulose, since the pair-wise hydrogen bond interactions involving water-water, carbohydrate-water, and carbohydrate-carbohydrate hydrogen bond interactions are about the similar magnitude, about 5 kcal/mol [12]. Therefore, hydrogen bonds might be responsible for keeping the linear cellulose chains arranged in sheets. On the other hand, as discussed above, the stacking of these sheets into the three-dimensional crystal structures of the cellulose material involves hydrophobic interactions. A theoretical work on the mean force calculations for the separation of cello-oligomers, have suggested that hydrophobic interactions contribute favorably to stabilizing a crystal-like stacked structure [85]. In fact, the driving force for

association is not exclusively van der Waals interactions [86, 87], but rather hydrophobic association driven by the liberation of structured water molecules [88]. The role of hydrophobic interactions in the cellulose solubility pattern is supported by some significant examples in literature.

A clear support to this view comes from the work of Isobe et al., which described that urea even if it does not have direct interaction with cellulose, favours the alkali penetration into the cellulose crystalline regions by stabilizing the swollen cellulose molecules, while following the cellulose dissolution in the NaOH/urea based solvent [89]. The authors concluded that such stabilizing effect may result from the fact that urea prevents the hydrophobic mutual association of cellulose chains.

Various substances of intermediate polarity such as poly(ethylene glycol), thiourea and urea can enhance the aqueous solubility of cellulose; also amphiphilic species, such as surfactants, have a positive impact in dissolution rate of cellulose [6]. Actually, urea is normally used as agent for protein denaturation and it is rational to assume that the role of urea in cellulose dissolution is similar to protein denaturation [90]. Concerning protein denaturation, using urea, it was demonstrated that urea molecules accumulate around less polar side chains forming an interface between less polar protein surface and water. The resulting displacement of water molecules from the protein surface into bulk water is entropically and enthalpically favorable and reduces the hydrophobic effect, such that unfolding of the protein becomes favorable [91]. Urea is less polar than water and is well known for its ability to reduce/eliminate hydrophobic association in water. One other example of this is the increase in critical micelle concentration (cmc) promoted by the addition of urea to aqueous surfactants systems; this increment in cmc is driven by the inhibition of hydrophobic association of surfactants [92]. Obviously, the key point here is the nature of urea which can establish polar and/or apolar interactions with other molecules; this has been demonstrated using molecular modeling in protein denaturation process [91], but also the enhancement of its concentration close to model hydrophobic surfaces [93] and inside hydrophobic nanotubes [94] are examples of it.

The investigation carried out by Xiong et al., using an aqueous NaOH based system, is another interesting example that supports the importance of hydrophobic interactions in cellulose behaviour. It was clearly shown that urea can improve the rate of dissolution by interaction *via* van der Waals forces with the hydrophobic regions of cellulose to prevent dissolved molecules from re-gathering [95]. In perfect agreement, the study carried out by Bergenstrahle-Wohlert et al., combining MD simulations and solid state

NMR on cellulose in pure water and in urea aqueous solutions [96] demonstrated that the local concentration of urea is significantly enhanced at the cellulose/solution interface. The study also showed that urea has a preferential orientation when binding to cellulose, having the carbonyl oxygen ("hydrophilic part"), on average, pointing slightly away from the cellulose backbone and the nitrogen atoms ("hydrophobic part"), pointing in the direction of the cellulose backbone.

Ionic liquids (ILs), a very promising group of solvents for cellulose, as discussed in the previous section, are composed of typically bulky cations with amphiphilic properties [62, 97, 98]. Even if there is no clear understanding on the role of individual ionic species in dissolution, it becomes clear that the high asymmetry in the IL species is fundamental and necessary for an efficient dissolution [6]. Such amphiphilicity is normally not considered when discussing the mechanism of cellulose dissolution, but is believed that this is determinant to understand their action in cellulose solubility. The dissolution of an amphiphilic polymer, such as cellulose, would be facilitated in solvents with amphiphilic properties and therefore the amphiphilic properties of all cations in ILs clearly fit this suggestion.

Mostofian et al. presented a notable work supporting this idea, suggesting a synergistic approach for cellulose dissolution in ILs [99]. The authors performed all-atom MD simulations of a cellulose fiber in 1-butyl-3-methylimidazolium chloride (BmimCl) in order to clarify the role of cations and anions during dissolution and the preferential interactions of the IL ions with cellulose surfaces. The study reveals that while the Cl$^-$ anions predominantly interact with the cellulose surface hydroxyl groups, the Bmim$^+$ cations stack preferentially on the hydrophobic cellulose surfaces, governed by non-polar interactions with cellulose. It is also suggested that the stacking interaction between solvent cation rings and cellulose pyranose rings can compensate the interaction between stacked cellulose layers, thus stabilizing detached cellulose chains. This work not only reinforces the idea that ILs are a very promising class of solvents for cellulose, but also provides an essential molecular understanding of how ILs act, and more notably, highlights the concerted and distinct action of anions and cations on the hydrophobic and hydrophilic regions of cellulose surfaces, respectively, as the key to an efficient dissolution of an amphiphilic molecule such as cellulose.

Another interesting study, recently presented by Isobe et al. [100] focused on the molecular regeneration of cellulose, both using a coagulant media or upon heating, in an aqueous alkali-urea solvent system, monitored by time resolved synchrotron X-ray

radiation. It is suggested that the gelation process is driven by the stack of the glucopyranose rings (conducted by hydrophobic interactions) to form monomolecular sheets, which then line up by hydrogen bonding to form Na-cellulose IV, a hydrate form of cellulose II). This idea has been hypothesized and supported by molecular dynamics first by Hermans [101] and later by Hayashi [102]. Afterwards, the theoretical work of Miyamoto et al. [23] simulated the regeneration of cellulose by MD, and supports the hypothesis of Hermans and Hayashi. However, this work of Isobe et al. constitutes the first experimental evidence of the development of hydrophobically stacked monomolecular sheets.

Östlund et al. stated that the properties of the regenerated cellulose material can be tuned by the proper choice of the experimental conditions such as temperature and coagulation medium [103]. It is suggested that coagulation media of different polarity lead to regenerated materials with different morphologies and properties and this can be used to tune the properties of the end materials. As the polarity of the coagulant is increased, more ordered (crystalline) materials are obtained, the hydrophobic interactions between the polymer chains during regeneration being governed by the increased polarity of the coagulant.

Rein et al. have used cellulose as novel and efficient eco-friendly emulsifying agent to form stable oil-in-water or water-in-oil dispersions, taking advantage of its amphiphilicity [104]. The authors interpret the dispersion stability as due to the ability of the hydrophilic hydroxyl groups to interact with the water while the more hydrophobic planes of the glucopyranose rings are situated towards the hydrocarbon oil. These dispersions were found to be stable for large periods of time, mainly the oil-in-water dispersion with stability of more than one year, where neither flocculation nor coalescence was observed.

Also Nawaz et al. noticed the amphiphilic properties of cellulose while studying the mechanism of mediated imidazole-catalysis acylation of cellulose, suggesting that the sub-sequent decrease in enthalpy during the N-butanoyl- to N-hexanoylimidazole conversion may be related to favorable hydrophobic interactions between the carbon chains of the N-acylimidazole and cellulosic surface, whose lipophilicity has increased, due to its partial acylation [105]. Closely related Hauru et al. found that cellulose regeneration from IL solutions goes via the hydrophobic association of the less polar regions of cellulose [106].

An additional curious example comes from the deposition of carboxymetylcellulose (CMC) on polymer surfaces. Kargl et al. suggest that the amphiphilicity of cellulose surfaces is important for the irreversible deposition of CMC over a polymeric substrate with appropriate properties, i.e. better results were obtained in substrates not highly hydrophilic or very hydrophobic [107].

Regarding the composite area, in the cellulose-acrylated epoxidized soybean oil (AESO) based biocomposite the presence of oil molecules was found in the cellulosic material, suggesting the lack of covalent or hydrogen bonding between the two components [108]. The authors proposed that the dispersion of AESO molecules in the cellulose matrix is held by hydrophobic interactions between hydrocarbon chains of the AESO and hydrophobic domains of cellulose, playing a crucial role in the composite.

From the facts mentioned above, it is indeed very striking that cellulose is amphiphilic in nature and hydrophobic interactions play an important role both in dissolution and regeneration.

Motivation and scope

As pointed out in the first chapter of this thesis, there are different points of view regarding which are the governing forces involved on the cellulose dissolution and regeneration processes. Also the level of dissolution, i.e. molecular dispersed cellulose chains vs. colloidal aggregates, is still a non consensual theme. Using a set of different techniques, described in chapter 2, in particular rheology, optical and electron microscopy, light scattering, small and wide angle X-ray scattering and NMR we have strengthened the molecular understanding of the cellulose dissolution. Part of the work was also performed in collaboration with the Department of Physical Chemistry at Lund University, Sweden and the Laboratory of Plant Biotechnology at the University of Algarve.

The central scope of the thesis is to understand the balance between the interactions involved in cellulose dissolution and its impact on the degree of dissolution, solution state (i.e. molecular solutions or colloidal aggregates), and on the resultant regenerated

materials. This can contribute to the development of new efficient and environmental friendly solvents for cellulose.

Until now, only a few solvent systems are described as able to dissolve cellulose into a molecular level [77] and the same applies for cellulose derivatives. Cellulose modifications are expected to adversely affect the degree of crystallinity. However, cellulose derivatives are surprisingly highly crystalline and therefore can be used as sources for nanocrystalline cellulose. In chapter 3, section 3.1, the extraction and characterization of cellulose nanocrystals using cellulose derivatives is described and also there is a discussion on dissolution at a molecular level or the presence of colloidal aggregates.

In section 3.2, is discussed a new NMR method, polarization transfer solid-state NMR, as applied to cellulose solutions. The advantage of the technique to provide robust information on the molecular-level about the dissolved and solid fractions of cellulose in aqueous dissolution media is demonstrated.

In chapter 3, section 3.3 the dissolution of cellulose in alkali based aqueous solutions and the influence of additives on the dissolution performance are discussed.

To a better understanding of the dissolution mechanism, a wide range of solvents for cellulose is used. In chapter 3 the main results are described for basic and acidic solvents.

The balance between the interactions involved in cellulose dissolution and the stability of the cellulose solutions are discussed in section 3.5 of chapter 3. The results clearly indicate the improvement of the thermal and storing stability of the solutions when amphiphilic additives are in the solution. The thermal gelation is shifted to higher temperatures when surfactants are added to the solution, which provides support to the role of the hydrophobic interactions also in cellulose regeneration.

The influence of the different solvent systems on the sample properties, regarding morphology and crystallinity of the regenerated materials, is discussed in chapter 3, section 3.6.

In chapter 4 the main conclusions are gathered.

CHAPTER 2

Materials and Methods

Materials

Microcrystalline cellulose (MCC) (Avicel PH-101, average particles size of 50 μm and degree of polymerization of ca. 260), carboxymethyl cellulose (CMC) (Mw = 7 × 10^5 Da, degree of substitution of 0.9), zinc oxide (> 99% purity), sulfuric acid (98% purity ACS reagent), urea (99.5% purity), thiourea (>99% purity), alkyl-polyglucoside (APG), 50% solution, 1-butyl-3-methylimidazolium chloride (BmimCl) (>98% purity), 4-methylmorpholine N-oxide monohydrate (NMMO) (>95% purity), tetrabutylphosphonium hydroxide (40% solution in water) and tetrabutylammonium hydroxide (TBAH) of chromatographic grade (as a 40 wt.% solution in water), methanesulfonic acid (anhydrous), glycerol (purity >99.5%), an aqueous surfactant solution (~35% active substance) of a derivative of betaine (N-(Alkyl C10-C16)-N,N-dimethylglycine betaine), 3-(trimethylsilyl)propionic-2,2,3,3-d4 acid sodium salt and zinc chloride (reagent grade, purity >98%) were acquired from Sigma Aldrich. High molecular weight cellulose (Domsjö Pulp, degree of polymerization of ca. 745) was obtained from Domsjö Fabriker, Sweden. NaOH pellets (>98% purity) and ortho-phosphoric acid (purity 99%) were obtained from Fluka. Hydroxypropyl methylcellulose (HPMC, Methocel® K15M Premium), 19–24% methoxyl and 7–12% hydroxypropyl, Mw = 4.3 × 10^5 Da, was purchased from Dow Chemical Company. Dialysis bags (molecular weight cut-off 2000, Cellu Sep H1) were purchased from

Orange Scientific. The ^{1}H NMR samples were prepared using D_2O (99.8%) supplied by EURISO-TOP (France)

Sample preparation

Cellulose dissolution was obtained following the adapted standard procedures in literature [53, 109, 110]. Briefly, a known amount of cellulose was dispersed in a 85 wt.% phosphoric acid pre-cooled at 5 ℃, the solution was stirred for 12 h until complete dissolution of MCC and achievement of a clear solution [109]. The dissolution of cellulose in H_2SO_4/glycerol was obtained by addition of a known amount of MCC in a solution of 66 wt.% of H_2SO_4 and 33 wt.% glycerol. The solution was heated at 60 ℃ for 15 min to complete dissolution of cellulose. Dissolution in the highly concentrated salt system was achieved by dissolving the desired amount of MCC in a 60 wt.% $ZnCl_2$/H_2O solution at 80 ℃ for 15 min [53].

Solutions in alkali-based systems were prepared by addition of a known amount of cellulose in a 8 % NaOH/H_2O solution and then allowed to freeze at -20 ℃ for 24 h. This was followed by thawing the solid frozen mass at room temperature under simultaneous vigorous mixing. The same procedure was followed with amphiphilic additives in the NaOH based systems but the additives were added before freezing the samples. On the other hand, for the TBAH based solvent, the dissolution procedure was simply the mixture of a known amount of cellulose with a 40 wt.% TBAH aqueous solution at room temperature for 30 min.

The extraction procedure of CNCs was based on a previously reported method [111]. Briefly, 5 g of MCC powder was added to a 100 mL H_2SO_4 (65 wt.%) aqueous solution. The hydrolysis was carried out during 30 min at 65 °C and afterwards the reaction was quenched by the addition of a large excess of deionised water (250 mL) and the mixture was centrifuged at 3800 rpm for 15 min at room temperature. This centrifugation step was repeated several times before the suspension was dialyzed against distilled water for one week to neutralize the pH of solution and remove undesired salts. The resulting suspension was kept refrigerated for later use. The same procedure was followed for the extraction of CNCs from cellulose derivatives, HPMC and CMC.

Experimental techniques

Polarized light microscopy

Optical microscopy is used in a wide range of applications, in different science fields such pharmacy, medicine, chemistry, biology and geology [112-115]. This technique is quite useful for a fast and facile analysis of the particle size and shape in solid compounds and also to analyze particles in a suspension. The use of polarized light microscopy (PLM) as a tool for crystallography extends back at least 200 years [112].

The simplest PLM is essentially a bright field microscope with a rotating stage and plane-polarizing filters placed below (the polarizer) and above (the analyzer) the specimen these being generally the main differences from a standard transilluminating microscope [116].

Light from an ordinary light source (natural light) that vibrates in random directions is called nonpolarized light. In contrast, light with vertical vibration that travels within a single plane is called linearly polarized light. Circularly polarized light and elliptically polarized light are obtained when the vibration plane rotates forward. In figure 2.1 the three types of polarized light are represented.

linearly polarized light **circularly polarized light** **elliptically polarized light**
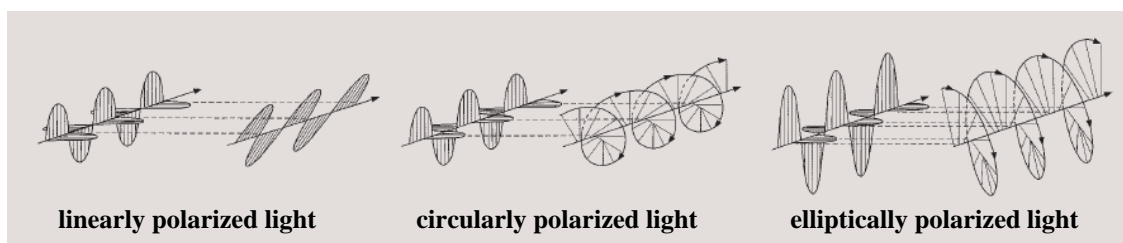
Figure 2.1: Types of polarized light [117].

A polarizing plate (polarizing filter) or polarizing prism is often used as the device to change natural light to linearly polarized light (figure 2.2). Configuring the primary and secondary polarizing devices in the orthogonal directions of each transmitting linearly polarized ray will "cut" the light. Such a state in which the primary light polarizing device is the polarizer and the secondary device is the analyzer is called crossed nicols. Parallel nicols is the state in which the analyzer is rotated to make the direction of the transmitting linearly polarized light match with the polarizer, and the amount of light transmittance is maximized.
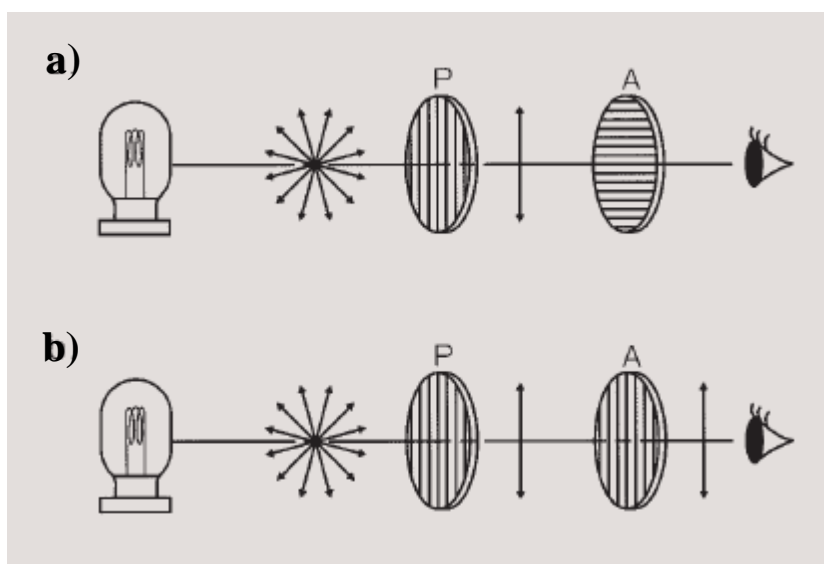
Figure 2.2: a) crossed nicols and b) parallel nicols. (P) polarizer; (A) analyzer [117].

A Linkam LTS 120 microscope equipped with a Q imaging station (Qicam) Fast 1394 camera was used to evaluate cellulose dissolution in the solvent systems used. Samples were kept between cover slips and illuminated with linearly polarized light and analyzed through a crossed polarizer. Images were captured and analyzed using an appropriate Qcapture software.

In figure 2.3 two examples of images obtained for the dissolution of cellulose in the TBAH/H_2O system are presented. A large amount of birefringent areas (bright) are clearly visible on the left side (0 min) while no insoluble material is detected after 30min.
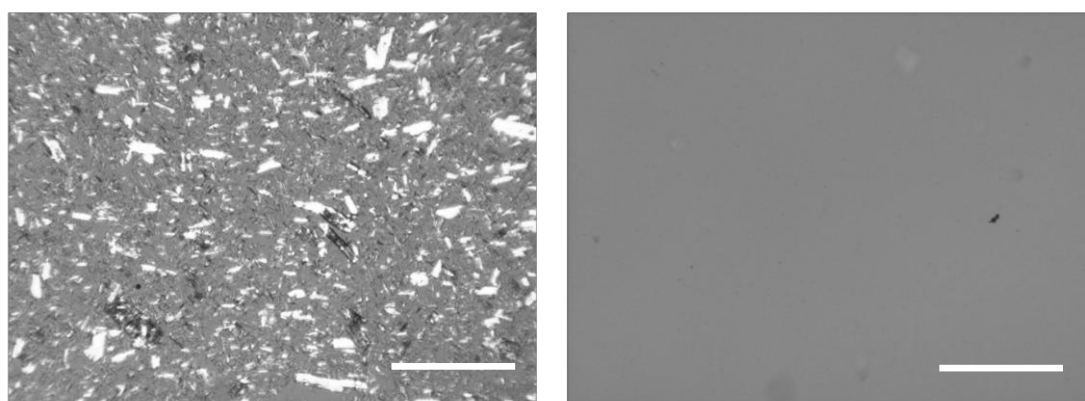
Figure 2.3: Images of 5.0 wt.% of MCC in TBAH/H_2O (40:60), at t = 0 min (left) and t = 30min (right). Temperature was kept at 20 °C. The scale bars represent 100 μm.

Scanning Electron Microscopy

The scanning electron microscopy (SEM) is routinely used to generate high-resolution images. This technique uses a high-energy focused beam of electrons to generate a variety of signals at the surface of the solid specimens. The electron source used in SEM can be a tungsten filament a LaB6 or Schottky emitter, or even a tungsten field-emission tip. Because the maximum accelerating voltage (typically 30 kV) is lower than for a transmission electron microscope (TEM), the electron gun is smaller, requiring less insulation [118]. Accelerated electrons in an SEM carry significant amounts of kinetic energy, and this energy is dissipated as a variety of signals produced by the electron-sample interactions, which result when the incident electrons are deccelerated in the solid sample. These signals include secondary electrons (that produce SEM images), backscattered electrons (BSE), diffracted backscattered electrons (EBSD that are used to determine crystal structures and orientations of minerals), photons (characteristic X-rays that are used for elemental analysis and continuum X-rays), visible light (cathodoluminescence–CL) and heat.

The signals that derive from electron-sample interactions reveal valuable information about the sample including external morphology (texture), chemical composition, and crystalline structure and preferred orientation of materials composing the sample. In most applications, data are collected over a selected area of the surface of the sample, and a 2-dimensional image is generated displaying spatial variations of these properties. Modern SEM equipments are capable of providing an image resolution typically between 1 nm and 10 nm. This is not as good as the ones obtained with TEM but nevertheless much superior when compared to common light microscopy. In addition, SEM images have a relatively large depth of focus: specimen features that are displaced from the plane of focus appear almost sharply in focus. This feature results from the fact that electrons in the SEM (or the TEM) travel very close to the optic axis, a requirement for obtaining good image resolution [119].

The major advantages of a SEM, compared with a TEM, are the easy preparation of the sample specimens and the fast data acquisition [118]. In figure 2.4 a schematic illustration of a scanning electron microscope is presented.
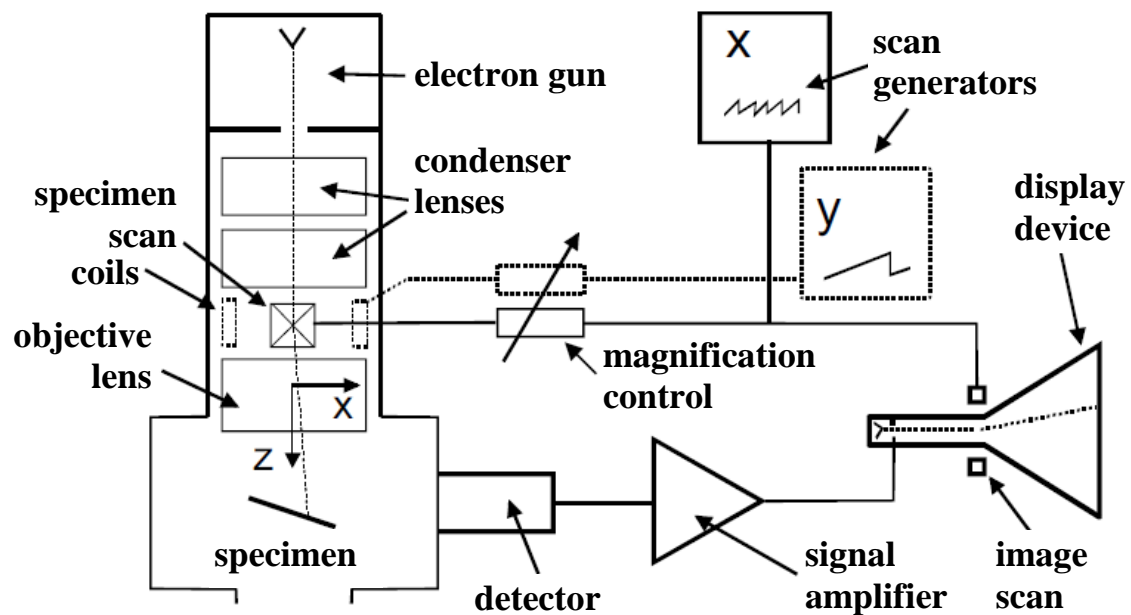
Figure 2.4: Schematic diagram of a scanning electron microscope with a CRT display (adapted from [118]).

The SEM is also capable of performing chemical analysis of selected areas on the sample; this approach is particularly useful for a qualitative or semi-quantitative determination of the chemical composition (using energy-dispersive spectrometry, EDS), crystalline structure, and crystal orientations (using EBSD). Secondary electrons and backscattered electrons are commonly used for imaging samples: while secondary electrons are most valuable for showing morphology and topography of samples, backscattered electrons are particularly relevant for illustrating contrasts in composition in multiphase samples (i.e. for rapid phase discrimination) [120].

The EDS analysis is based on the X-ray generation that is produced by inelastic collisions of the incident electrons with electrons in discrete orbitals (shells) of atoms in the sample. As the excited electrons return to lower energy states, they yield X-rays that are of a fixed wavelength (that is related to the difference in energy levels of electrons in different shells for a given element). Thus, characteristic X-rays are produced for each element in a mineral that is "excited" by the electron beam. SEM analysis is considered to be "non-destructive"; that is, x-rays generated by electron interactions do not lead to volume loss of the sample, so it is possible to analyze the same material repeatedly.

A high resolution (Schottky) Environmental Scanning Electron Microscopy (FEG-ESEM), equipped with the analytical systems X-ray microanalysis (EDS) and backscattered electron diffraction pattern analysis (EBSD) was used to observe the morphology and microstructure of the samples (model Quanta 400FEG ESEM/EDAX Genesis X4M). Typically, 50 μL of a suspension was dropped onto a clean glass lamella followed by drying for 24 h in a kiln and then sputtered with an approximately 6 nm thin Au/Pd film by cathodic pulverization using a SPI Module Sputter Coater before SEM analysis. The same procedure was followed for the regenerated and starting materials which, after being dried at room temperature, were also placed onto a glass lamella using an appropriate support tape and then sputtered as previously described for the suspension case. The accelerating voltage ranged from 5 to 15 kV. In figure 2.5 an example of an SEM micrograph obtained for a raw cellulose sample is displayed.

The cryo-scanning electron microscopy (Cryo-SEM) was carried out using a JEOL JSM-6301F (Tokyo, Japan), an Oxford Instruments INCA Energy 350 (Abingdon, UK), and a Gatan Alto 2500 (Pleasanton, CA, USA). Cryo preparation techniques for SEM have become essential for the observation of wet or beam-sensitive specimens to minimize potential morphological particle changes. The cellulose derivatives dispersions were dropped on a grid, rapidly cooled in a liquid nitrogen slush (- 210 °C), and transferred under vacuum to the cold stage of the preparation chamber. Here, the samples were fractured, sublimated (4 minutes, - 90 °C) to reveal greater detail, and coated with a gold-palladium alloy. Finally, the specimens were moved under vacuum into the SEM chamber where they were observed at - 150 °C).
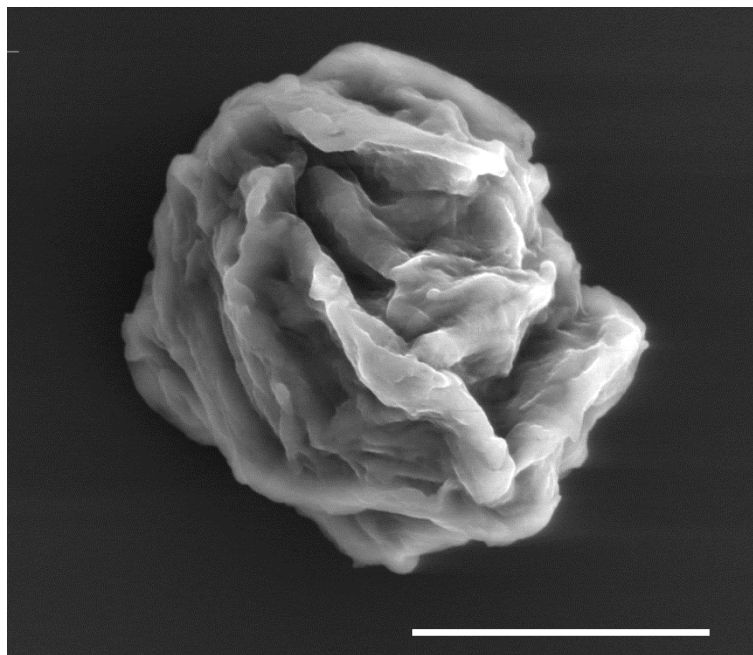
Figure 2.5: SEM micrograph of microcrystalline cellulose after dispersion in water. The scale bar represents 10 μm.

X-Ray diffraction

Since the first X-ray diffraction experiment on a single crystal in 1912, performed by Max von Laue, X-ray crystallography is recognized to be of major importance in natural sciences [121]. Max von Laue discovered that crystalline substances act as three-dimensional diffraction gratings for X-ray wavelengths similar to the spacing of the planes in a crystal lattice. X-ray diffraction (XRD) is a reasonably rapid analytical technique primarily used for phase identification of a crystalline material and can provide information on, for instance, unit cell dimensions. Typically, the analyzed material is finely ground, homogenized, and the average bulk composition is determined.

Diffraction effects are observed when electromagnetic radiation impinges on periodic structures with geometrical variations on the length scale of the wavelength of the radiation. The interatomic distances in crystals and molecules, ca. 0.15 to 0.4 nm, correspond to the wavelengths of X-rays, with photon energies between 3 and 8 keV and wavelengths in a range of 0.1 to 10 Å [121]. Accordingly, phenomena such as constructive and destructive interference should become observable when crystalline and molecular structures are exposed to X-rays [122].

There are three different types of interaction in the relevant energy range. Two inelastic processes (photoionization and energy transference) and one elastic, useful for structural investigations, the Thomson scattering [122]. The wavelength λ of X-rays is conserved for Thomson scattering in contrast to the two inelastic scattering processes mentioned earlier.

The high degree of order and periodicity in a crystal can be envisioned by selecting sets of crystallographic lattice planes that are occupied by the atoms comprising the crystal. The planes are all parallel to each other and intersect the axes of the crystallographic unit cell. Any set of lattice planes can be indexed by an integer triple *hkl* with the meaning that *a/h*, *a/k* and *a/l* now specify the points of intersection of the lattice planes with the unit cell edges. This system of geometrical ordering of atoms on crystallographic planes is known as the Miller indices *hkl*.

Up to now, what has been known as the "Laue conditions" and the "Bragg equation" has formed the basis of X-ray diffraction of crystalline materials. The interaction of the incident X-rays with the sample produces constructive interference (and a diffracted ray) when conditions satisfy Bragg's Law ($n\lambda=2d \sin \theta$). This law relates the wavelength of electromagnetic radiation to the diffraction angle and the lattice spacing in a crystalline sample. These diffracted X-rays are then detected, processed and counted. By scanning the sample through a range of 2θ angles, all possible diffraction directions of the lattice should be attained due to the random orientation of the powdered material. Conversion of the diffraction peaks to d-spacings allows identification, for instance, of a given mineral because each mineral has a set of unique d-spacings. Typically, this is achieved by comparison of d-spacings with standard reference patterns [122]. In figure 2.6 a schematic representation of a $\theta/2\theta$ diffraction in Bragg-Brentano geometry is represented.
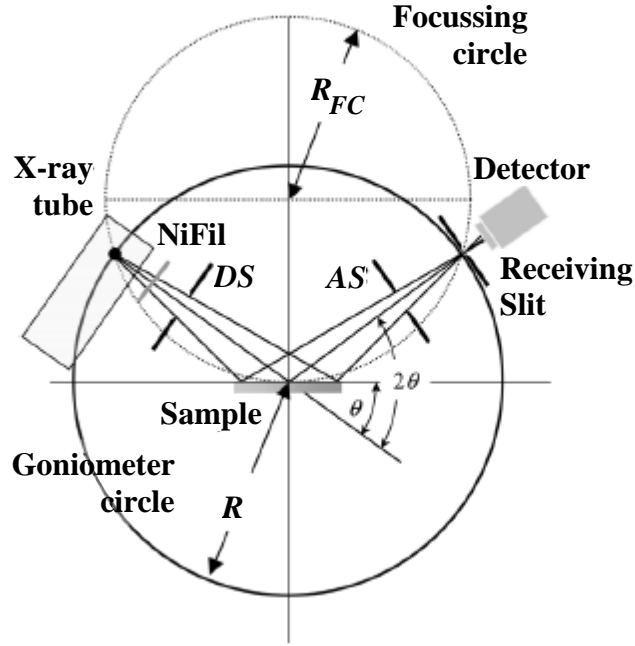
Figure 2.6: Schematic representation of a θ/2θ diffraction in Bragg-Brentano geometry (adapted from [122]).

The X-Ray Diffraction (XRD) experiments were performed on a Siemens D5000 X-ray diffractometer, sensitive to crystalline phases down to 3% of the bulk. This equipment consists of a θ/2θ diffraction instrument operating in the reflection geometry. $CuK_{\alpha 1}$ is used as radiation source with $\lambda = 1.54056$ Å, focused by a primary Ge crystal monochromator. The detector is a standard scintillation counter. The Cu tube runs at 40 mA and 40 kV. The cooling is supplied by an internal water-filled recirculation chilling system, running at approximately 16 ℃ with a flow rate of 4-4.5 L/min. The slit arrangement is a 2 mm pre-sample slit, 2 mm post-sample slit and a 0.2 mm detector slit. The footprint size used was 0.005 degrees. The crystallinity index (CrI) was estimated from the diffracted intensity data using the method suggested by Segal et al., equation 2.1 [123]:

$$(\text{CrI}) = \frac{I_{002} - I_{am}}{I_{002}} \times 100 \tag{2.1}$$

where I_{002} is the maximum intensity of the (002) lattice diffraction and I_{am} is the intensity of diffraction at $2\theta = 18°$.

An example of the obtained spectra for native microcrystalline cellulose is presented in figure 2.7. In the obtained diffraction pattern it is possible to observe a major peak centred at around ca. 22.5° (002) with a side peak at 20.5° (021) typical for the cellulose

I crystalline polymorph [124]. Other characteristic reflections for a cellulose I type structure can be found at 14.7° (101), 16.6° (101) and 34.7° (040).
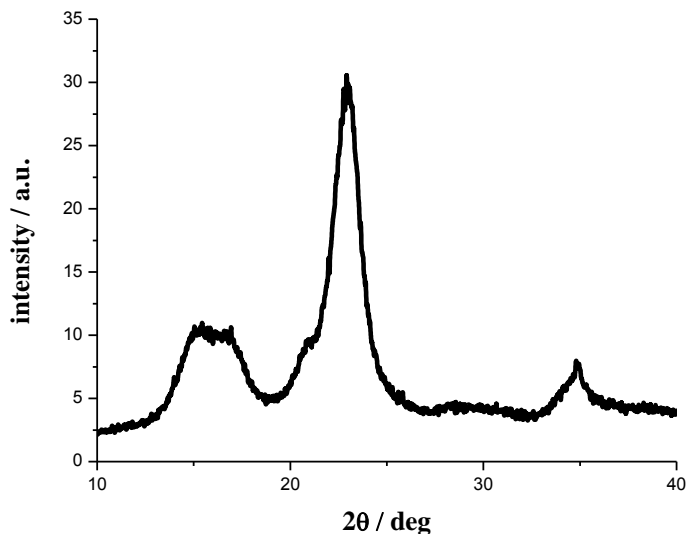
Figure 2.7: XRD diffraction pattern obtained for native microcrystalline cellulose.

Optical transmittance measurements

The turbidity of a sample can be easily determined by using Ultraviolet/Visible absorption spectroscopy (UV/VIS). UV/VIS has been used as routine research method in ordinary chemistry laboratories for many years. The technique is almost universal in its application [125].

In UV/VIS spectroscopy, one studies how a sample interacts to light. The way light interacts with matter can be summarized in four different manners: absorption, transmission, emission and scattering [126]. When a light beam passes through a substance or a solution, part of it may be absorbed and the remainder transmitted through the sample. The ratio between the intensities of the incident light (I_0) to that exiting the sample (I_t), at a particular wavelength, is defined as the transmittance (T). This is often expressed as the percentage of transmittance (%T), which is the transmittance multiplied by 100 (equation 2.2).

$$\%T = \left(\frac{I_t}{I_0}\right) \times 100 \qquad (2.2)$$

The transmittance and absorbance are deeply related. Mathematically, absorbance is the negative logarithm of transmittance ($A=-log\ T$). There is an exponential relationship

29

between the relative absorption (I_t /I_0) and the concentration (c) and path length (l) of the absorbing substance [127]. The linear relationship between absorbance (A), concentration (c) and path length (l) is known as the Beer-Lambert law ($A=\varepsilon cl$). In this relation, ε is the molar attenuation coefficient of the attenuating specie. The linearity can be highly affected by scatter [125]. If the sample is turbid, the incident light will be scattered and, as result, less radiation will fall on the detector and a falsely high absorbance reading will be observed.

If the experimental setup is made in a way to use a wavelength where the involved chemical species do not absorb, it can be assumed that all apparent absorbance is actually due to light scattering from the non-dissolved particles, and in this case the turbidity can be related with undissolved cellulose particles in solution.

A single beam T70 UV–vis spectrophotometer (PG Instruments Ltd) was used for the optical transmittance measurements. Essentially, the cellulose solutions were placed in a couvette cell (dimensions of 1 cm × 1 cm × 5 cm) and the transmittance was fallowed at 600 nm. In figure 2.8 the variation of the transmittance of a solution of cellulose in strong alkali medium (tetrabutylammonium hydroxide) as function of the addition of a salt (KCl) is presented.
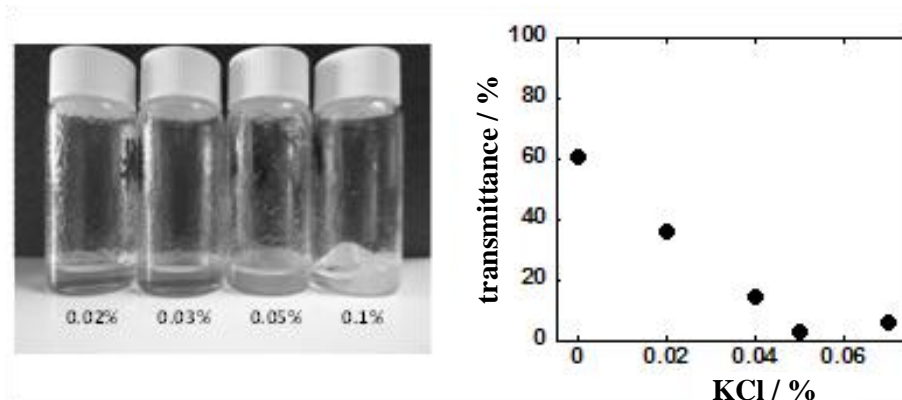
Figure 2.8: Photos (left) and transmittance (right) of cellulose dissolved in strong alkali (TBAH solution) with progressive addition of KCl.

Rheometry

The understanding of the flow behavior of a certain material when subjected to a deformation force is the basis of the rheological studies. The type of deformation depends on the state of matter; for example, gases and liquids will flow when a force is

applied, whilst solids will deform and are expected to regain their shape when the force is removed (pure elastic behaviour). In other words, rheology studies the *"handling properties of materials"*. The utility of many of the materials we make use every day is due to their unique rheological behaviour and that is one of the reasons why many chemists spend a lot of time in developing formulations to have specific textures, flow properties, etc. [128].

Rheological techniques help to understand the molecular organization and to anticipate the mechanical properties of materials, thus having applications in a large number of industrial processes in which, for instance, the viscosity control is required. Two main groups of rheological tests can be applied: rotational and oscillatory tests. In figure 2.9 the forces applied to a certain sample using a parallel plate geometry are depicted.
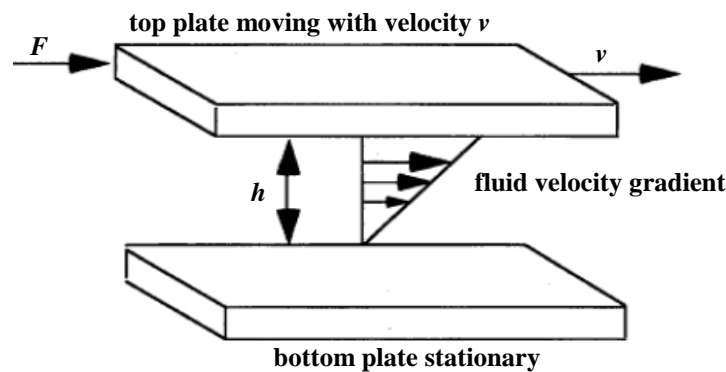
Figure 2.9: Parallel plats depiction of shear rate (adapted from [129]).

The height, *h*, is much smaller when compared with the dimensions of the plates, usually in the range of μm. The velocity profile can be considered linear and its gradient is constant. Shear rate (γ̇) defines how quickly a fluid is induced to flow, and is related with the applied force (σ) by a constant of proportionality, viscosity (*η*), as described in equation 2.3.

$$\sigma = \eta\dot{\gamma} \tag{2.3}$$

The oscillatory linear viscoelastic experiments measure the response function, or the complex modulus, $G^*(\omega) = G'(\omega) + iG''(\omega)$. This provides information about the relaxation of the microstructure of the system as a function of the frequency of oscillation, ω. The elastic component is described by the rheological variable G', storage modulus, and represents the mechanical energy stored and recovered (per period of oscillation). The viscous component is described by the rheological variable G'', the loss modulus, and it measures the mechanical energy lost as heat during the viscous

flow [130]. Solutions presenting G'>G'' have a solid-like behavior and solutions were G''>G' have a liquid-like behavior. Given the proper conditions, some samples can show a solid-to-liquid transition (G'=G'') [131]. The more solid the sample is the more energy is necessary to provide in order for the material to flow.

Cellulose solutions are often not stable and gelation occurs either with time or with temperature. Therefore, the determination of shear viscosity of the cellulose samples is a critical parameter for processing both regarding dissolution and regeneration issues.

All the rheological experiments were conducted using a controlled stress Reologica Stresstech rheometer equipped with an automatic gap setting. All samples were allowed to equilibrate for 10 min before the measurements. A cone-and-plate measuring geometry (1º, 50 mm diameter) was used with a solvent trap to prevent sample evaporation. A temperature control unit ensures a temperature variation in the sample chamber not larger than 0.1 ℃ of the set value. The oscillatory studies with temperature ramps were performed either on a heating or cooling mode at a fixed rate of 1 °C/min. The storage (G') and loss (G'') moduli were recorded at a constant frequency (1 Hz) and stress (2 Pa). Flow curves were determined using the same equipment setup and a shear rate range of 1-100s^{-1}, keeping the temperature constant at 20 ℃. The effect of the amphiphilic additives on the shear viscosity of cellulose solutions in NaOH/H$_2$O is presented in figure 2.10.
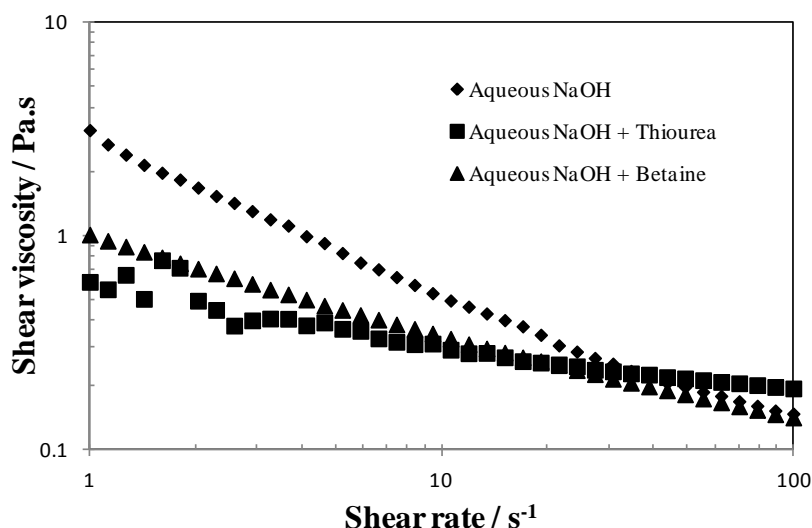
Figure 2.10: Flow curves of 5 wt.% microcrystalline cellulose in aqueous alkali solution, without additives and in the presence of additives (thiourea and surfactant).

Fourier Transform Infrared spectroscopy (FTIR)

Infrared spectroscopy is one of the most versatile techniques used in chemistry and certainly one of the most important analytical methods available. It is a versatile experimental technique and it is relatively easy to obtain reliable spectra from samples in virtually any state. Liquids, solutions, pastes, powders, films, fibers, gases and surfaces can all be examined with a judicious choice of the sampling technique. As a consequence of improved instrumentation, a variety of new sensitive techniques have now been developed in order to examine formerly intractable samples [132].

The FTIR technique is based on the vibrations of the atoms in a molecule. An infrared spectrum is commonly obtained by shining infrared radiation (wave number range from 400 to 4000 cm^{-1} [133]) through a sample and determining what fraction of the incident radiation is absorbed at a particular energy. The energy at which any peak in an absorption spectrum appears corresponds to the frequency of a vibration of a part of molecule. In order to produce a measurable absorption signal in infrared spectroscopy the vibrational mode must cause a change in the dipole moment of the molecule. The larger this change is, the more intense will be the absorption band [132].

Historically, dispersive instruments, available since the 1940s, were used to obtain infrared spectra. In recent decades, a very different method has replaced the dispersive instrument. Fourier-transform infrared spectrometers (FTIR) are now predominantly used and have dramatically improved the acquisition of infrared spectra [134].

| Source | Interferometer | Sample | Detector | Amplifier | Analog-to-digital converter | Computer |
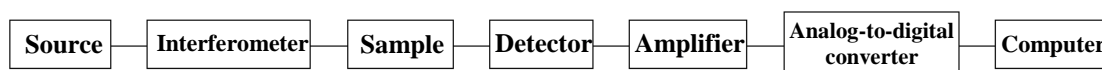
Figure 2.11: Basic components of a FTIR spectrometer (adapted from [134]).

The sample preparation is a crucial step in analytical chemistry. The traditional transmittance methods can be limited in terms of the analysis of some peculiar samples. Reflectance techniques may be used for samples that are difficult to analyse by the conventional transmittance methods. Attenuated total reflectance (ATR) spectroscopy utilizes the phenomenon of total internal reflection, in which a beam of radiation entering a crystal will undergo total internal reflection, when the angle of incidence at the interface between the sample and crystal is greater than the critical angle. The latter is a function of the refractive indices of the two surfaces. The beam penetrates a fraction

of a wavelength beyond the reflecting surface when a material, that selectively absorbs radiation, is in close contact with the reflecting surface. This technique has several advantages when compared with transmittance methods, such as the minimal sample preparation and the capability of the analysis of almost all types of samples. FTIR can be applied in the cellulose field in order to study the structure and arrangements of the cellulose molecules, estimate the degree of crystallinity, and also in investigations involving modifications of cellulose, such as after cellulose oxidation [135].

The segments in the cellulose polymer chain are expected to vibrate differently in well-ordered crystalline phases in comparison to less ordered amorphous phases and, therefore, it is possible to assign absorption bands to crystalline and amorphous regions and estimate a kind of crystallinity index (CrI) from FTIR. This is one of the simplest methods but one should keep in mind that the extracted values are not absolute. O'Connor et al. [135] established that the absorption band at around 1430 cm^{-1} is characteristic of crystalline areas in the polymer and the absorption band at 890 cm^{-1} typical of amorphous regions; the ratio of these two bands was established as a "crystallinity index", later referred to as the "lateral order index" (LOI). Later, Nelson and O'Connor [136] defined another crystalline parameter from the ratio of absorption bands at 1370 cm^{-1} and 2900 cm^{-1}, the so called "total crystallinity index" (TCI). The TCI is said to be proportional to the crystallinity degree of cellulose while LOI is correlated to the overall degree of order in cellulose [137, 138].

The infrared spectra were recorded at 25 °C with an ATR-FTIR spectrophotometer Thermo Nicolet, IR300 (USA), using an universal ATR sampling accessory. The FTIR spectral analysis was performed within the wave number range of 400-4000 cm^{-1}. A total of 256 scans run to collect each spectrum at a resolution of 1 cm^{-1} in the transmission mode. The CrI (also referred to as "lateral order index" - LOI) was estimated from the ratio between the absorption band at 1430 cm^{-1} and the absorption band at 890 cm^{-1} [135, 139]. Additionally, the "total crystallinity index" (TCI) was estimated from the ratio between the bands at 1370 cm^{-1} and 2900 cm^{-1} [136]. In figure 2.12 the obtained IR spectrum for microcrystalline cellulose is presented.
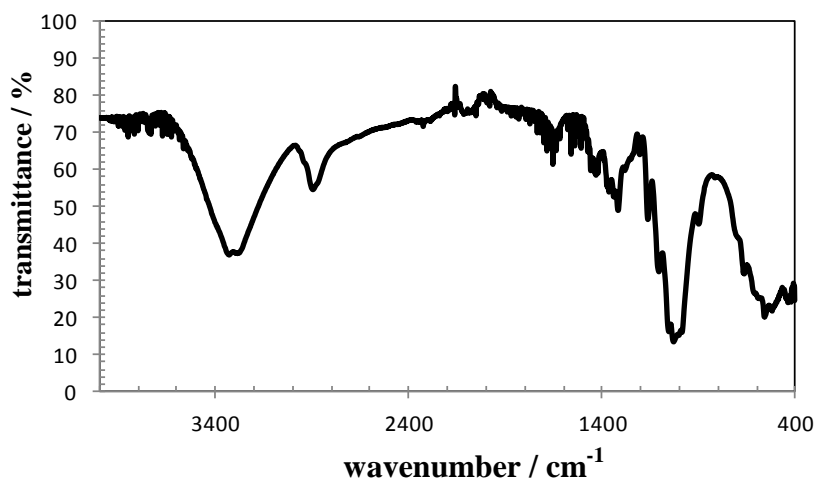
Figure 2.12: FTIR spectrum of native microcrystalline cellulose.

Nuclear Magnetic Resonance

One of the most important spectroscopic techniques for structure elucidation is nuclear magnetic resonance (NMR) spectroscopy. The physical foundation of NMR spectroscopy is based on the magnetic properties of the atomic nuclei. The interaction of the nuclear magnetic moments with an external magnetic field, B_0, leads, according to the rules of quantum mechanics, to different nuclear energy levels because the magnetic energy of the nucleus is restricted to certain discrete values, E_i, the so-called "*eigenvalues*". Associated with the eigenvalues are the "*eigenstates*", also called stationary states, which are the only states in which an elementary particle can exist. Through a radiofrequency (RF) transmitter, transitions between these states can be stimulated. The absorption of energy is then detected in an RF receiver and recorded as a spectral line, the so-called resonance signal (figure 2.13) [140]. In this way, a spectrum can be generated for a molecule containing atoms whose nuclei have non-zero magnetic moments. Among these nuclei are the proton, ^{1}H, the fluorine nucleus, ^{19}F, the nitrogen isotopes, ^{14}N and ^{15}N, and many others of chemical interest. The carbon nucleus, ^{12}C, which is extremely important in chemistry, has, like all other nuclei with even mass and even atomic number, no magnetic moment. Therefore, NMR studies with carbon are limited to the stable isotope ^{13}C, which has a natural abundance of only 1.1% [141].
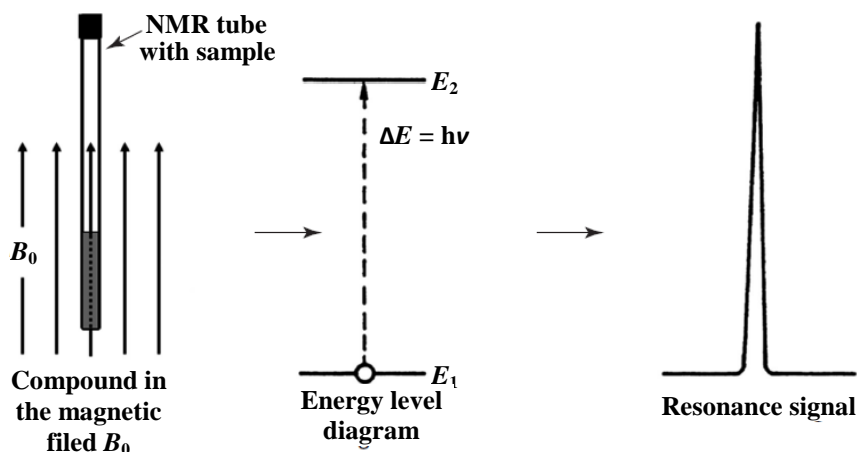
Figure 2.13: Generic formation of a NMR signal (adapted from [140]).

NMR studies are very useful in the cellulose field. They are applied, for example, in the determination of the cellulose polymorph type and to analyse the crystalline or non crystalline cellulose fractions [142, 143]. NMR can also be used as an alternative method to X-ray diffraction or as a complementary technique. Among the different NMR experimental techniques, the widely used ^{13}C NMR Cross-Polarization/Magic Angle Spinning (CP/MAS) is of valuable relevance for cellulose chemists [142, 143].

As alluded to this technique is an excellent tool for the determination of the structure and the crystallinity of solid samples. NMR has in its high-resolution and solid-state features been applied to both dissolved and solid cellulose. An innovative approach has been recently suggested for polarization transfer solid-state NMR (PT ssNMR) that combines features of both high resolution and solid-state NMR, thus enabling studies of all the constituent phases in complex materials with solid, liquid and liquid crystalline domains [144].

This new approach demonstrates potential for the detailed characterization of both the liquid and the solid phases in cellulose dissolution media. The PT ssNMR method gives information about molecular structure, conformation, and packing through the ^{13}C chemical shifts. It also provides information about molecular dynamics *via* the signal intensities obtained with the polarization transfer schemes CP (cross polarization) and INEPT (insensitive nuclei enhanced by polarization transfer).

^{1}H NMR measurements: ^{1}H NMR spectra were recorded at 25.0 (±0.1) ºC on a Varian 500 MHz spectrometer using a 5 mm NMR probe. Spectra were obtained with residual solvent (HOD) presaturation and the acquired parameters included 24 k data points covering a spectral width of 8 kHz, a radiofrequency excitation pulse of 45º and a scan

repetition time of 15 s to allow for full magnetic relaxation of proton nuclei. The resonance at 0 ppm due to the $Si-(CH_3)_3$ signal, from 3-(trimethylsilyl)propionic-2,2,3,3-d4 acid sodium salt (TSP) at tracer concentration (below 3 μM), was used as internal reference.

The method of continuous variation has been used to determine the stoichiometry of the β-cyclodextrin:tetrabutylammonium hydroxide (β-CD:TBAH) interaction; for that, samples were prepared by dissolving an amount of the solids in D_2O to achieve a concentration of β-CD and TBAH of 1.01 and 1.02 mM, respectively. The TBAH was previously lyophilized overnight just before using and the pH of D_2O was adjusted to 12.08 with the addition of NaOD, in order to keep the pH of β-CD:TBAH solutions constant.

The binding constant was computed by using experimental ^1H NMR chemical shifts of TBA^+ nuclei for mixed solutions with different $[\beta$-CD]/[TBAH] molar ratios, and keeping the [TBAH] constant and equal to 1.20 mM.

PT ssNMR measurements: The NMR spectra were recorded using a 4 mm HR-MAS rotor (Bruker, Germany) specifically designed for retaining liquids during magic angle spinning (MAS). NMR experiments were performed at 25 ºC on a Bruker AVII-500 spectrometer operating at ^1H and ^{13}C Larmor frequencies of 500 and 125 MHz, respectively, with a 4 mm $^{13}C/^{31}P/^1H$ E-free probe (Bruker, Germany). PT ssNMR data was recorded using 5 kHz magic angle spinning (MAS), 88 kHz two pulse phase modulation (TPPM) decoupling, 20 ms acquisition time, 300 ppm spectral width, and 80 kHz nutation frequency for 90º and 180º pulses. CP was performed with t_{CP} = 1 ms, 80 kHz ^{13}C nutation frequency, and linear ramp from 72 to 88 kHz ^1H nutation frequency. The time delays for refocused INEPT were τ = 1.8 ms and τ' = 1.2 ms. Each spectrum was recorded by accumulating 3072 transients with 5 s recycle delay, giving a measurement time of 12.5 h per sample. The time-domain data was zero-filled from 755 to 8192 complex points, Fourier transformed with 100 Hz line broadening, automatically phase corrected, and baseline corrected using customized Matlab scripts based on matNMR. In figure 2.14 the pulse sequences used are presented and in figure 2.15 the obtained spectrum for microcrystalline cellulose (solid) is depicted.
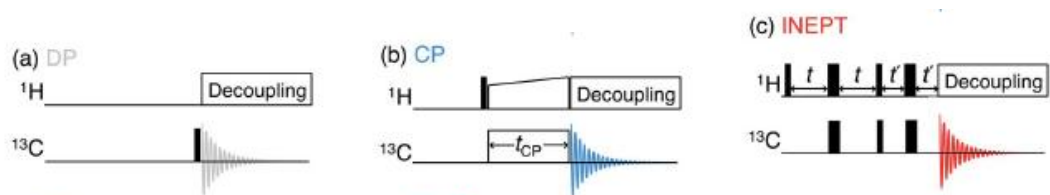
Figure 2.14: Polarization transfer solid-state NMR (PT ssNMR) pulse sequences (a–c) with detection of the ^{13}C signal under ^{1}H decoupling and magic-angle spinning (MAS). Direct polarization (DP) is using the thermal equilibrium polarization of ^{13}C, while CP and INEPT rely on polarization transfer from ^{1}H to ^{13}C. Narrow and broad vertical lines indicate 90º and 180º radiofrequency pulses [144].
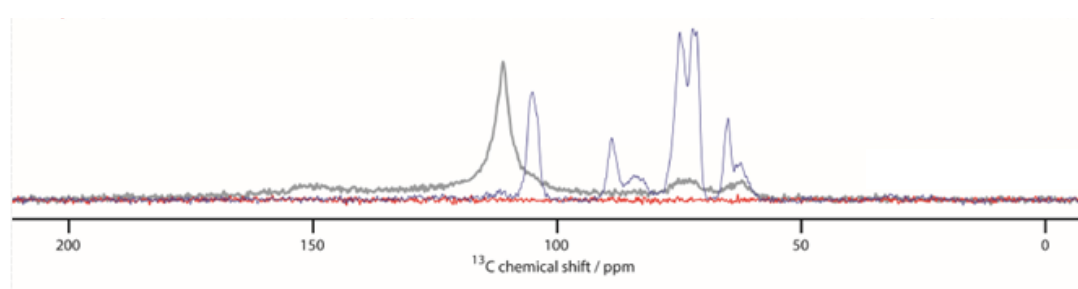
Figure 2.15: PT ssNMR spectrum for microcrystalline cellulose in the initial dry state.

Dynamic Light Scattering

Dynamic light scattering (DLS, also known as photon correlation spectroscopy, PCS, or quasi-elastic light scattering, QELS) is widely used as an effective technique for the estimation of the average particle size in colloidal suspensions, typically ranging from 2 nm to 2 μm [145, 146].

In a DLS experiment, a laser source provides the monochromatic incident light, which interacts with the small particles in solution, in Brownian motion. Then, through the Rayleigh scattering process, particles whose sizes are sufficiently small compared to the wavelength of the incident light will diffract the incident light in all directions with different wavelengths and intensities as a function of time. The larger the particle, the slower the Brownian motion will be. Since the scattering pattern of the light is highly correlated to the size distribution of the analyzed particles, the size-related information of the sample can be acquired by mathematically processing the spectral characteristics of the scattered light.

In this method, the diffusion coefficients of the scattering particles are firstly determined, and the average diameters are then calculated from these coefficients using the Stokes–Einstein relationship (equation 2.4), where $d(H)$ is the hydrodynamic diameter, k is the Boltzmann's constant, T is the absolute temperature, η is the viscosity and D is translational diffusion coefficient [147].

$$d(H) = \frac{kT}{3\pi\eta D} \tag{2.4}$$

The relation between the translational diffusion coefficient (or hydrodynamic radius) and the actual dimensions of non-spherical particles depends on the particle shape.

The size is obtained from the correlation function, which describes the decay of the intensity of the scattered light as a function of time, and contains the diffusion coefficient information required in the Stokes-Einstein equation. The diffusion coefficient is obtained by fitting the correlation function with a suitable algorithm, such as the cumulants analysis, which determines a mean size and polydispersity index (PI). In the case of polydisperse samples a different algorithm should be used such as the non-negatively constrained least squares (NNLS) or CONTIN to deconvolute the measured intensity autocorrelation function of the sample into a number of intensity values each associated with a discrete size band [148]. The size distribution can be extracted from the fluctuations in the data of the scattered light using cumulant expansion or other methods; the obtained results can be expressed using one of three kinds of distribution index, usually used in size analysis: number weighted distribution, volume weighted distribution, and intensity weighted distribution. In figure 2.16 the correlation function and the size distribution by intensity obtained for a sample of microcrystalline cellulose are presented.
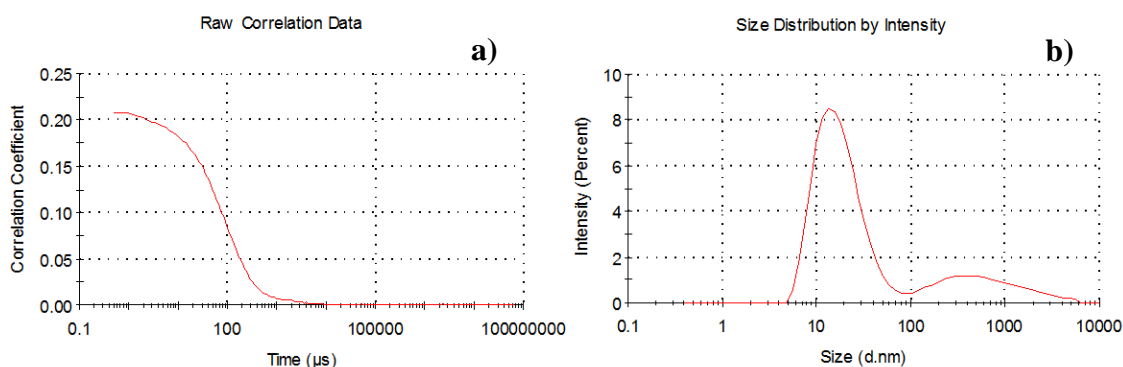
Figure 2.16: Correlogram and size distribution by intensity obtained for 0.5 wt.% microcrystalline cellulose in TBAH/H_2O system. Temperature was kept at 25 ºC.

CHAPTER 3

Results and discussion

3.1 - Cellulose derivatives: Crystallinity and solution state.

In theory, a successful polymer dissolution completely eliminates the supramolecular structure resulting in a clear solution where the polymer is molecularly dispersed. Experience with synthetic polymers reveals that these solutions are typically mostly fully dispersed down to the molecular level. This has led to the simplified conclusion that either a polymer is dissolved or not. However, this two-option rule does not always hold; intermediate stages between swelling and complete solubility exist and cellulose and its derivatives are clear examples of it [149].

In the majority of the cases, cellulose and its derivatives only rarely form molecularly dispersed solutions; cellulose is not dissolved down to a molecular level but rather forms stable colloidal dispersions where ordered cellulose aggregates are present (aggregation numbers between 10 to 800 have been estimated) [76].

On the other hand, cellulose derivatives are known as being highly soluble. This high solubility of cellulose derivatives is excellent for applications such as in food, pharmaceuticals or drug delivery [9]. In general, cellulose derivatives result from the non-homogeneous substitution of the hydroxyl groups in each anhydroglucose ring by other functional groups. Cellulose modification occurs first in the amorphous domains and later in the crystalline regions. Nevertheless, during this process, a large decrease in

the crystallinity of the substance is expected to occur [150]; this is one of the arguments to explain the high solubility of these derivatives. From such high solubility the formation of molecularly dispersed solutions can be anticipated; Kamide et al. reports that a cellulose derivative (CMC), with high degree of substitution, forms a gel-like solution while the residual small crystalline regions act as cross-linking points [150]. Therefore, at a first glance, one could argue that cellulose derivatives are not an obvious choice as a source of nanocrystals. To our knowledge, cellulose nanocrystals, CNCs, have never been extracted from cellulose derivatives and therefore we here report the initial results regarding their extraction and characterization. Scanning electron microscopy (SEM) and dynamic light scattering (DLS) were used to study the morphology while FTIR and X-ray diffraction were further used to infer about more detailed molecular information of the extracted CNCs.

Materials and methods

The materials and methods used are described in chapter 2.

Results

The chemical modification of cellulose includes activation of the polymer by dissolution in suitable solvents, conversion of the dissolved cellulose with reactive compounds, and control of the functionalization pattern by using protecting groups [151]. Suitable solvent systems, such as DMAc/LiCl or ionic liquids typically present a high cellulose dissolution efficiency, which consequently makes possible to achieve a high substitution degree, as well as a homogenous distribution of the substitutions. At the end of the derivatization process the obtained product is usually highly soluble in water or in other solvents.

The cellulose derivatives (commercial samples) used in the present work form clear solutions when dispersed in water. Thus, from a macroscopic point of view, cellulose is completely dissolved. However, looking into these samples using electronic microscopy (Cryo-SEM) it is possible to observe polymer aggregates, even at very low concentration, below the estimated overlap concentration (ca. 0.7 wt.% [152]). In figure 3.1 micrographs of cellulose derivatives in water are presented.
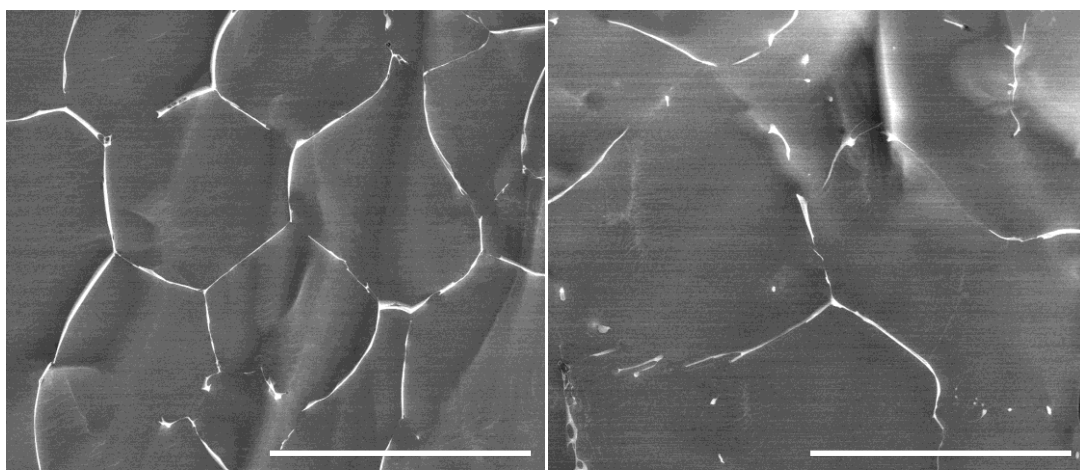
Figure 3.1: Cryo-SEM micrographs of 0.1 wt.% of carboxymethyl cellulose (CMC) (left) and hydroxypropyl methylcellulose (HPMC) (right). The scale bars represent 30 μm.

These micrographs show aggregates of cellulose in solution, which suggest that we do not have molecular dispersed solutions. Carboxymethyl cellulose sodium salt (NaCMC) aqueous solutions have been found to form molecular dispersed solutions in aqueous medium [152]. Moreover, it has been found that the degree of solubility is strictly dependent on the degree of substitution; a less substituted (more hydrophobic) NaCMC shows a larger fraction of aggregates. Xiquan et al. indicate that for degrees of substitution above 1, the obtained CMC solutions are molecularly dispersed [153]. On the other hand, for samples with a degree of substitution below 0.82 the presence of crystalline aggregates (cellulose II polymorph) in solution is reported.

In this section, the extraction and characterization of CNCs from two cellulose derivatives, CMC and HPMC is reported and for comparison purposes, microcrystalline cellulose was also used.

In figure 3.2 the micrographs of the three starting materials used are presented.
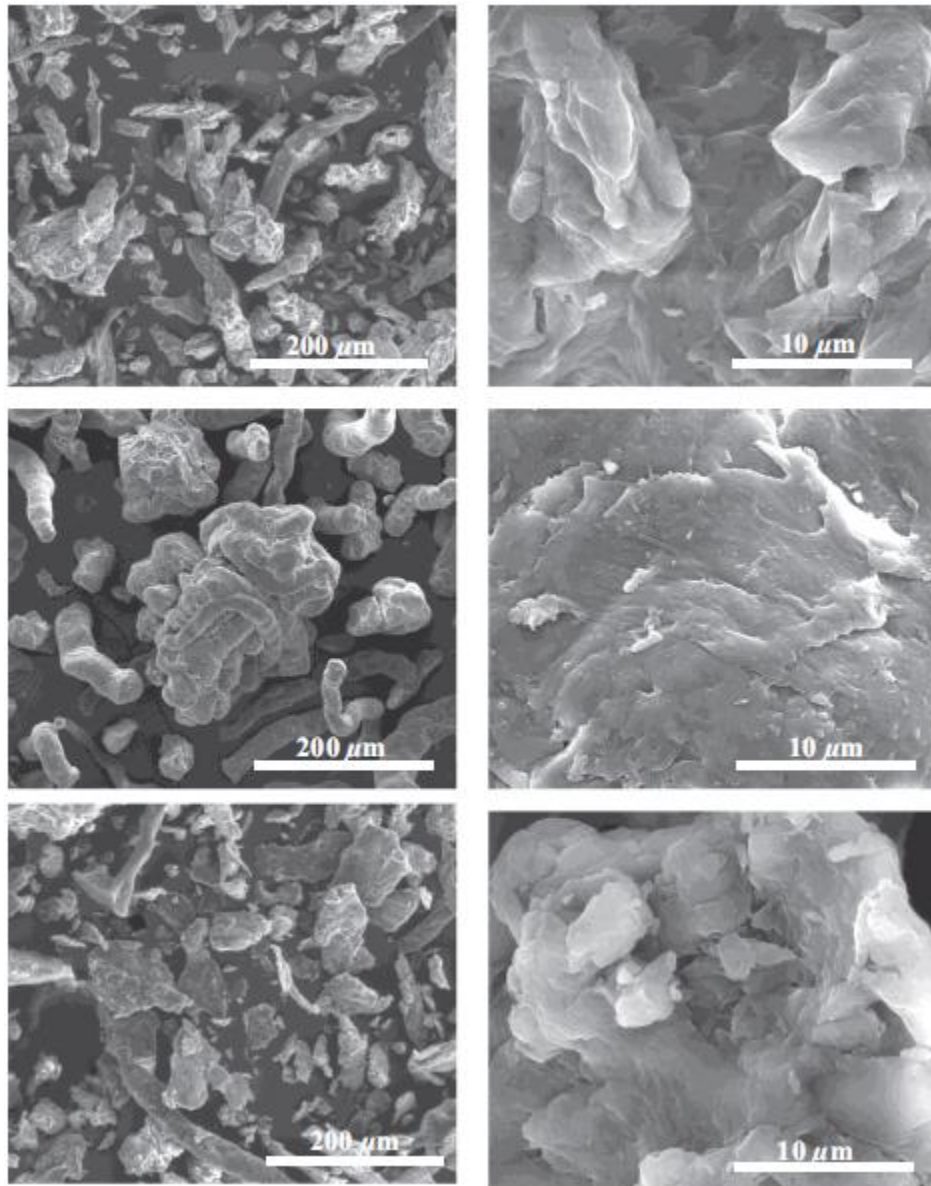
Figure 3.2: SEM micrographs of native celluloses used: MCC (top), CMC (middle) and HPMC (bottom) [154].

Coarse particles of different sizes are observed in all cases. Additionally, in the CMC case, soft elongated aggregates are also visible. When the dry powders are suspended in water, the crystalline cellulose sample (MCC) presents coarse particles with an average size around 50 μm, while the cellulose derivatives (for instance, HPMC) present particles with a smaller average size, i.e. between 2 and 5 μm (figure 3.3). The larger size of the MCC particles might also reflect some aggregation due to the lower solubility in water. On the other hand, the cellulose derivatives are water-soluble and, therefore, individual particles are expected to disperse more efficiently in the solvent.
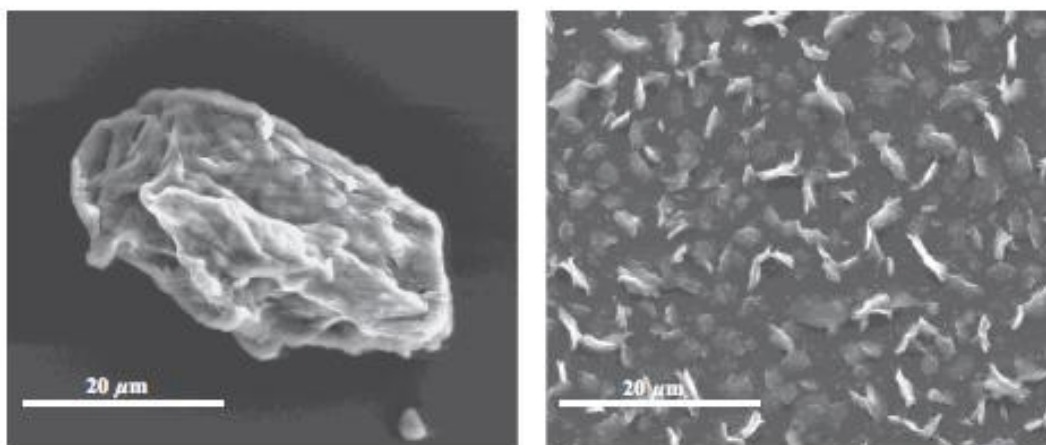
Figure 3.3: SEM micrographs of MCC (left) and HPMC (right). In both cases, 0.1% cellulose was dispersed in water [154].

The SEM micrographs of the cellulose nanocrystals (CNCs) suspensions extracted from the cellulose derivatives CMC and HPMC are shown in figure 3.4 (panels c, d and panels e, f, respectively). For comparison, micrographs of the CNCs from the MCC sample are shown on the top of figure 3.4 (panels a and b). The CNCs from MCC (figure 3.4, a and b) are wider (ca. 200-300 nm) and longer (ca. 1 μm) than the CNCs from the cellulose derivatives: CMC (figure 3.4, c and d) shows individual crystallites which are approximately 50-100 nm wide and 300-600 nm long while the crystallites from HPMC (figure 3.4, e and f) are approximately 50-100 nm wide and 300-400 nm long. In both systems, a small fraction of larger needle-like crystals can also be observed. One should mention that the dimensions estimated by SEM are significantly bigger than those obtained from AFM for the CNCs extracted from MCC [155]. Among other possible reasons, this might suggest self association of rods along a single axial direction already in the solution state, or during specimen preparation for SEM. Additionally, the mechanical treatment provided to disperse CNCs as a uniform stable suspension might not be enough to separate all CNCs rods as individual entities and thus the size is consequently overestimated.
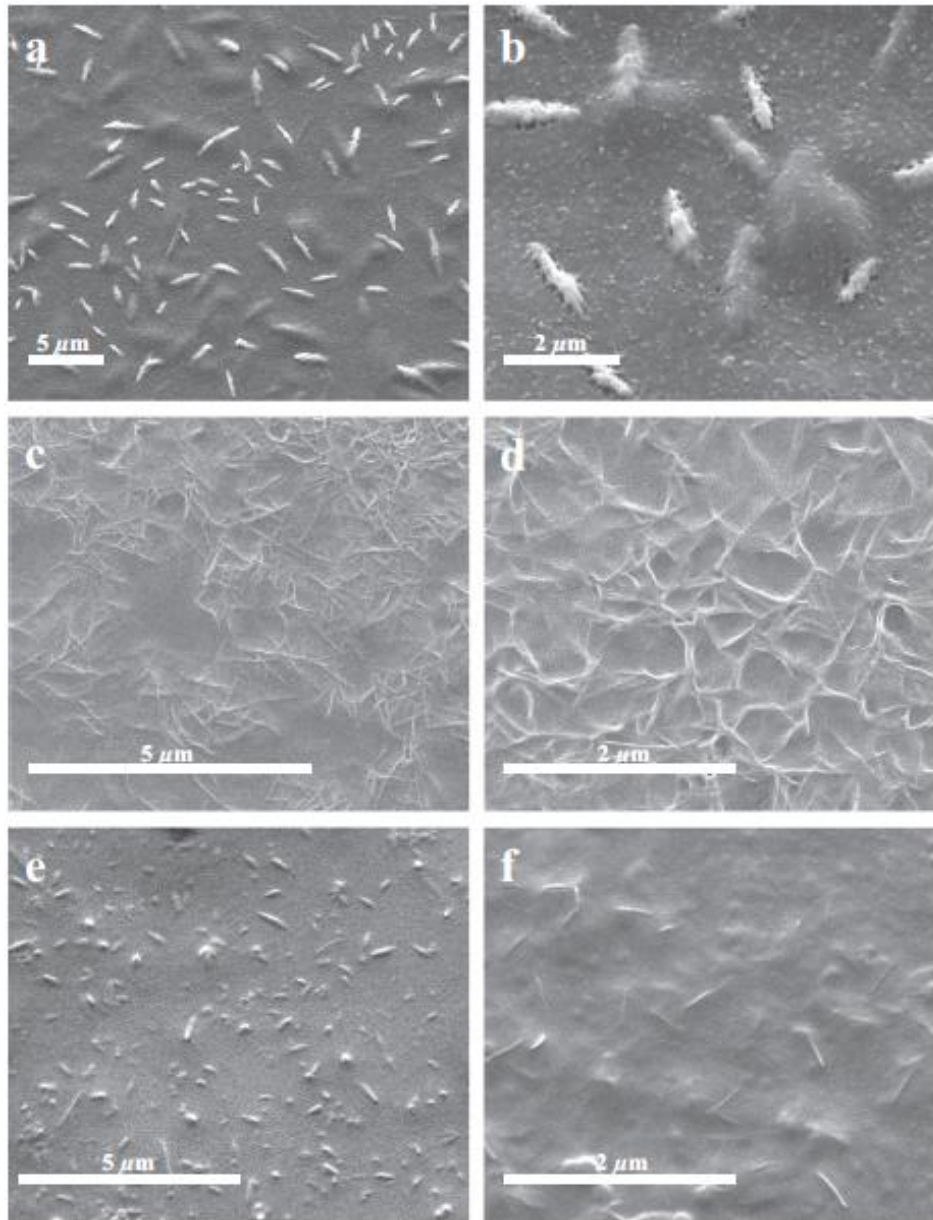
Figure 3.4: SEM micrographs of CNCs extracted from MCC (a and b), CMC (c and d) and HPMC (e and f) [154].

The size of the CNC particles was also estimated from photon correlation spectroscopy (PCS). Since PCS is a light-scattering method, the measured CNC particle size values are the z-average (intensity mean) hydrodynamic diameters of equivalent spheres and do not represent the actual physical dimensions of the rod-like CNC particles. However, the extracted values are valid for comparison purposes. In table 3.1 some structural parameters derived from the different techniques used are represented.

Table 3.1: Characteristics (i.e. dimensions, zeta potential and CrI) of CNCs extracted from HPMC, CMC and MCC.

| | L, Length (nm) | | Average width (d) (nm)[a] | Average Aspect ratio (L/d) | Zeta potential (mV) | Crystallinity | | |
| | SEM | DLS | | | | FTIR | | X-ray[d] (%) |
						LOI[b]	TCI[c]	
CNC$_{HPMC}$	300-400	260	50-100	3-8	-8.6	1.19 (0.53)	1.47 (0.95)	53 (81)
CNC$_{MCC}$	1000	820	100-300	3.3-10	-51.5	0.73 (0.70)	0.95 (0.87)	77 (75)
CNC$_{CMC}$	300-600	218	50-100	3-6	-33.2	1.29 (0.98)	1.34 (0.77)	59 (57)

[a] estimated from the SEM micrographs.
[b] "Lateral Order Index" (LOI) estimated from the ratio between the vibration band at 1430 cm^{-1} and the band at 890 cm^{-1} ([156])
[c] "Total Crystallinity Index" (TCI) estimated from the ratio of absorption bands at 1372 cm^{-1} and 2900 cm^{-1} ([157]).
[d] "Crystallinity index" estimated from the method suggested by Segal et al., equation 2.1 ([123]).

The first observation is that, not surprisingly, the average size estimated from PCS is smaller than the size estimated from SEM. More importantly, and in agreement with the SEM analysis, the average particle size of the CNCs extracted from HPMC and CMC is considerably smaller than the one from MCC. Another useful information is the aspect ratio (defined as the length-to-diameter, L/d) which is an important factor and a controlling parameter for the mechanical properties of nano-composites [155]. Typically, CNCs with a high aspect ratio tend to give the best reinforcing effect [158] and this parameter depends on the original cellulose characteristics and extraction conditions (i.e. temperature, acid concentration, time, etc.). Here, the L/d values found were very similar (L/d ∼ 3–10) and in agreement with previous reports for Avicel whiskers [158]. An additional important characteristic of CNCs, when prepared in sulfuric acid, is that the particles possess negatively charged surfaces coming from the esterification of hydroxyl groups by sulfate ions. This process is expected to enhance CNC colloidal stability in aqueous solutions due to the electrostatic repulsion among the charged particles. The determined zeta-potential is presented in table 3.1. Essentially, the zeta-potential measures the mobility of a distribution of charged particles as they are subjected to an electric field. The CNCs extracted from the MCC show an average zeta potential of -51.5 mV. On the other hand, the CNCs extracted from cellulose derivatives, HPMC and CMC, present an average zeta potential of -8.6 mV and -33.2 mV, respectively. The less negative zeta potential of the former might be important for biocompatibility issues, however the colloidal stability of the samples is poorer and flocculation is frequently observed. This lower absolute value of the zeta potential can be rationalized as follows: when the amorphous regions of the HPMC are hydrolyzed,

the remaining crystallites are expected to preserve their structure. It is reasonable to assume that the isolated crystals possess hydroxypropyl and methyl modifications from the original HPMC and, therefore, are less susceptible for esterification when compared with the hydroxyl groups in CNCs derived from MCC (i.e. the ether modifications are more stable in acidic media than the hydroxyls, which can be readily esterified). Thus, a higher surface charge is anticipated for the CNCs extracted from MCC while a much lower charge density is expected for the CNCs from HPMC. The same is valid for the CNCs derived from CMC with the difference that in this case even if no etherification occurs the crystallites possess already charged carboxylate groups and, therefore, the zeta potential of the CMC nanocrystals is found in-between the zeta-potentials of HPMC and MCC.

Figure 3.5 shows the FTIR spectra of native celluloses as well as of extracted CNCs. Both native cellulose and extracted CNCs are found to be very similar with only slight differences, mainly regarding intensity. In all cases, the characteristic bands can be identified [137, 138]; the broad absorption in the range of 3100–3600 cm^{-1} can be ascribed to the stretching of the –OH groups (with typical sharpening at 3400 cm^{-1}) [159-161] while the peak at 2900 cm^{-1} appears due to C-H stretching [159, 161]. An intense band between 1600 and 1650 cm^{-1} originates from the absorbed moisture (i.e. bending mode of water absorbed to cellulose) [162]. The deformation, wagging and twisting modes of anhydroglucopyranose vibration are shown from 600 to 1800 cm^{-1}. More specifically, the absorbance at around 900 cm^{-1} can be assigned to the C-H deformation mode of the glycosidic linkage between the glucose units [163, 164], while the absorbance bands between 1000 cm^{-1} and 1200 cm^{-1} are attributed mainly to the C-O stretching in major ether bands [164]. We note that the changes observed in the zeta potential measurements are not clearly evident in the FTIR analysis mainly due to the fact that some of the expected vibrational bands from the esterification are masked by other major bands (i.e. the vibrational modes of C-H and O-H superimpose and dominate the spectra). Nevertheless, in some cases, we can see in the extracted crystal signs of these vibration bands such as in figure 3.5 (top spectrum of CNCs from MCC shows a small peak at around 833 cm^{-1} which can be assigned to the S-O stretching) or the signal from the CNCs from the HPMC where a band at around 1250 cm^{-1} can be assigned to the C-O-S stretching mode.
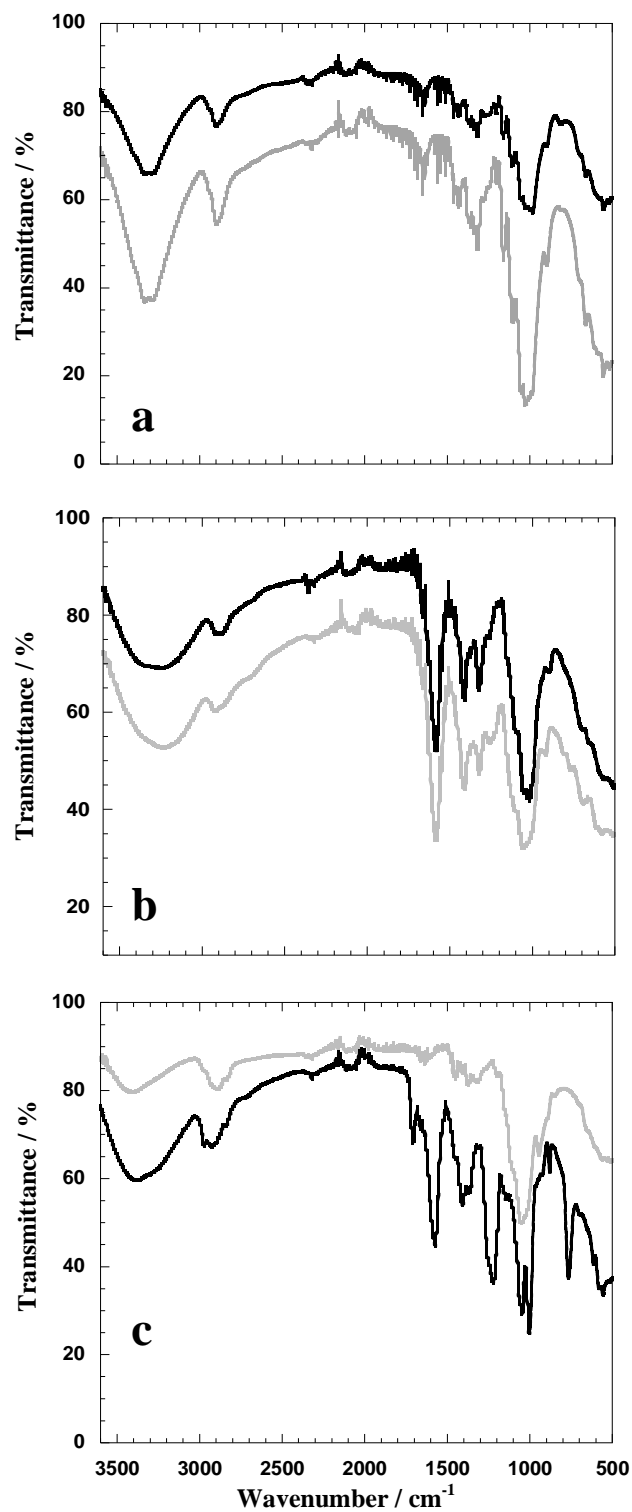
Figure 3.5: FTIR spectra of a) MCC (gray line) and extracted CNC_{MCC} (black line), b) CMC (gray line) and extracted CNC_{CMC} (black line) and c) HPMC (gray line) and extracted CNC_{HPMC} (black line) [154].

As described in chapter 2, it is possible to estimate a crystallinity index (CrI) from FTIR. In table 3.1, both TCI and LOI are presented. The numbers inside the parentheses represent the indices for the initial cellulose (MCC, CMC and HPMC). Regardless of the method of calculation, the CrI estimated from FTIR always increases for the CNCs. This is somehow expected since during the extraction and purification procedure the amorphous areas are likely removed and thus the crystallinity increases. Another important observation is that the native cellulose derivatives, CMC and HPMC, are already quite crystalline and the CNCs extracted from them present both TCI and LOI indices higher than the ones corresponding to the CNCs extracted from MCC.

This high crystallinity of the cellulose derivatives is not trivial to understand. Modifications are expected to affect adversely the good packing of cellulose chains in crystals (i.e. decrease the crystallinity and enhance solubility). This is why essentially any modification done on cellulose tends to make it more soluble in water; apart from HPMC and CMC, other notable examples are, for instance, methyl cellulose (MC) and hydroxyethylcellulose (HEC).

The former is highly soluble in water, even if from a polarity point of view it would be expected to be less soluble. In the latter case, also highly soluble, substitution would not change the number of hydrogen bonds (typical argument used to explain cellulose insolubility in water) compared to unmodified cellulose. Therefore, it is somehow surprising that the (water soluble) cellulose derivatives studied here present such a significant initial crystallinity. Although relevant, the data suggests that crystallinity is indeed not the critical parameter for cellulose solubility.

The X-ray diffraction patterns of cellulose starting materials and extracted CNCs are represented in figure 3.6. In line with the FTIR measurements, the first important observation is that, despite HPMC and CMC being modified polymers, it is clear that both are significantly crystalline in nature as can be inferred from the diffraction peaks.
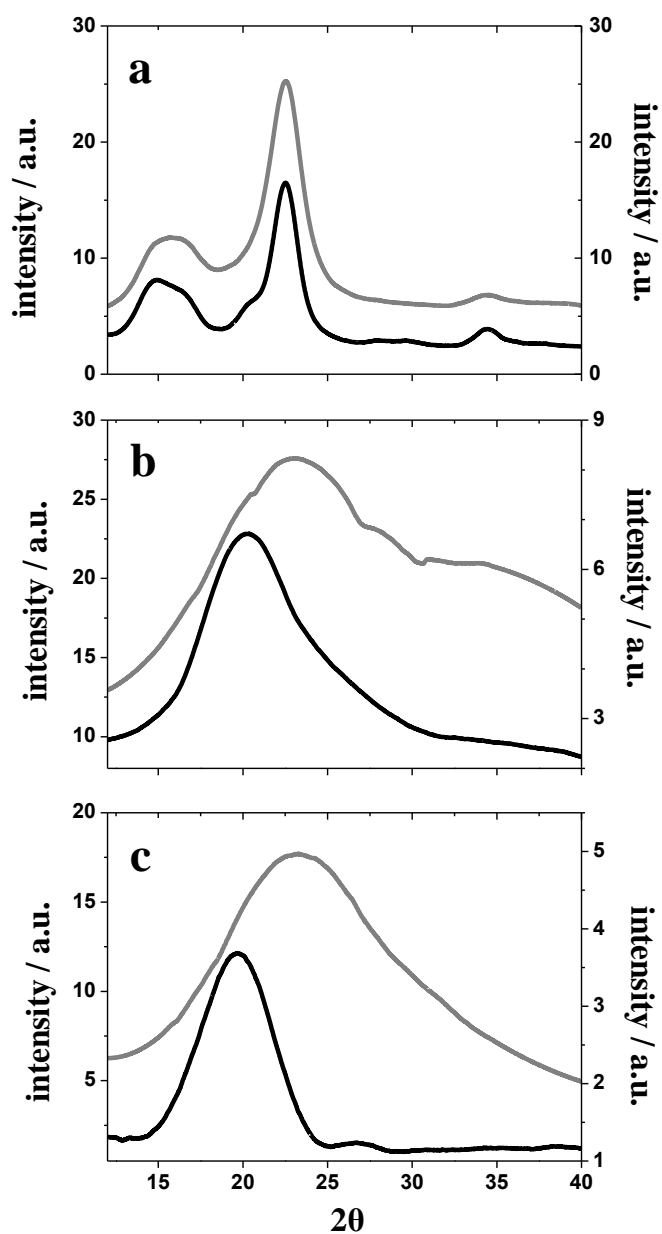
Figure 3.6: XRD diffraction patterns: smoothed raw data of a) MCC (black line) and extracted CNC_{MCC} (gray line), b) CMC (black line) and extracted CNC_{CMC} (gray line) and c) HPMC (black line) and extracted CNC_{HPMC} (gray line) [154].

While this is expected for the MCC, it is more striking for the cellulose derivatives CMC and HPMC. As one can see, the diffraction pattern of MCC is characterized by a major peak centered around 22.5° (002) with a side peak at 20.5° (021) typical for a cellulose I crystalline polymorph [165]. Other characteristic reflections for a cellulose I type structure can be found at 14.7° (101), 16.6° (101) and 34.7° (040). The extracted CNCs have the same diffraction pattern as the native MCC. The synthesis of the cellulose derivatives changes the crystalline structure to a cellulose II type polymorph,

where a diffraction pattern with a unique peak centered around 20.1° (101) can be observed for both CMC and HPMC. On the other hand, the CNCs extracted from the cellulose derivatives also show a single peak but centered around 22.5° (002) which, as previously discussed, can be attributed to a crystal structure of cellulose I type. Despite the fact that in XRD, intensity depends on several instrumental/sample conditions, such as sample mass/size and sample placement, so that intensity usually cannot be used to extract direct information through comparisons with other samples, we note that the diffraction intensities for CNCs from cellulose derivatives are considerably lower when compared with the native celluloses. This might mean that although the original material has a preferential cellulose II organization (due to the chemical synthesis), a small fraction of cellulose I is still present (but masked by the dominating cellulose II organization) and could be isolated in the CNCs. The degree of crystallinity was estimated following the method suggest by Segal et al. [123] and included in table 3.1. In qualitative agreement with the FTIR analysis, one can observe that the native cellulose derivatives are highly crystalline (the estimated CrI is in all cases above 50%) and the extracted CNCs, with exception of the HPMC case, show a higher CrI value than the original cellulose derivatives.

Synopsis

A successful extraction and characterization of CNCs from the cellulose derivatives CMC and HPMC is reported. Surprisingly, the cellulose derivatives were found to be significantly crystalline indicating an unusual extraction of CNCs. The average size of the CNCs extracted from HPMC and CMC was found to be smaller (and with lower zeta potential) than the ones extracted from microcrystalline cellulose (MCC). The estimated crystallinity indices show that the extracted material is more crystalline than the native one. However, while the MCC and CNCs share the same crystalline organization (cellulose I polymorph), the cellulose derivatives (starting materials) were found to be of cellulose II type. The extracted CNCs from the cellulose derivatives show a crystalline organization of cellulose I type, which probably indicates that the starting material has a small fraction of cellulose I (masked in the diffraction spectra by the main cellulose II diffraction pattern), which is the one isolated after dissolution in the acidic media and purification. In literature is described the obtainment of aggregated crystalline domains by X-ray diffraction in aqueous solution, for NaCMC derivative,

with degree of substitution (D.S.) below 1.06. No crystallinity was found for D.S. 1.06 [153]. These aggregates are assumed to be cellulose type II, contrary to the result obtained in the present work, keeping in mind that once dissolved, cellulose does not reorganize in a cellulose type I polymorph. Our data suggests that there are specific parts of cellulose chains that remain insoluble during all the modification process. The huge challenge of getting molecularly dispersed solutions will be discussed in the next sections.

3.2 - Polarization transfer solid-state NMR: A new method for studying cellulose dissolution

Several cellulose end-products such as fibers and films, typically involve pre-dissolution steps in solvents with toxic components such as carbon disulfide or copper ions. Therefore dissolution of cellulose in aqueous media is, for economical and environmental reasons, strongly preferred. Current aqueous dissolution media include NaOH based systems [166], with or without other additives such urea or thiourea [49, 50], or tetraalkylammonium salts [167].

Not only the mechanisms governing cellulose dissolution are still in debate but also the characterization of the dissolved state is still lacking. The development of facile and accurate techniques capable to provide a clear understanding on the level of dissolution and molecular organization of cellulose is obviously desired.

Solid, dissolved, and regenerated cellulose are usually separately investigated with a wide range of experimental techniques: infrared spectroscopy [137], fiber and powder X-ray diffraction [168, 169], transmission and scanning electron microscopy [109, 170], and neutron fiber diffraction [171] among others. Among the wide spectrum of techniques applied to cellulose research, mainly cryo-TEM and small angle X-ray scattering (SAXS) are recently introduced to study cellulose in solution [77]. Although all the techniques give useful information about particular aspects of the starting material or the final product, molecular-level information about both the dissolved and the solid polymer in the dissolution medium is still lacking.

High-resolution nuclear magnetic resonance (NMR) [172] and solid-state NMR [173] have been applied to both dissolved [174, 175] and solid [142, 176] cellulose. Recently Topgaard et al. suggested an experimental approach based on a new developed NMR methodology [177] that combines features of both high resolution and solid-state NMR, thus enabling studies of all the constituent phases in complex materials with solid, liquid, and liquid crystalline domains. The method has been applied to hydrated surfactants [177, 178], lipid biomembranes [179], lipid-amyloid fibril aggregates [180], and intact stratum corneum [181], all of which contain amphiphilic molecules in a wide range of physical states. In this section the potential of PT ssNMR for detailed characterization of both the liquid and the solid phases in cellulose dissolution media is discussed.

The CP and INEPT techniques are traditionally used to boost the signals for solids and liquids, respectively, in comparison to the ^{13}C direct polarization (DP). The ^{13}C signal is acquired under magic-angle spinning (MAS) and high power ^{1}H decoupling [182], giving spectra with reasonably high resolution for both liquids and solids.

Materials and methods

The materials and methods used are described in chapter 2.

Results

The preliminary experimental PT ssNMR results obtained for cellulose are displayed in figure 3.8 and the ^{13}C chemical shifts of the peaks assigned to cellulose are compiled in table 3.2. The blue and red colors, attributed to CP and INEPT spectra, respectively, are shown to give an intuitive visual impression of which peaks originate from segments with slow (CP) or fast (INEPT) molecular dynamics (see figure 3.7). As a reference, the DP spectra are shown in gray. The dry cellulose gives intense CP peaks while the INEPT signal is absent, which is consistent with cellulose being in a solid state.
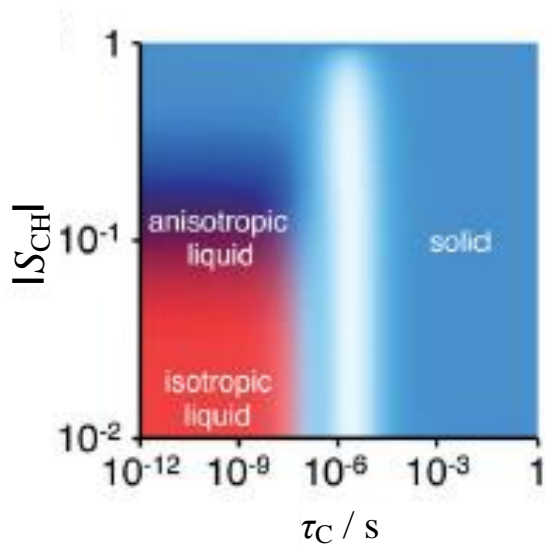
Figure 3.7: Theoretical CP (blue) and INEPT (red) signal enhancement vs. the CH-bond orientational order parameter S_{CH} and reorientational correlation time τ_C. The enhancement factor was calculated for a tertiary carbon atom as described in Nowacka et al. [178] using the experimental parameters of the current study, which were selected to, with least possible ambiguity, discriminate between isotropic liquids (only INEPT), anisotropic liquids (both INEPT and CP), and solids (only CP) according to the labeled areas in panel. White indicates lack of signal for both CP and INEPT [144].
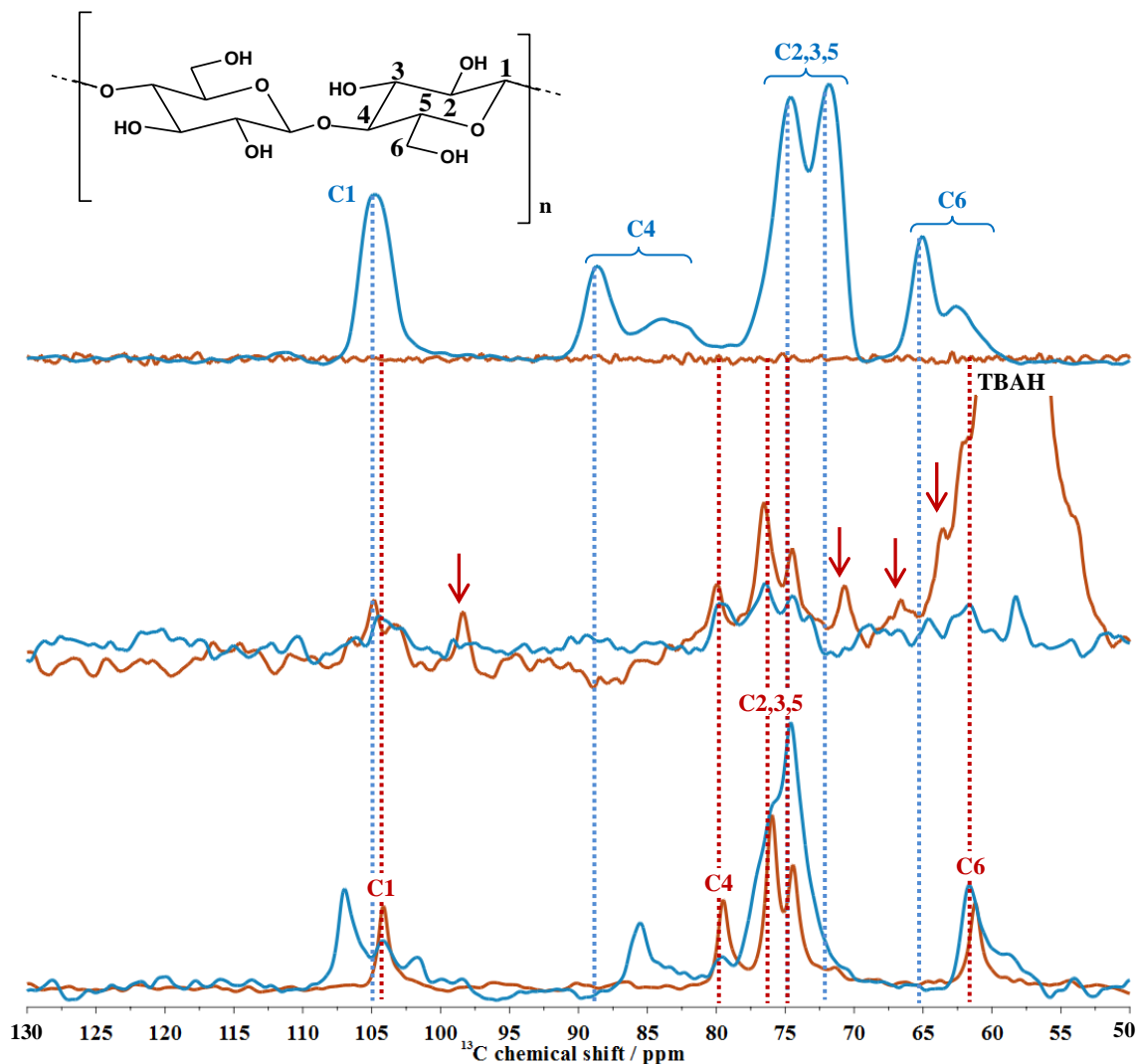
Figure 3.8: PT ssNMR data for microcrystalline cellulose in the initial dry state (top), as well as 10 wt.% cellulose dissolved in aqueous TBAH (middle) and in NaOH aqueous (bottom). CP and INEPT spectra are shown in blue and red, respectively. The assignments of the solid (blue) and dissolved (red) cellulose peaks refer to the carbon atom numbering in the structural formula. The blue and red dashed lines represent literature data for cellulose I in wood pulp fibers [142] and dissolved cellulose [174], respectively. The labels TBAH point out the truncated peaks from the TBA$^+$ ions, while the arrows indicate TBA$^+$ breakdown products. The data was acquired at 25 ºC and 125 MHz ^{13}C Larmor frequency with 5 kHz MAS and 88 kHz TPPM ^{1}H decoupling. The spectra are zoomed-in on the 50-130 ppm spectral region relevant for cellulose, and, independently for each sample, magnified to facilitate observation of the cellulose resonance lines [183].

The obtained spectrum for microcrystalline cellulose (starting material) is in good agreement with the one reported in literature for cellulose I [184, 185]. The chemical shift values obtained for dry cellulose (see table 3.2) are very similar to those reported by Kamide et al. [105.40 (C_1), 89.10 (C_4), 75.30/72.70 ($C_{2,3,5}$) and 65.50 (C_6)] [142] for wood pulp. The side peaks at ca. 85.0 ppm and 62.0 ppm can be assigned to the amorphous residual fraction present in the dry microcrystalline cellulose [186].

Table 3.2: Chemical shifts of partially dissolved cellulose[a] [183].

Sample	Fraction	Carbon atom				Polymorph
		C_1	C_4	$C_{2,3,5}$	C_6	
Dry	Solid	105.10	88.80	74.60, 72.10	65.00	Cellulose I
TBAH	Solid	105.10	88.70	74.40, 71.50	65.10	Cellulose I
aqueous	Dissolved	104.70	79.80	76.40, 74.50	61.70	
NaOH	Solid	107.10	85.60	75.80, 74.60	61.50	Na-Cell Q
aqueous	Dissolved	104.30	79.60	76.00, 74.50	61.30	

[a]Shifts are given in ppm with α-glycine at 176.03 ppm as external standard. The precision is limited to ±0.2 ppm by the acquisition time.

The sample containing cellulose dissolved in aqueous TBAH gives both CP and INEPT signals, showing that solid as well as liquid/dissolved material are present in the sample. The chemical shifts obtained for the solid fraction (CP signal) of the sample in aqueous TBAH and the initial dry cellulose are very similar, indicating that the residual undissolved material has an organization characteristic of cellulose I. The INEPT spectrum comprises a wide number of peaks, mainly from the inequivalent carbons of the tetrabutylammonium ion. Only one of these peaks is located inside the spectral window showed in figure 3.8. The remaining peaks can be assigned to dissolved cellulose, as well to degradation products of TBA[+], formed by Hofmann elimination, namely the tributylamine and 1-butene [187].

The peaks derived from degradation products of TBA[+] are indicated by the red arrows. Comparing the areas of the DP peaks from dissolved cellulose, TBA[+], and tributylamine it is possible to estimate the fraction of TBA[+] breakdown (ca. 4.9%), while the molar ratio between the tributylamine and the glucose units of the dissolved cellulose is approximately 1:9. The chemical shifts assigned to dissolved cellulose in the TBAH aqueous solution are very similar to the literature data for ultra-centrifuged samples of cellulose dissolved in 10 wt.% NaOH in D_2O: 104.7 (C_1), 79.9 (C_4), 76.4/75.0 ($C_{2,3,5}$), and 61.9 (C_6) ppm [174]. According to the theoretical calculations [144], the presence of INEPT peaks for cellulose implies that the C-H bonds reorient on a timescale faster

than 100 ns, which in turns is a strong indication that the "liquid fraction" of the cellulose solution is molecularly dissolved.

The NaOH aqueous solution also gives both CP and INEPT signals. While the INEPT peaks are similar to the ones assigned to dissolved cellulose in the aqueous TBAH sample, the CP peaks are noticeably different. Their comparison with the chemical shifts found in literature, [e.g. 106.9/104.2 (C_1), 85.5/83.0 (C_4) and 61.3 (C_6)] suggests that cellulose is organized in the so called "Na-cellulose Q", which is a highly swelled form of cellulose first identified by Sobue et al. [188]. This swelled state of cellulose is also characterized by a low order, which can be deduced from the chemical shifts of C_4, (85.52 ppm), and C_6 (61.65 ppm) [186]. Considering the suggested importance of hydrophobic interactions in cellulose systems [189], the effects of such unintentional hydrophobic or amphiphilic co-solutes (TBAH is an example) must be taken into account in any attempt of rationalizing the observed cellulose solubility.

Even if neither CP nor INEPT yields truly quantitative information, the comparison between their areas gives, at least, a rough estimative of the ratio solid/dissolved. Thus, the growth of one peak at the expense of the other is an indication that the ratio is changing. Additionally, the comparison between the DP, CP, and INEPT intensities gives qualitative information on the molecular dynamics [178]. Changes in properties such as molecular conformation and interactions with surrounding molecules and ions in the solution can be followed through the observation of the chemical shifts. Another potential of the method is the possibility to detect the presence of minor amounts of dissolved impurities, in the DP and INEPT spectra. In the case of aqueous TBAH, the impurities result from the chemical degradation of the major components, and are thus difficult to avoid.

Synopsis

These preliminary results show that both the solid and the dissolved cellulose components can be detected with PT ssNMR. This method reveals to be an excellent tool to study, in one single step, the arrangement of the solid fraction (undissolved material) as well as the dissolved fraction and the possible interaction of different additives with cellulose chains. These results are very useful for future studies on the mechanisms of cellulose dissolution.

Based on these promising results, additional studies were performed (using alkali based and acid based solvent systems). The obtained results for PT ssNMR were complemented with light and electronic microscopy and presented in sections 3.3 and 3.4.

3.3 - Cellulose dissolution in alkali medium

Since cellulose is not meltable, typically it has to be dissolved first in a suitable solvent before further processing. However, most of the common solvents usually fail in this respect. Through the years, several suitable solvents for cellulose dissolution have been developed and the list provides a wide variety of quite unusual options: from simple or multi-component mixtures, aqueous and organic media, to inorganic and organic salts, with peculiar experimental conditions (e.g. high and low temperatures, high and low pH), etc. [17, 20].

In this section we pay attention to solvent systems with a high hydroxide concentration. Cellulose dissolution at extreme pHs can be related to the fact that cellulose molecules acquire net charges either by protonation (low pH) or deprotonation (high pH). This observation is based on the general finding that polyelectrolytes are more soluble in water than nonionic polymers, due to the dissociation of counterions and the concomitant large gain in counterion entropy. Whereas the fact that a high concentration of hydroxide ions facilitates dissolution is rather trivial, the role and nature of the cation needs further considerations. Here we are interested in the question whether there are differences between hydroxides with different cations, particularly between inorganic and organic cations. Thus, by means of scanning electron microscopy (SEM), polarized light microscopy (PLM), polarization transfer solid state NMR (PT ssNMR) and dynamic light scattering (DLS) the effect of distinct solvents, i.e. cold NaOH solutions and aqueous solution of tetrabutylammonium hydroxide on the degree of dissolution of cellulose samples was studied. Additionally, the effect of different additives on the cold NaOH system was evaluated.

Materials and methods

The materials and methods used are described in chapter 2.

Results

The dissolution of cellulose in water is not feasible; when mixed with this solvent a cloudy dispersion is formed, which phase separates after a certain time as figure 3.9a) illustrates.
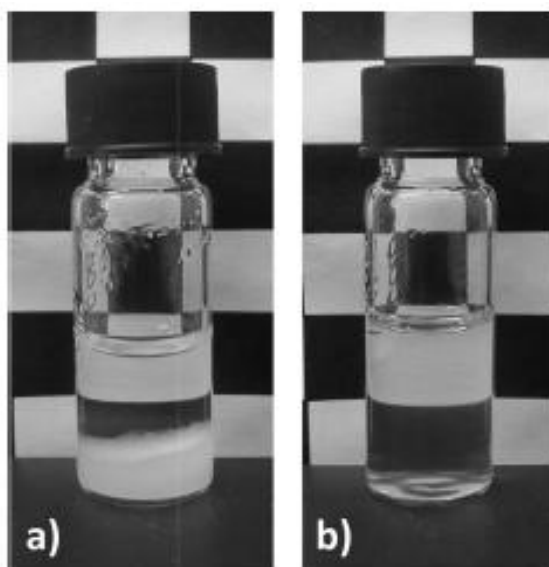
Figure 3.9: Cellulose dissolution: water (a) and 8 wt.% NaOH/H_2O solvent (b). Macroscopically, the 1 wt.% cellulose dissolved in the 40 wt.% TBAH/H2O system looks the same as the sample dissolved in the cold alkali system [190].

In figure 3.9b) 1 wt.% cellulose is dissolved in a 8 wt.% (2.00 M) NaOH aqueous solution. The same successful dissolution is found for a 40 wt.% (1.54 M) aqueous solution of TBAH.

A simple naked-eye inspection reveals a clear and transparent one-phase solution in both cases; the polarized light microscopy pictures in figure 3.10 reveal that the initial cellulose fibers, rich in birefringent domains, are significantly reduced in both solvents. In the cold alkali, it is still possible to see a few cellulose disks and fragments while in the TBAH solution the PLM micrograph shows no signs of undissolved material.

For several practical applications, such as the formation of films and fiber spinning, these solutions are quite acceptable. However, even if from a macroscopic and

microscopic point of view, cellulose seems reasonably dissolved, there are already a few indications that the state of the solutions must be different for the two solvents used.
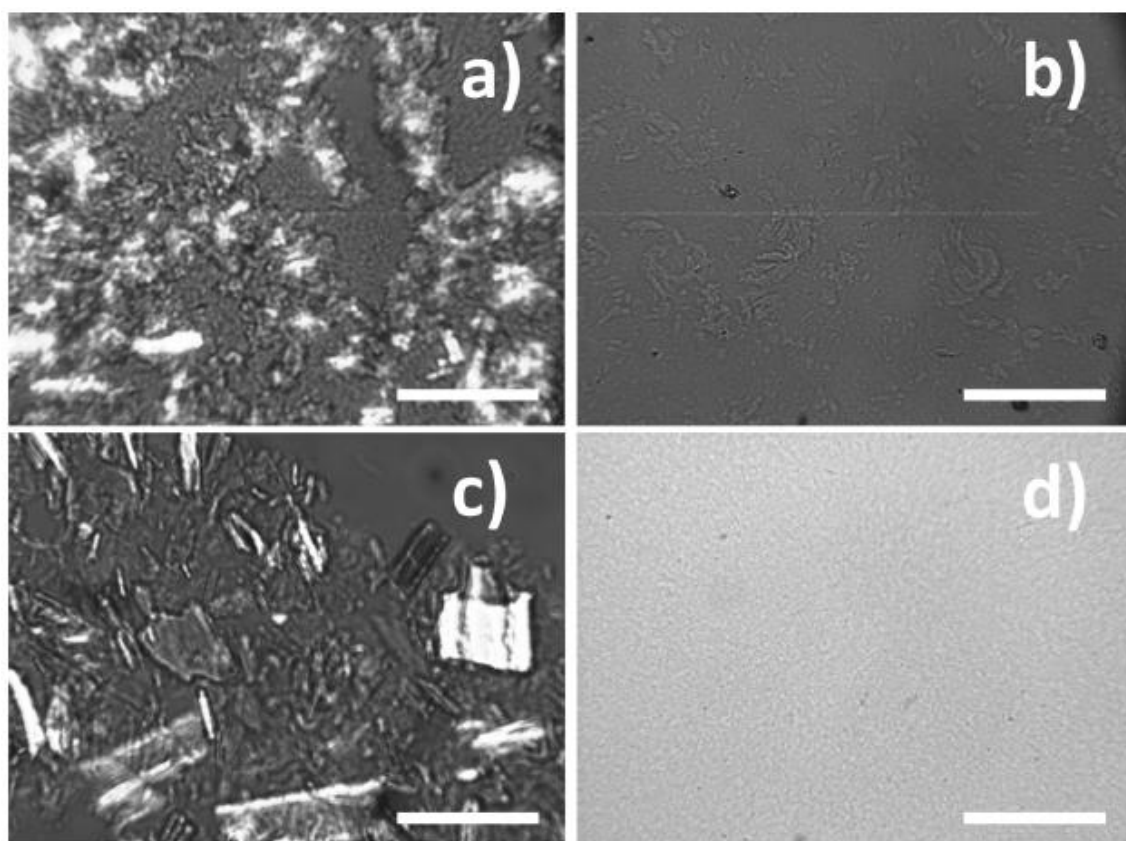
Figure 3.10: Polarized light micrographs of native (a and c) and dissolved cellulose in the cold 8 wt.% NaOH/H_2O solvent (b) and in 40 wt.% TBAH/H_2O solvent (d). The birefringent domains of the native fibers are clearly observed. The scale bars represent 100 µm [190].

In figure 3.11, one can see SEM images of the above mentioned cellulose solutions after being deposited onto a clean glass lamella.
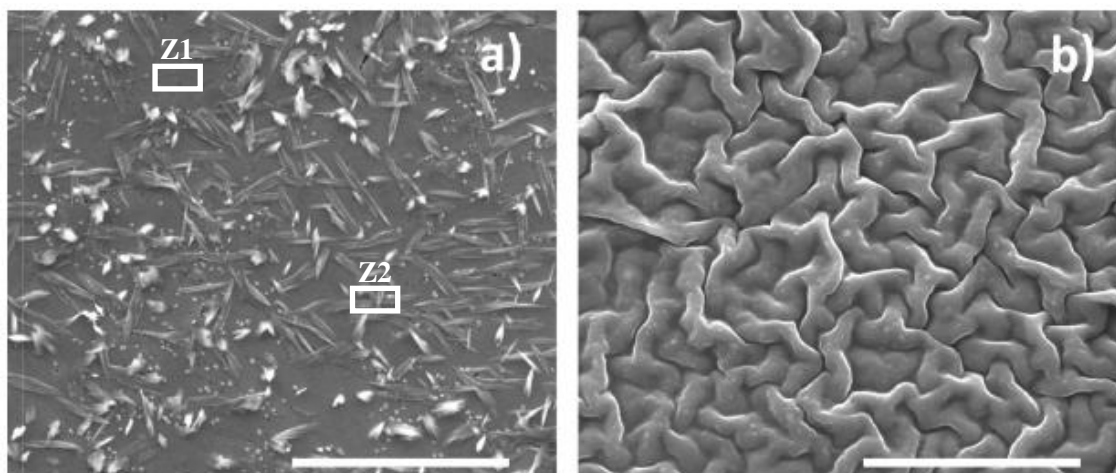
Figure 3.11: SEM images of the cellulose solutions after being deposited onto a glass lamella followed by solvent evaporation. "Needle-like" crystallites are observed in the 8 wt.% NaOH/H$_2$O solvent (a) while a "continuous wrinkled-film type" morphology is observed in the 40 wt.% TBAH/H$_2$O system (b). The scale bar represents 5 μm (adapted from [190]).

The texture and morphology are markedly different between the two solvent media; while needle-like crystallites (with lengths ranging from several hundred nanometers up to a few micro-meters) are observed in the cold alkali solvent, a "continuous wrinkled-film type" texture is observed in the TBAH based solvent. In the latter case, no sharp crystals are observed but rather more flexible and soft cellulose surfaces. It is important to note that the energy dispersive spectroscopy (EDS) spectra indicates that the needle-like crystals are indeed cellulose and not NaOH crystallites or other dry inorganic compounds (figure 3.12). From such analysis it is possible to calculate the ratio between Na and C in two distinct areas (bulk solution, Z1, and needle-like crystals, Z2) and clearly there is an increase in the C/Na ratio when going from the bulk region (without crystals) to a crystals area. Moreover, the presence of sodium carbonate crystals also can be discarded since the O/C ratio decreases considerably when going from the bulk solution area to a needle-like crystal area.
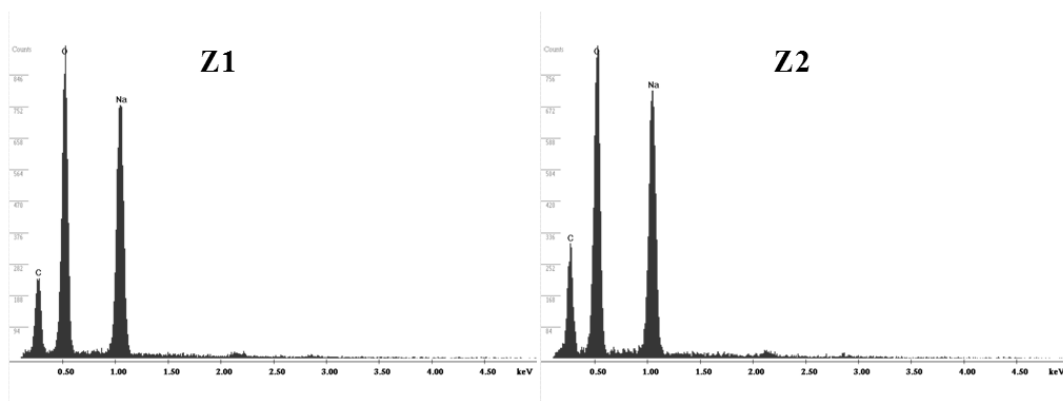
Figure 3.12: Energy dispersive spectra of bulk solution, Z1, and needle-like crystals, Z2, of a dried sample of cellulose in 8 wt.% NaOH/H_2O solution.

Interestingly, the DLS measurements indicate the presence of particles with an average size between 10 and 20 nm in the TBAH system while the mean particle size estimated from the NaOH based solutions is, at least, one order of magnitude higher (ca. 200 nm). We note that very rarely cellulose is found to be dissolved on a molecular level [77]. For instance, in the cadmium complexing Cd-tris (2-aminoethyl) amine solution, the size of cellulose particles is estimated to be ca. 20 nm [42, 149]. In diluted solutions of cellulose in N-methylmorpholine-N-oxide (NMMO) a mean size of 200 nm has been reported [191-193] and even in some ionic liquids, such as the 1-ethyl-3-methylimidazolium acetate (EMIMAc) [194-197] there is evidence for aggregates with rather large radius of gyration, ca. 150 nm, considerably higher than that of a single cellulose macromolecule [198]. In the NaOH-urea system, a mean size of ca. 60–160 nm [199] has been observed for the self-assembled solvent-cellulose clusters which is in good agreement with our DLS measurements. It is clear that in the cold alkali, dissolution is not complete since rather larger particles are detected in DLS measurements and individual crystals can be found dispersed in the glass lamella (figure 3.11). On the other hand, dissolution in the TBAH based solvent is considerably more efficient, since the estimated particle size is significantly smaller suggesting us that in this solvent we get, if not truly molecular solutions, at least, small molecular aggregates which explain the apparent softness and flexibility of the deposited cellulose solutions (figure 3.11).

The obtained PT ssNMR data obtained for cellulose dissolved in NaOH and TBAH aqueous, shown in figure 3.8, are in good agreement with the results of PLM, SEM and DLS here reported. The MCC sample dissolved in the aqueous TBAH gives both CP

and INEPT signals. However, the weak CP signal indicates a good level of dissolution; the estimated fraction of undissolved cellulose is below 1 wt.%. Similar results were obtained for tetrabutylphosphonium hydroxide in aqueous solution. The obtained chemical shifts for solid and dissolved fraction, as well the polymorph attribution are discussed in section 3.2.

The MCC sample dissolved in an aqueous NaOH solution gives both CP and INEPT signals. The discussion about the polymorph of solid fraction and the INEPT spectrum, based on the chemical shifts obtained, is provided in section 3.2. Additionally, the NaOH sample presents a well defined CP spectrum (good signal to noise ratio), which is indicative of a significant amount of undissolved material, in opposition to the CP spectrum obtained for the TBAH sample, where the signal to noise ratio is poor.

Effect of additives on dissolution in cold alkali systems

The cold alkali based solvent systems are a group of very interesting cellulose solvents because of the typical associated low cost and low environmental impact issues. However, the dissolution of cellulose in these systems is quite limited. Several studies have been carried out in order to improve the dissolution and capacity of cold alkali systems and also to allow the use of high molecular weight cellulose pulps [200, 201]. Additives such as urea, thiourea, zinc oxide, surfactants and polyethylene glycol (PEG) demonstrate a good potential to improve the dissolved amount of cellulose in cold alkali based systems [48, 186, 199-201]. Nevertheless, the majority of these alkali-water based systems only allow the dissolution of cellulose with a relatively low degree of polymerization (typically, less than 300). In figure 3.13 PLM micrographs of cellulose solutions in 8 wt.% NaOH are presented, in the absence of additives and in the presence of 12 wt.% of urea and thiourea (1.97 M and 1.57 M respectively). The effect of these additives is remarkable, decreasing the birefringent domains of the native cellulose in solution when compared with the standard aqueous NaOH system without additives. Thiourea demonstrates to be a more efficient additive leading to a completely clear solution, without the presence of undissolved material, in accordance with the work of Zhang et al. [200].

These results, that clearly indicate an improvement in the solvent quality, can be discussed in terms of amphiphilicity. Urea and thiourea are clearly less polar than water and these species are possibly capable to reduce the hydrophobic interactions between cellulose chains. The reduction in hydrophobic interactions among cellulose chains seems to be reached through the interaction of molecules of intermediate polarity with the hydrophobic part of cellulose. This is also supported by a recent molecular dynamics simulation where it has been found that urea interacts directly with cellulose through hydrophobic interactions [202].
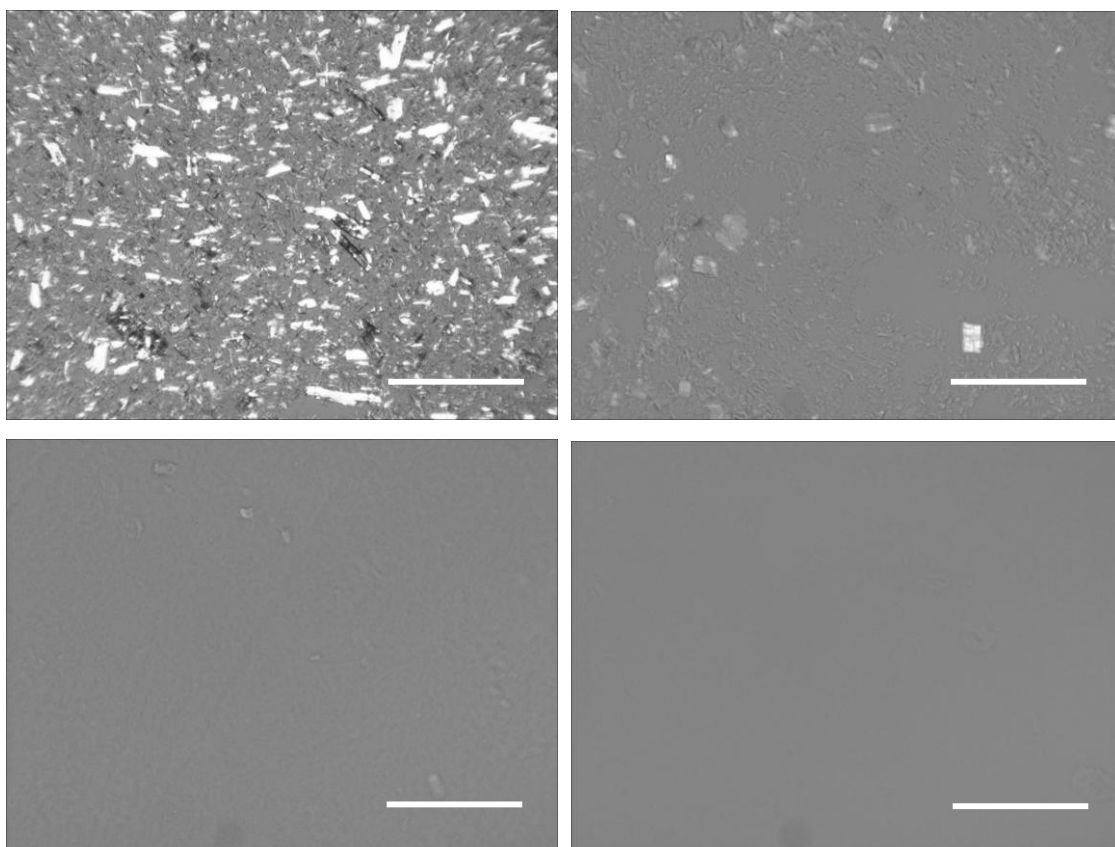
Figure 3.13: Polarized light micrographs of native (top left), dissolved cellulose in the cold 8 wt.% NaOH/H$_2$O solvent (top right), in 8 wt.%NaOH/12 wt.%urea/H$_2$O solvent (bottom left) and in 8 wt.%NaOH/12 wt.%thiourea/H$_2$O solvent (bottom left). Cellulose concentration is 5 wt.%. The scale bars represent 100 μm.

In electronic scanning microscopy it is possible to see relevant differences on the morphology of the samples. In figure 3.14 (top) micrographs of cellulose samples prepared in cold alkali aqueous solution, with the addition of 12 wt.% of thiourea, are presented. A continuous and "melted" film is obtained, contrasting with the undissolved

crystals obtained in the case of NaOH aqueous solution (see figure 3.11a). The lack of crystallites and the film-like morphology reveals an improvement of the dissolution power of cold alkali system when thiourea is added. Similar results were obtained with urea (figure 3.14 (bottom)).
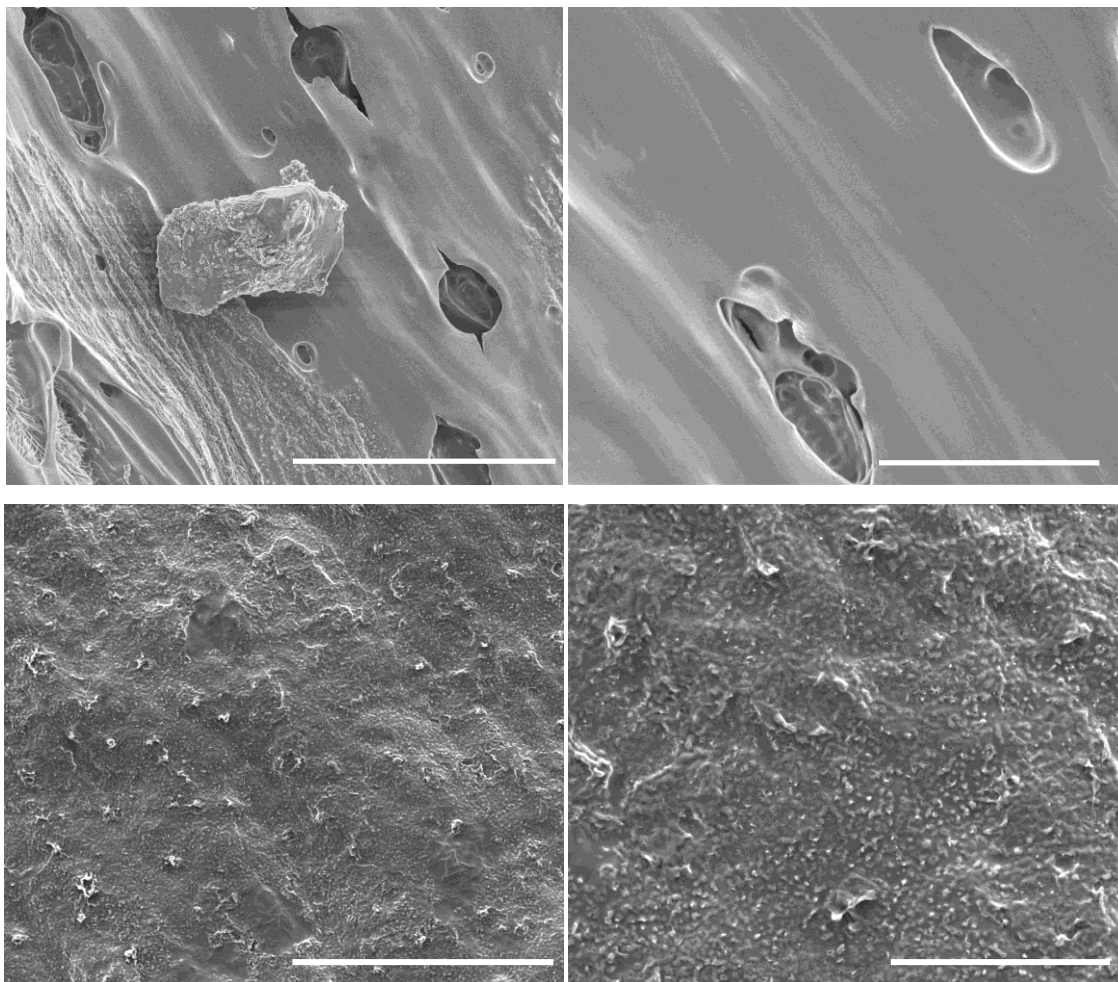
Figure 3.14: SEM images of the cellulose solutions in 8 wt.% NaOH/12 wt.% thiourea/H_2O (top) and in 8 wt.% NaOH/12 wt.% urea/H_2O (bottom), after being deposited onto a glass lamella followed by solvent evaporation. The scale bar represents 30 μm and 10 μm respectively.

In figure 3.15 the CP and the INEPT spectra for MCC dissolved in NaOH/thiourea aqueous solution are depicted and in table 3.3 the polymorph type of the solid fraction and main chemical shifts are summarized for several NaOH systems doped with different additives.
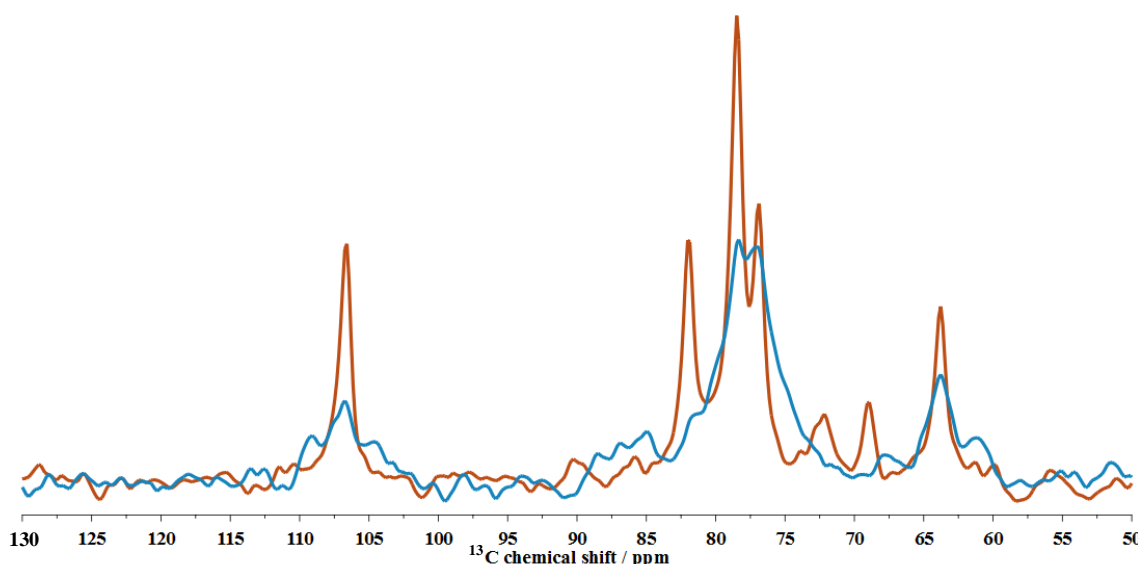
Figure 3.15: CP (blue line) and INEPT (red line) spectra for 10 wt.% microcrystalline cellulose dissolved in aqueous 8 wt.% NaOH/12 wt.% thiourea. The data was acquired at 25 ºC and 125 MHz ^{13}C Larmor frequency with 5 kHz MAS and 88 kHz TPPM ^{1}H decoupling. The spectra are zoomed-in on the 50-130 ppm spectral region relevant for cellulose, and, independently for each sample, magnified to facilitate observation of the cellulose resonance lines [183].

As observed for the NaOH aqueous solvent, clear CP and INEPT signals are also detected for the cellulose dissolved in the NaOH/thiourea system thus indicating that dissolution is not complete. However, the ratio between the CP and INEPT peaks is different. For the NaOH system the CP peaks are slightly more intense than the INEPT peaks while this relation is inverted for NaOH/thiourea system. This suggests that the additive improves the dissolution efficiency as manifested by the enhancement in the INEPT signal. The chemical shifts obtained for the solid fraction of cellulose (CP signal) in the NaOH/thiourea system, [106.80 (C_1), 88.03 (C_4), 78.42/77.08 ($C_{2, 3, 5}$) and 63.85 (C_6) ppm], can be assigned to a cellulose II, an anti-parallel arrangement of the cellulose molecules in the crystal, which is in good agreement with literature [186].

It is worth noting that the INEPT spectrum of cellulose dissolved in the NaOH/thiourea solvent presents a downfield shifting of ca. 2.0 ppm. This might be a result from a defective calibration or due to strong thiourea-cellulose interactions, which not only facilitates dissolution but also influences the carbon chemical shifts of cellulose [80]; presently, additional studies are in progress in order to clarify the origin of the chemical shift changes. Recent studies tend to support this observation regarding a preferential additive-cellulose interaction. For instance, Bergenstråhle-Wohlert et al. combining MD

simulations and solid state NMR on cellulose in water and in aqueous urea solutions found that the local concentration of urea is significantly enhanced at the cellulose/solution interface [203]. In another related study, Xiong et al., while working in the NaOH/urea system, state that the addition of urea in the NaOH solvent can reduce the hydrophobic effect of cellulose since urea plays its role through interacting with the hydrophobic part of cellulose [202].

Other additives have been used and in table 3.3 the main chemical shifts for solid and dissolved fractions of cellulose in 8 wt.% NaOH based systems are summarized together with the type of crystalline arrangement of the undissolved cellulose (i.e. solid fraction).

Table 3.3: ^{13}C chemical shifts of the dissolved and solid fractions of MCC in NaOH doped with different additives [183].

Sample	Fraction	Chemical shift				Polymorph
		C_1	C_4	$C_{2,3,5}$	C_6	
NaOH	Solid	106.97,104.18,101.69	85.52	74.60	61.65	Na-Cell. Q*
	Dissolved	104.15	79.50	75.96, 74.44	61.21	
NaOH/ZnO	Solid	109.29, 107.11	88.03	78.45, 77.18	64.18	Cellulose II
	Dissolved	106.59	81.94	78.53, 77.09	63.75	
NaOH/Urea	Solid	105.70, 104.49	86.68	77.73	61.93	Amorphous
	Dissolved	106.58	81.92	77.87	63.50	
NaOH/Thio.	Solid	106.80	88.03	78.42, 77.08	63.85	Cellulose II
	Dissolved	106.69	82.01	78.52, 76.96	63.86	
NaOH/APG	Solid	108.91	88.02	77.10	63.72	Na-Cell. II
	Dissolved	107.04	82.00	78.78, 76.21	64.19	

* Na-Cellulose Q is a highly swelled form of cellulose identified by Sobue et al. [188].

Comparing the NMR spectra it is possible to conclude that the addition of selected additives to the NaOH solvent results in an enhancement of the dissolution of cellulose. Additionally, we have also found that intermediate polarity additives delay or even prevent gelation induced by time or temperature. In figure 3.16 the flow curves obtained for samples of cellulose in cold alkali, fresh and after 7 days, in the absence of additives and in the presence of thiourea are represented. A significant decrease in viscosity is obtained in the presence of thiourea, which indicates a good dissolution state of cellulose. Additionally, the sample does not show signs of gelation (increase in viscosity) even after 7 days of being stored. On the other hand, the system without additives shows an increase in the zero-shear viscosity which may indicate a progressive gelation. It is remarkable to notice that the zero-shear viscosity of the system without additives is almost two orders of magnitude higher than the system with additives.
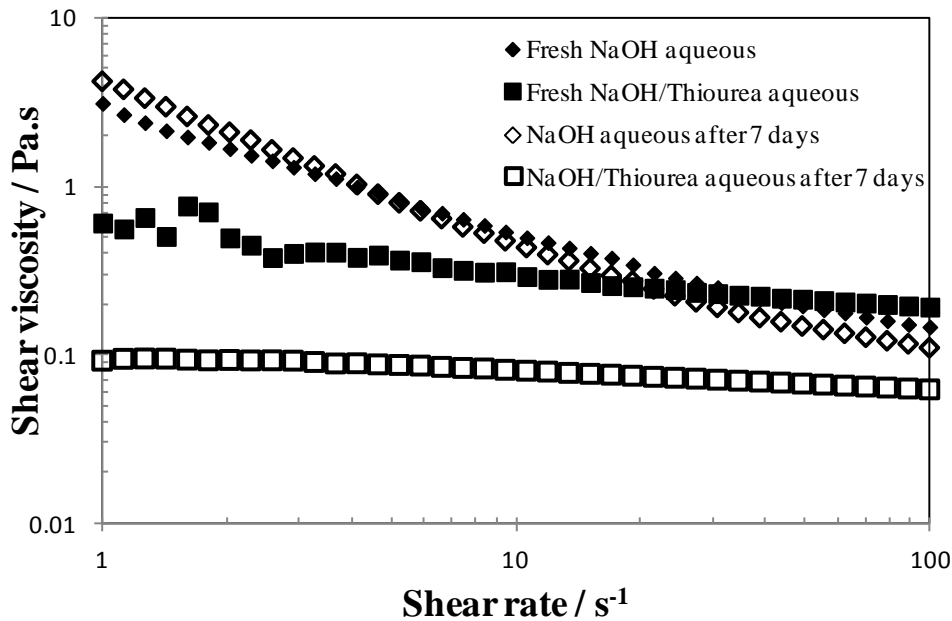
Figure 3.16: Flow curves of 5 wt.% microcrystalline cellulose in 8 wt.% NaOH/H$_2$O and 8 wt.% NaOH/12 wt.% thiourea/H$_2$O, fresh and after 7 days. Gelation is prevented by the addition of thiourea. Temperature was kept at 25 ºC.

As discussed above, cold alkali solvent systems are suitable for the dissolution of cellulose with relatively low molecular weight (degree of polymerization < 300). Additives, such as thiourea or urea, can improve the dissolved amount and dissolution rate (for low degree of polymerization celluloses). In figure 3.17, PLM micrographs of high molecular weight cellulose pulp (Domsjö pulp) dissolved in alkali aqueous systems are presented.
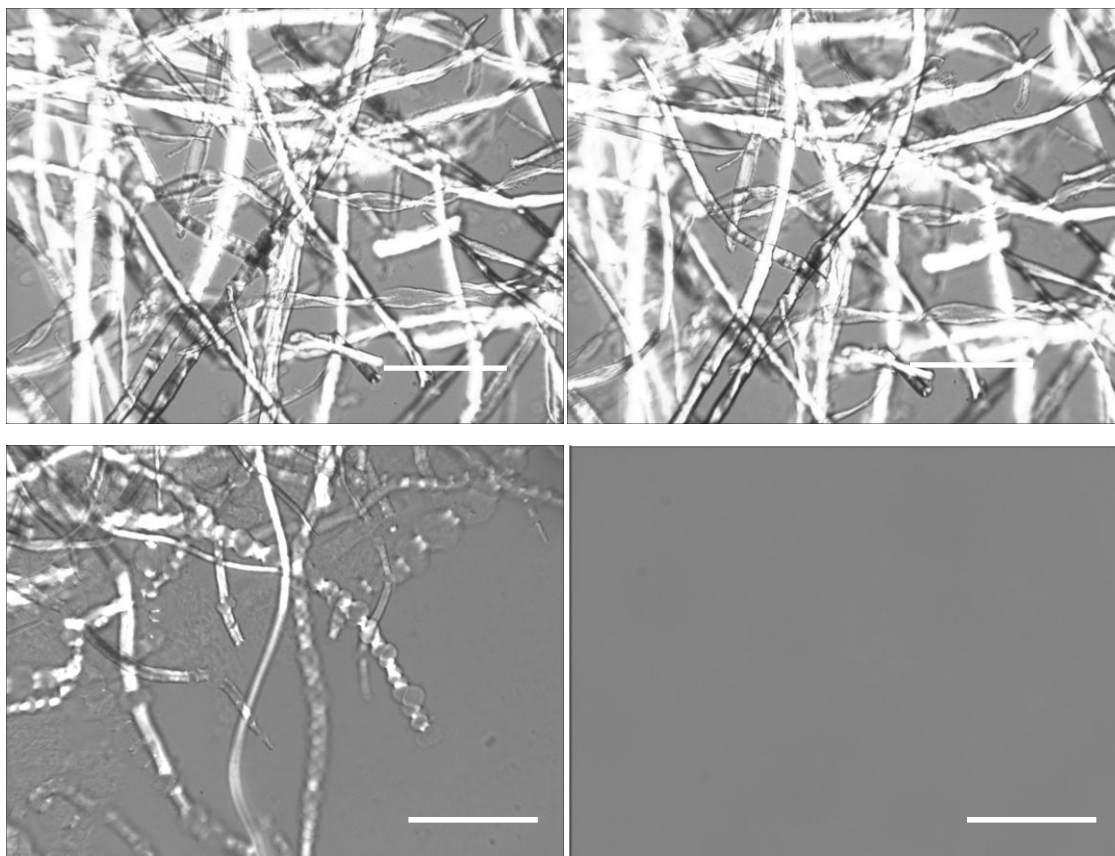
Figure 3.17: PLM micrographs of 1 wt.% of cellulose pulp dissolved in 8 wt.% NaOH/H$_2$O (top left), 8 wt.% NaOH/12 wt.% urea/H$_2$O (top right), 8 wt.% NaOH/12 wt.% thiourea/H$_2$O (bottom left) and 40 wt.% TBAH/H$_2$O (bottom right). The scale bars represent 100 μm.

As expected, the NaOH based solvent is not able to dissolve cellulose with high degree of polymerization. Undissolved and unswelled native fibers dispersed in solution are observed in both NaOH aqueous systems (with and without additives). The addition of thiourea to the cold alkali system improves the swelling of the fibers (the "ballooning effect" is observed) and promotes partial dissolution of the fibers. A distinct result is obtained when using tetrabutylammonium hydroxide. In this case, cellulose pulp can be dissolved, leading to clear solutions. These results also point out the positive effect on dissolution promoted by a more amphiphilic cation (TBA$^+$). The mechanism suggested involves the weakening of the hydrophobic interactions of cellulose via the more hydrophobic moieties of the cation which facilitates the dissolution of cellulose.

Tuning the solvent quality: role of salt and urea

Compared with nonionic polymers, charged polymers can be easily dissolved in water, due to the entropy gain of the counterions, therefore, charging up a polymer is always expected to be helpful for solubility [82]. For a nonionic polymer such as cellulose, this can be done either by the association of an ionic charged specie (such as an ion or a surfactant) or via deprotonation or protonation of the hydroxyls groups [12, 204].

In our point of view, the mechanism of dissolution in strong alkaline environment is based on the (weak partial) deprotonation of the hydroxyl groups, with the translational entropic gain associated, due to the release of the counterions (figure 3.18). It is our conviction that even if a low deprotonation level is obtained, this might be enough to produce significant changes in solubility. However, this does not represent the more consensual visions of the dissolution mechanism in cold alkali. One of the common opinions is that the alkali forms hydrates with water capable to break the inter- and intramolecular hydrogen bonds between cellulose molecules [205].
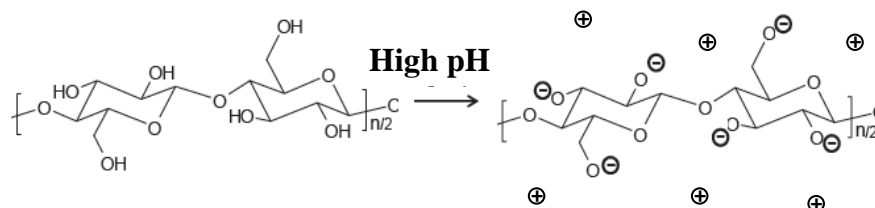
Figure 3.18: Conversion of neutral cellulose into a polyelectrolyte by pH change: schematic representation of the ionization of the hydroxyls of cellulose in strong alkali medium (extremely high pH) [206].

A strong indication of cellulose ionization is that the addition of a simple salt, such as KBr (also verified for KCl [206], LiCl and NaCl [207]), changes the cellulose dope (in aqueous TBAH solution) from a homogenous and transparent solution to an opaque solution, which eventually phase separates after a certain amount of salt (figure 3.19).

| [KBr] / mM | 0.0 | 20.0 | 40.0 | 60.0 | 80.0 | 100.0 |
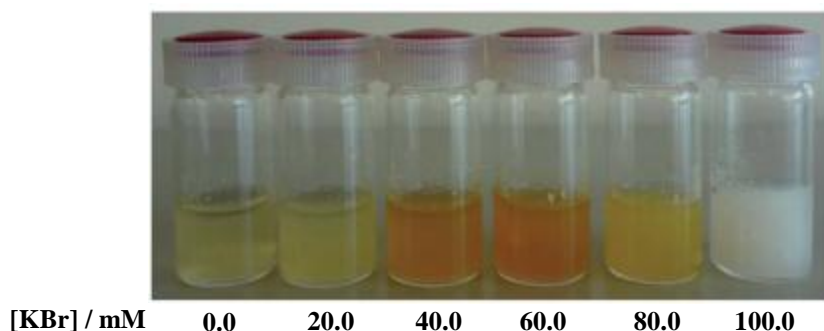
Figure 3.19: Turbidity increase of samples of cellulose dissolved in strong alkali (40 % TBAH solution in water) with progressive addition of KBr. As the salt concentration increases the quality of the solution decreases (increase in turbidity) (adapted from [207]).

The situation can be reversed by the addition of a reagent capable of capturing K^+ ions. When a selected crown ether (18-crown-6 (18C6)), known as an excellent ligand for K^+, is added to the solution the transparency of the solution increases and even a better dissolution power is observed than that without 18C6. Surprisingly, the solution containing 18C6 (3.0 M) was found to be clearer than that containing no KBr (figure 3.20).

| [18C6] / M | 0.0 | 0.0 | 0.5 | 1.0 | 2.0 | 3.0 |
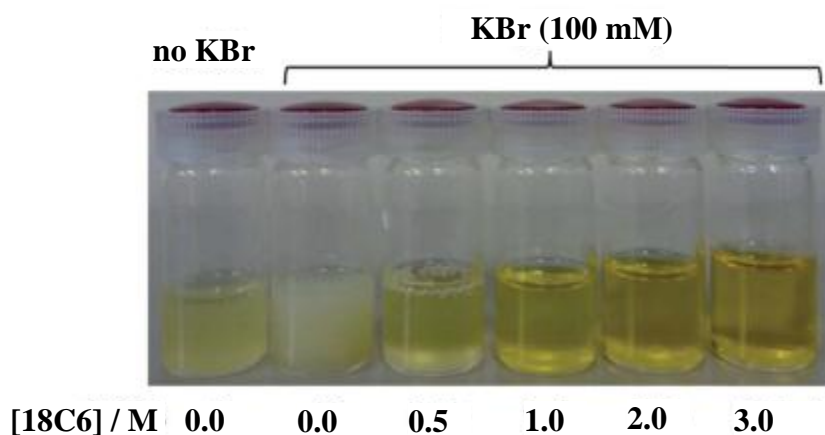
Figure 3.20: Effect of the addition of 18C6 to a solution of cellulose in TBAH aqueous containing 100 mM of KBr (adapted from [207]).

This is a good indication that cellulose is, at least, partially ionized in solution due to the extremely high pH and, upon salt addition, charges are progressively screened and the polymer becomes less hydrophilic until eventually the hydrophobic interactions are dominant over the electrostatic repulsion. Similar results were obtained with the addition of KCl to a solution containing cellulose in TBAH, followed by addition of the

crown ether. It should be noted that this is not a simple salting out effect since the precipitation/gelation of the system is always observed regardless of the use of kosmotropic or chaotropic salts.

On the other hand the addition of urea to a cellulose solution (in TBAH/H_2O) does not change the quality of the solution [206], figure 3.21. The addition of 3.33 M (20.0 wt.%) of urea does not lead to a phase separation, but rather improves cellulose dissolution and the rheological properties. As mentioned above, urea can weaken the hydrophobic interactions among cellulose chains, in a similar way as it does during protein unfolding, increasing cellulose solubility and preventing the hydrophobic regions of cellulose to come together to form a gelled network [208].
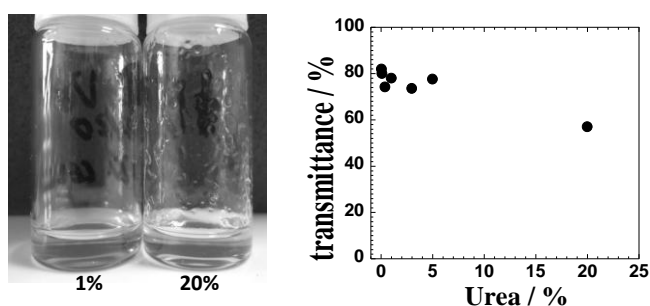
Figure 3.21: Photos (left) and transmittance (right) of cellulose dissolved in strong alkali (TBAH aqueous solution) with progressive addition of urea. The addition of urea does not produce significant changes in transmittance [206].

Synopsis

It is remarkable that while the samples of MCC dissolved in NaOH exhibit needle-like crystallites (observed in SEM), the cellulose samples dissolved in the TBAH/H_2O demonstrate a considerable reduction in crystallinity, showing a flexible continuous wrinkled-film type morphology. This is illustrative of the different levels of dissolution; while for TBAH the lack of crystallinity and high flexibility of the materials indicate that dissolution progresses down to the molecular level (in agreement with the PT ssNMR results), in the case of the NaOH, dissolution is not complete and stable cellulose aggregates (crystallites) can be observed in solution. The light scattering data indicates the presence of rather small cellulose particles in the TBAH system (ca. 10-20 nm), while considerably larger cellulose particles (above 200 nm) are found for the NaOH system. In any case, both cellulose dopes are macroscopically transparent. In the

same direction, PT ssNMR studies indicate a better dissolution performance when amphiphilic cations are used; the CP signal is weak in the case of TBAH and TBPH aqueous solutions, while in case of NaOH based systems the CP signal is well defined. Moreover, the chain arrangement of undissolved material is dependent on the solvent used. Cellulose I is observed when amphiphilic cations are used and a highly swelled form of cellulose, the so called "Na-Cellulose Q", or cellulose II is obtained when NaOH aqueous based systems are used.

In the present study we found fundamental differences between a small inorganic cation of high charge density and a large organic cation with amphiphilic character. The use of an amphiphilic cation leads to cellulose dissolution down to the molecular level whereas this is not the case for the sodium ion. That dissolution into molecular solutions is strongly assisted by an amphiphilic ion provides good support for the view that cellulose molecules have both polar and non polar regions and have a strong tendency to associate by hydrophobic interactions. There are several other illustrations in the same direction, such as the effect of urea [89], well-known to eliminate hydrophobic interactions, thiourea, surfactants and acids with organic anions on cellulose dissolution [45], some of them also explored in this work.

Dissolution and dope stability are found to be clearly influenced by the presence of amphiphilic species. Moreover, we have seen that combining cellulose ionization (either achieved by extreme pH or adsorption of ionic species) with the weakening of the hydrophobic effect (for example by adding urea or thiourea) makes dissolution more efficient. In the TBAH system, we have seen that this effect can be controlled and even reversed, thus decreasing the solvent capabilities, by the addition of salt (i.e. reducing the counterion entropy effect).

3.4 - Cellulose dissolution in acidic medium

The effort to develop new efficient, environmentally and human friendly solvents for cellulose is a hot topic in the cellulose field. Cellulose is insoluble in most common solvents, but can be dissolved in some specific solvent systems, such as strong alkaline (previously discussed) or strong acid media. The reduced accessibility of the

solvent molecules to the interior of cellulose fibrils, promoted by the cohesion of the cellulose chains, reduces its efficiency. This cohesion is due to the extended hydrogen bond network and hydrophobic interactions (via *van der Waals* forces) [12, 202].

Acidic solvents are very effective systems to dissolve cellulose. This high performance is usually attributed to the fast diffusion of the hydrogen ion from acid compounds; this fast diffusion is related to the very small size of the ion that can easily diffuse into the heterogeneous cellulose matrix [209]. However, the cases are rare, where dissolution is not accompanied by chemical hydrolysis of cellulose. Such cellulose degradation might be useful in some cases, such as fundamental chemical analysis or 2nd generation biofuel production but it is definitely not desired or beneficial for other applications, such as fiber spinning [210]. Therefore, the solution state of dissolved cellulose is an important parameter to consider not only to develop new efficient solvents, but also to understand and prevent undesired side effects.

The general mechanism for cellulose dissolution in acidic systems is suggested to be related to protonation of the hydroxyl groups. This charging up effect has been extensively explored and observed to be very useful in the polymer field, in particular with cellulose derivatives [211].

In this section we focus on the dissolution of cellulose in highly concentrated acid solutions. Cellulose dissolution in acids can basically be related to the fact that cellulose molecules acquire net charges, by protonation at extremely low pH. As done for the alkaline media, the effect of different anions and solvent polarity (using glycerol) will be addressed using techniques such as scanning electron microscopy (SEM), polarized light microscopy (PLM), PT ssNMR and rheology.

Materials and methods

The materials and methods used are described in chapter 2.

Results

Although acid based systems are a very interesting class of cellulose solvents, the dissolution is often accompanied by the degradation of the biopolymer. In literature several examples can be found where the border between dissolution and degradation is

quite subtle [212, 213]. Ioelovich et al. report on the dissolution of cellulose in concentrated sulfuric acid solution. The authors found that cellulose regenerated from 65 wt.% sulfuric acid shows a degree of polymerization of 70-80 while the starting material presented a degree of polymerization of 170 [110]. Increasing the sulfuric acid concentration above 65 wt.% led to a diminution in the yield of the regenerated cellulose. After treatment of the initial MCC sample with 70 wt.% sulfuric acid, the dissolved cellulose cannot be regenerated from the acidic solution by dilution with water due to fast acidic depolymerization and the formation of water-soluble oligomers. It should be noted that the procedure to isolate nanocrystalline cellulose uses similar acid concentrations.

A similar system, using glycerol instead of water, was tested in the present work. The addition of glycerol intends to facilitate dissolution by reducing the polarity of the medium and decreases the kinetics of degradation. Figure 3.22 shows the polarized light micrographs of microcrystalline cellulose dissolved in different acidic media.
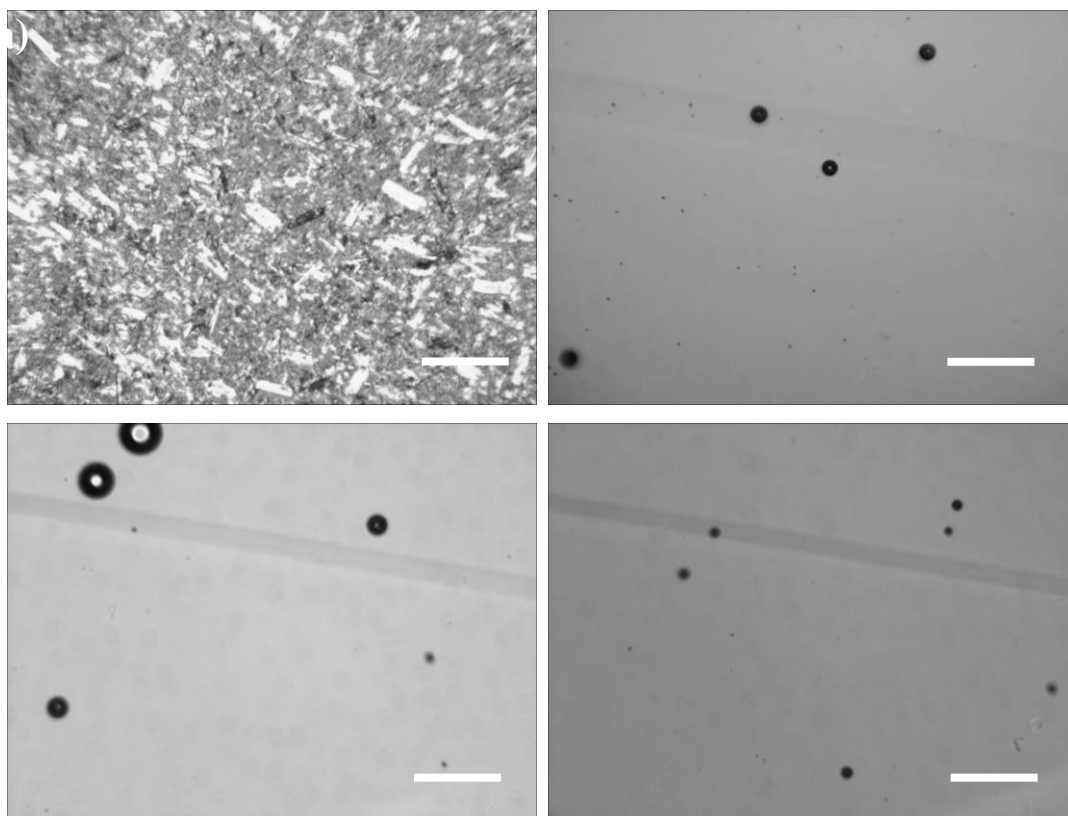
Figure 3.22: Polarized light micrographs of 10 wt.% microcrystalline cellulose dispersed in water (top left) and dissolved in H_2SO_4/glycerol (2:1) solution (top right), in 85 wt.% H_3PO_4 aqueous solution (bottom left) and in 65 wt.% zinc chloride aqueous solution (bottom right). The scale bars represent 100 µm. Black dots are air bubbles.

The samples appear to be quite well dissolved when observed in PLM. The absence of visible undissolved material is achieved in all cases, which means that if cellulose aggregates are still present, they have a very small size (sub micron). The presence of trapped air bubbles is due to the high viscosity of the samples. In fact, the high viscosity of cellulose dopes in acidic systems is one of the main concerns for a process implementation on industrial scale.

The observation in electron microscopy of a sample containing cellulose in aqueous zinc chloride solution, figure 3.23 shows a "melted" morphology, which indicates that the super-molecular structure of the cellulose is "destroyed" and no signals of crystallites are observed in the dissolved sample.
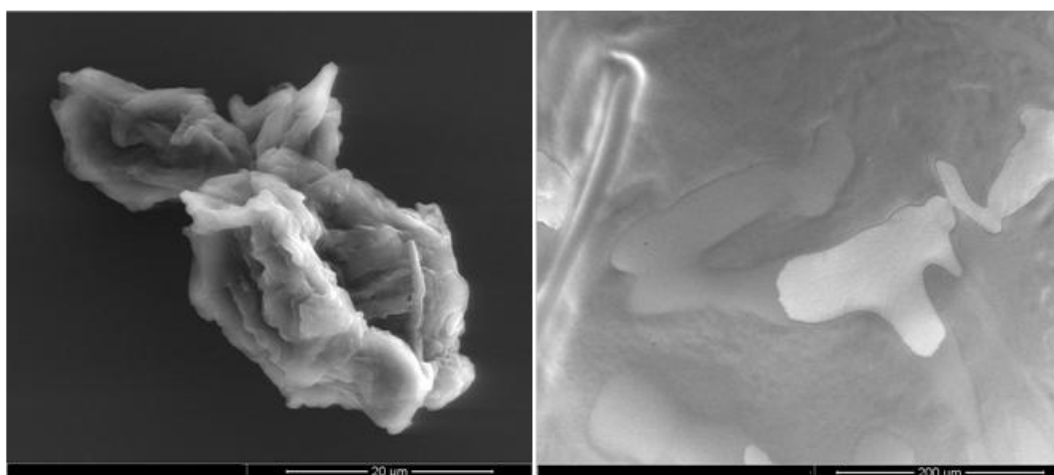
Figure 3.23: Scanning electronic micrographs of microcrystalline cellulose; dispersed in water (left) and dissolved in 65 wt.% zinc chloride aqueous (right).

In order to have a better understanding of the dissolved state of cellulose in the acidic solvents, NMR techniques were again applied. As discussed in section 3.2, PT ssNMR is able to give us information not only about the cellulose in solid state, but also about the dissolved cellulose, in a single experiment.

In figure 3.24 the PT ssNMR spectra of microcrystalline cellulose dissolved in aqueous phosphoric acid, recorded at 25 ºC and 60 ºC, as well the spectra of the starting material, are depicted.
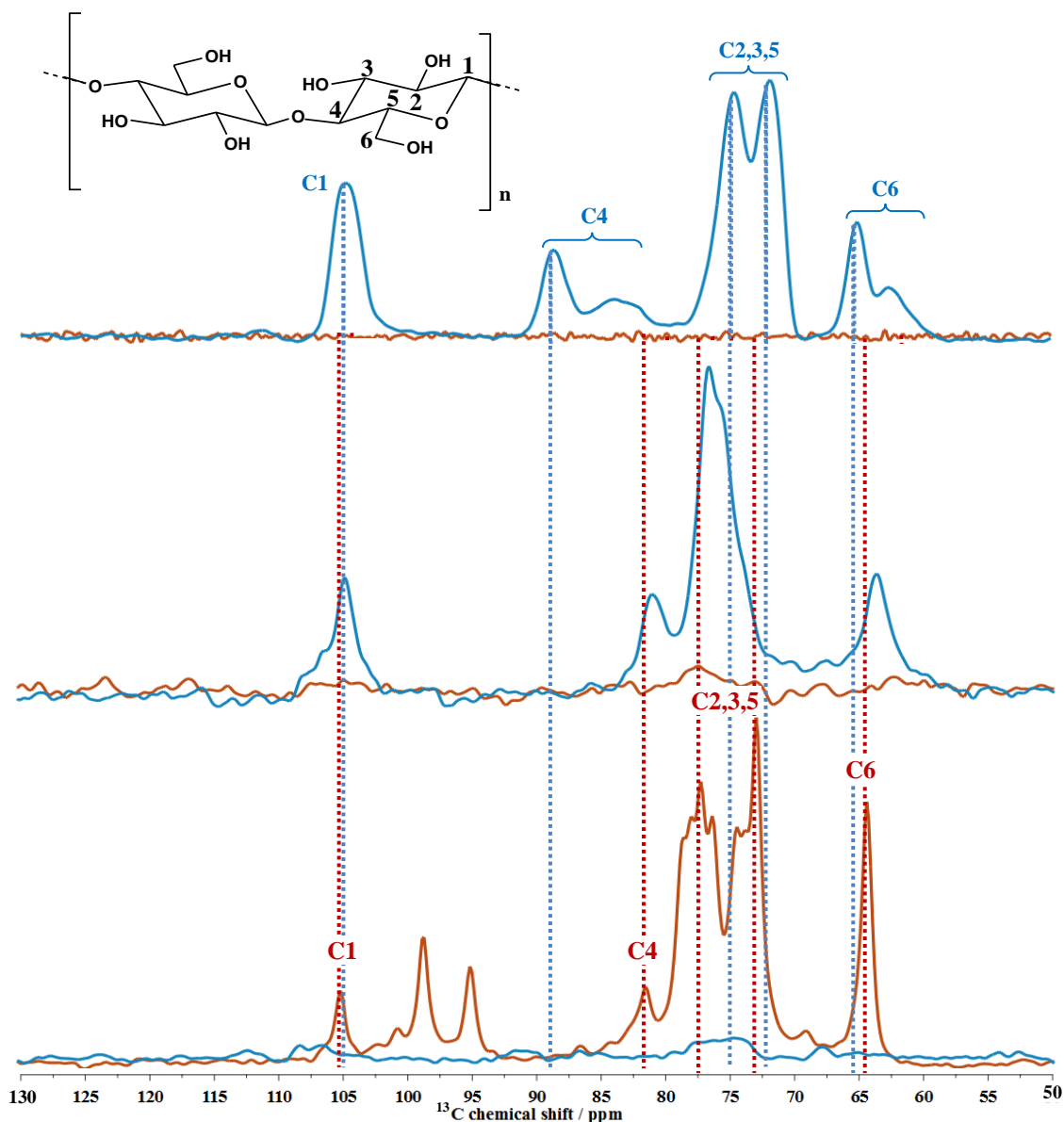
Figure 3.24: PT ssNMR data for microcrystalline cellulose in the initial dry state at 25 ℃ (top), as well as 10 wt.% cellulose dissolved in aqueous H_3PO_4 (middle and bottom); recorded at 25 ℃ (middle) and recorded at 60 ℃ (bottom). CP and INEPT spectra are shown in blue and red, respectively. The assignments of the solid (blue) and dissolved (red) cellulose peaks refer to the carbon atom numbering in the structural formula. The blue and red dashed lines represent chemical shifts for cellulose I (starting material) and dissolved cellulose, respectively, in order to a better visualization of the data. The data was acquired at 125 MHz ^{13}C Larmor frequency with 5 kHz magic angle spinning (MAS), 88 kHz two pulse phase modulation (TPPM) decoupling ^{1}H decoupling. The spectra are zoomed-in on the 50-130 ppm spectral region relevant for cellulose, and, independently for each sample, magnified to facilitate observation of the cellulose resonance lines [214].

In table 3.4 the chemical shifts for microcrystalline cellulose dissolved in aqueous H_3PO_4 (two temperatures) as well as the attribution of the polymorph type for the solid fraction present in each sample are reviewed.

Table 3.4: ^{13}C chemical shifts of microcrystalline cellulose dissolved in acidic aqueous solutions [214].

Sample	Fraction	Chemical shift				Polymorph
		C_1	C_4	$C_{2,3,5}$	C_6	
Dry	Solid	104.77	88.65	74.60, 71.82	65.05	Cellulose I
H_3PO_4 at	Solid	104.74	81.02	76.65	63.71	Amorphous
25ºC	Dissolved	----	----	----	----	
H_3PO_4 at	Solid	106.41	86.64	77.48, 76.23, 74.72	65.19	Cellulose I
60ºC	Dissolved	105.06	81.53	77.28, 72.99	64.46	

The dry cellulose (starting material) gives intense CP peaks while INEPT is absent, which is consistent with cellulose being in the solid state. As discussed in sections 3.2 and 3.3, the observed CP chemical shifts are typical for cellulose I [188]. The sample containing cellulose in aqueous phosphoric acid gives a good CP signal and a poor INEPT signal; at a first glance this would suggest that we are mainly in the presence of a solid material with a small dissolved fraction. This would contradict the results obtained by light microscopy and previously reported for this solvent system [209]. However, it is important to note that the solutions formed are very viscous (see figure 3.25), which can lead to an increase in the reorientation time of the C-H bonds in the cellulose chains; if this reorientation time is increased above 100 ns (see figure 3.7) the INEPT signal is expected to be lost and "converted" into the CP signal. An indication that possibly the CP signal is coming from dissolved cellulose is that the chemical shifts obtained in the CP spectrum are typical for dissolved, low order and amorphous cellulose.
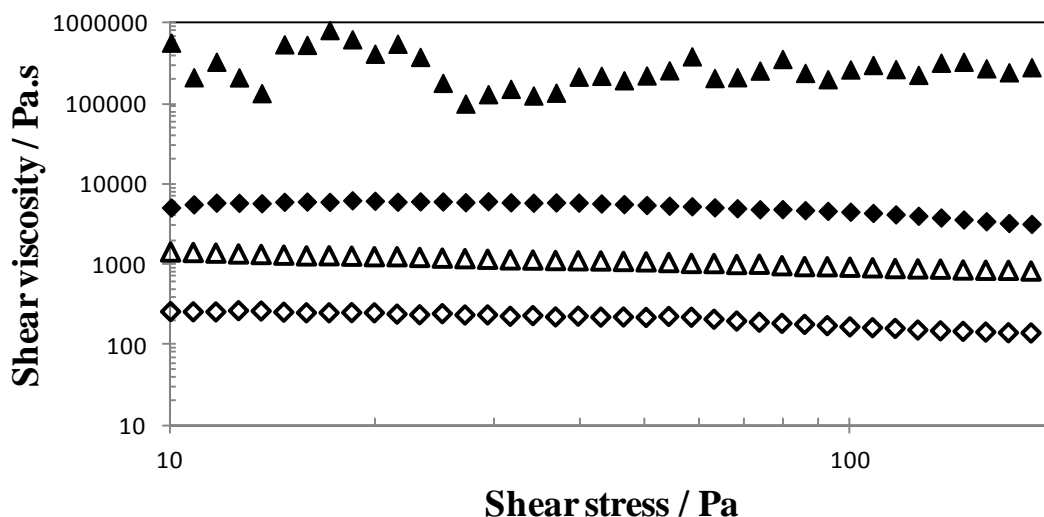
Figure 3.25: Flow curves of 10 wt.% microcrystalline cellulose in aqueous H_3PO_4 ($\blacklozenge$) and in aqueous $ZnCl_2$ ($\blacktriangle$), at 25 ºC (filled symbols) and at 60 ºC (empty symbols).

The acquisition of the spectra was also performed at 60 ºC (figure 3.24, bottom). As one can observe, the CP signal dramatically decreases and the INEPT signal increases; this inversion in the signals intensities is most likely due to the considerable decrease in viscosity induced by the temperature raise. The chemical shifts obtained in the INEPT spectra [105.06 (C_1), 81.53 (C_4), 77.28/72.99 ($C_{2,3,5}$), and 64.46 (C_6) ppm] are in good agreement with the ones reported for dissolved cellulose [174]. Two new peaks appearing at 98.68 ppm and 95.05 ppm can possibly be attributed to degradation products of cellulose in the acidic medium [215], most likely small oligomers from polymer degradation.

The weak CP signal at 60 ºC reveals a good dissolution efficiency of the aqueous H_3PO_4 solvent (less than 1% of undissolved starting material is estimated to remain in the sample). Furthermore, the chemical shifts for the solid fraction of cellulose in solution indicate that we are in the presence of the cellulose I polymorph.

Another interesting system that shows good ability for cellulose dissolution is the aqueous $ZnCl_2$. This strongly concentrated salt system displays Lewis acid character. In figure 3.26 (top) the CP and the INEPT spectra for microcrystalline cellulose dissolved in an aqueous 65 % $ZnCl_2$ solution are represented.
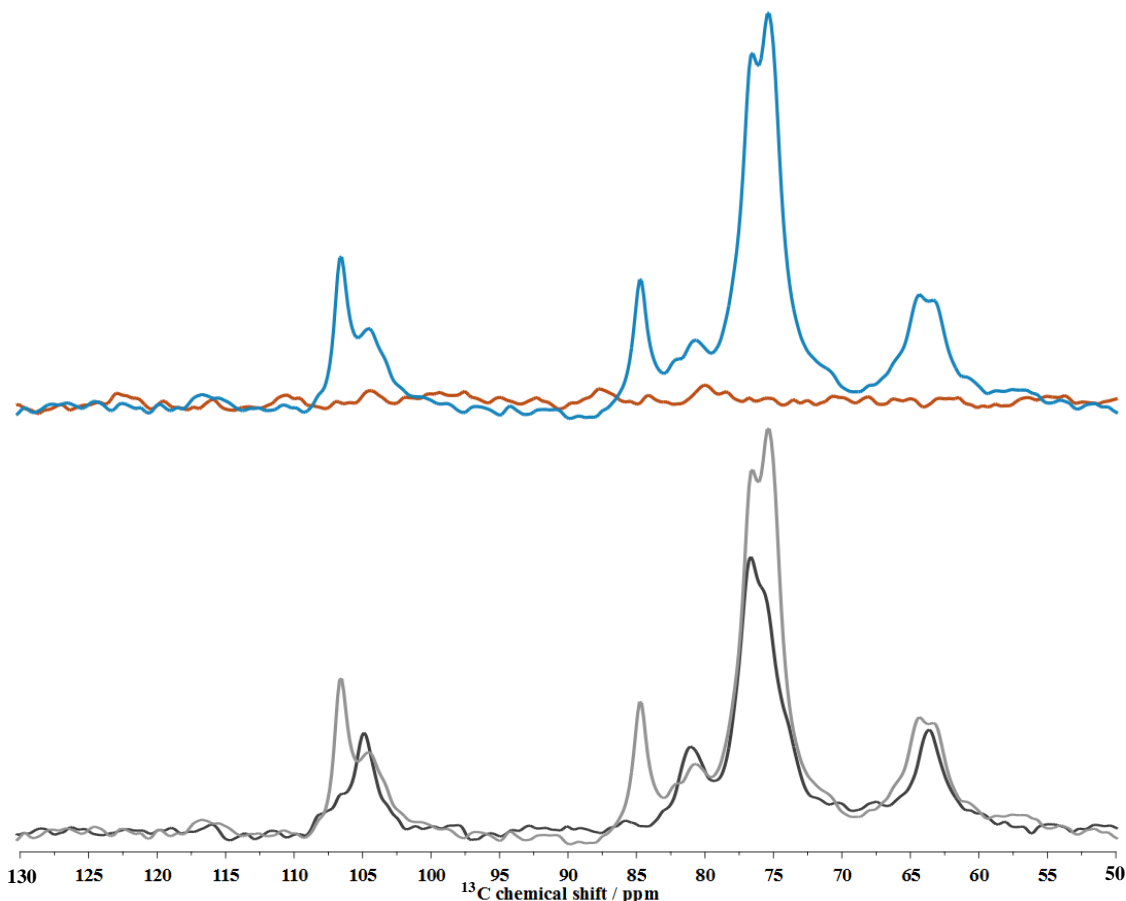
Figure 3.26: (top): CP (blue line) and INEPT (red line) spectra for 10 wt.% microcrystalline cellulose dissolved in aqueous $ZnCl_2$ (65%). (bottom): CP spectra of cellulose in H_3PO_4 aqueous (black line) and in $ZnCl_2$ aqueous (grey line). The data was acquired at 25 °C and 125 MHz ^{13}C Larmor frequency with 5 kHz MAS and 88 kHz TPPM ^1H decoupling. The spectra are zoomed-in on the 50-130 ppm spectral region relevant for cellulose, and, independently for each sample, magnified to facilitate observation of the cellulose resonance lines [214].

As observed for the H_3PO_4 aqueous system, the cellulose dope in $ZnCl_2$ gives also a good CP signal and a poor INEPT signal. Due to the high viscosity of the dopes formed in $ZnCl_2$ we believe that the C-H reorientation time is higher than predicted this being the main contribution to the CP signal. The reported ^{13}C spectrum for cellulose in an aqueous $ZnCl_2$ solution at 65 °C, is coherent with the suggested hypothesis [51] since a good signal for dissolved cellulose is obtained at high temperature.

Comparing the CP spectra of cellulose in H_3PO_4 and in $ZnCl_2$ it is possible to observe minor differences in the chemical shifts of C_1 and C_4. In figure 3.26 (bottom), two new peaks at 106.42 ppm and 84.67 ppm are detected. These differences are suggested to result from the formation of a complex zinc-cellulose [51, 216]. For the cellulose dope produced from the $ZnCl_2$ based system, no degradation products are detected. Another

example of an acidic solvent already reported for cellulose is the H_2SO_4/glycerol (2:1) mixture [217]. The addition of glycerol is intended to stabilize the cellulose solution, reducing the harsh degradation that is usually observed in common acidic solvents. In figure 3.27 the CP and INEPT spectra for microcrystalline cellulose dissolved in the sulfuric acid/glycerol mixture are presented.
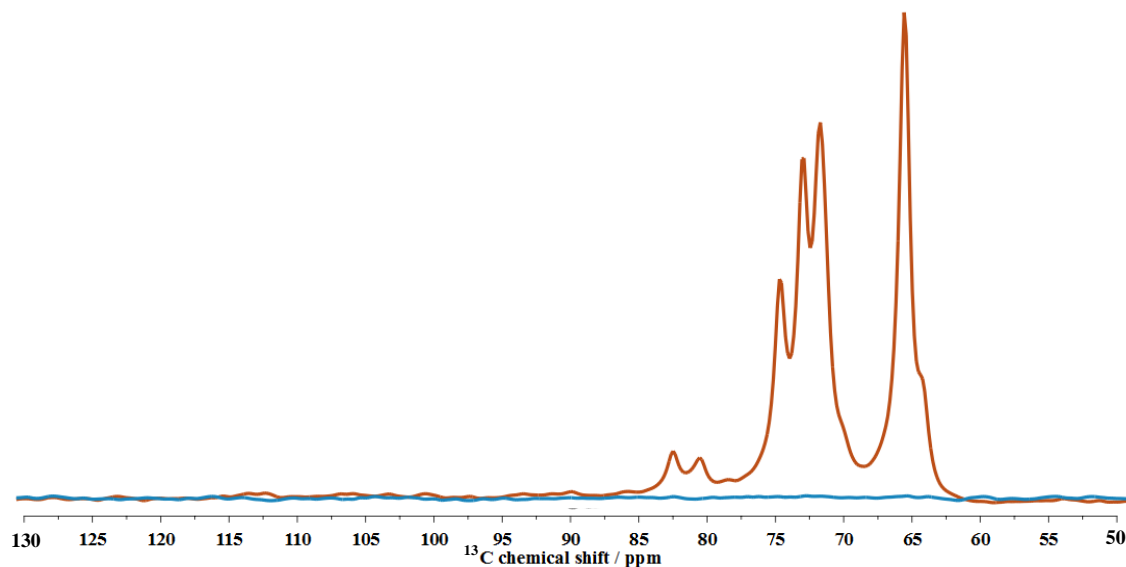

Figure 3.27: CP (blue line) and INEPT (red line) spectra for 10 wt.% microcrystalline cellulose dissolved in H_2SO_4/glycerol (2:1) solution. The data was acquired at 25 ºC and 125 MHz ^{13}C Larmor frequency with 5 kHz MAS and 88 kHz TPPM ^1H decoupling. The spectra are zoomed-in on the 50-130 ppm spectral region relevant for cellulose and, independently for each sample, magnified to facilitate observation of the cellulose resonance lines [214].

The CP signal is inexistent, which suggests that the dissolution is complete. However, the obtained INEPT spectrum is significantly different from the spectra obtained for cellulose in other solvents or even in the dry state. The chemical shifts obtained [75.01 (C_2), 73.37 (C_4), 72.15 ($C_{3,5}$) and 66.06 (C_6) ppm] suggest the presence of D-gluconic acid in solution [218]. The signal for the C_1 carbon is lost due to the absence of C-H bond in the D-gluconic acid. The appearance of this compound in the dope is due to cellulose degradation [219]. Moreover, the presence of two additional peaks at 82.72 ppm and 80.80 ppm possibly indicates that besides D-gluconic acid, the major degradation product, other compounds from cellulose degradation are present in solution.

The strong cellulose degradation in the H_2SO_4/glycerol system (and also found in other acidic systems) reduces the applications of these systems in situations where high degrees of polymerization are required, such as fiber spinning. However, this solvent might be very useful for other applications such as biofuel production [219].

Synopsis

Although quite efficient, acidic systems usually lead to unwanted cellulose degradation, which can be an important drawback for certain applications. Here we have shown by PLM the absence of large aggregates of undissolved material which is supported by PT ssNMR (weak CP signal). However, PT ssNMR also demonstrates to be very sensitive to the viscosity of the system; highly viscous solutions can lead to a long reorientation time (C-H bond), which results in an enhancement in the CP signal even if the sample is well dissolved (similar results were also obtained when true gelation of the solutions occurs, such as the DMSO/H_2O/TBAH or TBAF/DMSO/H_2O systems [220]). This might be regarded as a weakness of the technique, which can wrongly induce the less accurate determination of the solid/liquid fractions. Nevertheless, it seems clear that even for gelled systems important information can be obtained by PT ssNMR, especially when combined with other techniques. PT ssNMR is also useful to detect degradation products; for example, D-gluconic acid is found in the H_2SO_4/glycerol system.

3.5 - Stability of cellulose dopes: Role of cyclodextrins and surfactants.

Usually, cellulose dopes are unstable with the self-association of cellulose chains resulting in gelation of the system. Molecular association of cellulose is many times explained based on an extended reformation of intra- and intermolecular hydrogen bonds [174, 221-223]. However, as argued cellulose is an amphiphilic molecule and thus the stability of the cellulose solutions is also governed by hydrophobic interactions. During the regeneration process, the hydrophobic interactions are expected to be responsible for the stacking of the cellulose chains and formation of molecular sheets, the hydrogen bonds being responsible for the association of these sheets into thin planar

crystals [74]. Recently, Isobe et al. reported the first experimental evidence of such molecular aggregation [100]. The gelation phenomenon of cellulose solutions most likely is also driven by hydrophobic interactions. In the previous section 3.3, the enhancement of dissolution performance of NaOH based systems, promoted by the addition of selected cosolutes such as urea or thiourea, was discussed. In this section the stability of the dopes is evaluated.

Materials and methods

The materials and methods used are described in chapter 2.

Results

As discussed above the effect of amphiphilic solvents on the efficiency of dissolution of cellulose samples is remarkable. In alkali based systems, a "simple" change of an inorganic cation, Na^+, by an amphiphilic cation (organic TBA^+) results in a significant enhancement in performance. Higher concentrations of cellulose with larger degrees of polymerization can be dissolved in solvents with the amphiphilic TBA^+. The introduction of molecules with intermediate polarity on the NaOH based solvents also improves not only the dissolution capacity of the solvents but also their stability. As presented in figure 3.16 the shear viscosity of an alkali based solution doped with thiourea, is reduced after 7 days of storage. The same sample without the additive shows an increase in shear viscosity, possibly demonstrating a small aggregation of the cellulose chains.

Stability of cellulose solutions: influence of cyclodextrins

The cellulose dopes produced in aqueous TBAH or TBPH solutions are stable (no gelation is observed) during a long period of time (figure 3.28). Such stability is typically not observed with systems containing inorganic cations. For instance cellulose solutions produced via the viscose process typically gel after one week, limiting the time window for processing.
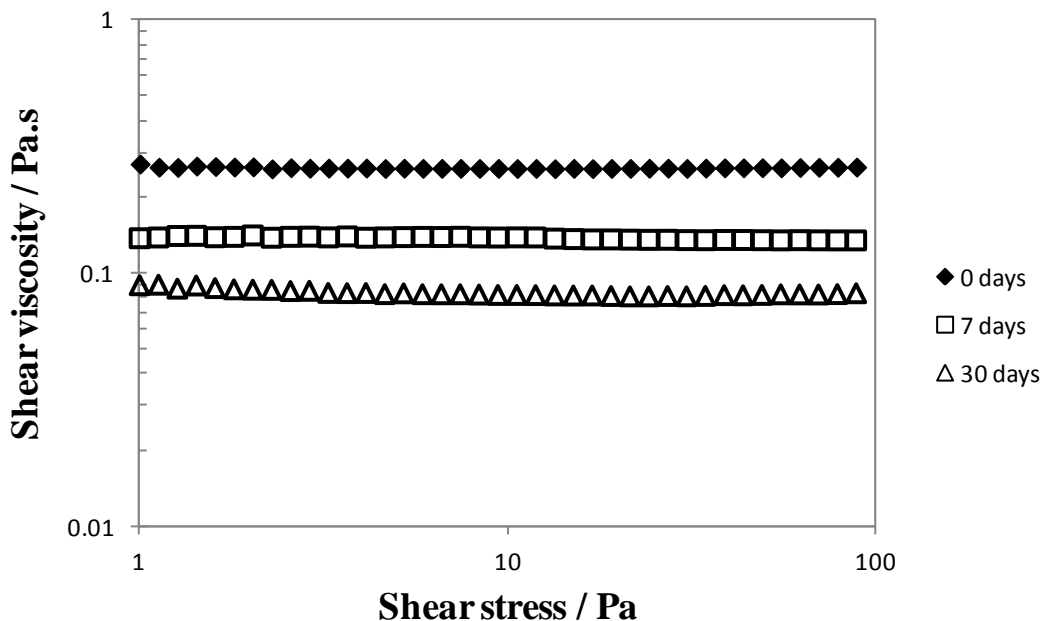
Figure 3.28: Flow curves of 5 wt.% microcrystalline cellulose in aqueous TBAH (1.54 M), as a function of time. Temperature was kept constant at 25 ºC.

In section 3.3 the changes in the quality of cellulose solutions (aqueous TBAH) as a function of salt addition have been discussed. The solubility is observed to decrease by salt addition. However this behavior can be reversed by the addition of a specific ligand to the cation used. The solvent quality is also very much influenced by the concentration of amphiphilic cations available in solution. For instance, in an aqueous solution the reduction of the concentration of TBAH from 1.54 M (40 wt.%) to 1.35 M (35 wt.%) leads to a dramatic decrease in solvent quality. Similar results can be obtained by the addition of a compound capable to encapsulate less hydrophilic species, such as cyclodextrins. In figure 3.29 the transmittance results obtained with the addition of *β*-CD to a solution of cellulose in aqueous TBAH are presented.
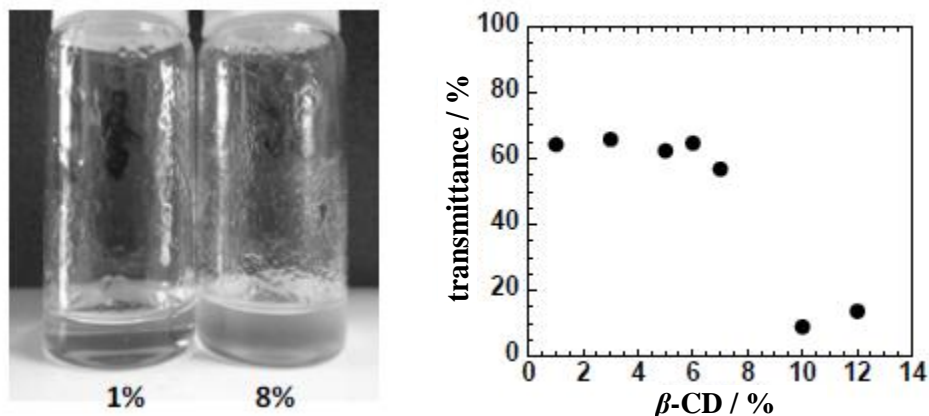
Figure 3.29: Photos and transmittance of cellulose dissolved in strong alkali (TBAH/H$_2$O solution) with progressive addition of β-cyclodextrin. The addition of β-cyclodextrin phase separates the solution (adapted from [206]).

As can be observed, the addition of CD turns a good solvent into a bad solvent, with a clear increase in turbidity of solution and later gelation. A possible mechanism to explain this reduction in solubility is the association of the tetrabutylammonium cation (TBA$^+$) with cyclodextrin, decreasing its availability in solution. As a consequence, the solvent quality becomes poorer and the transmittance considerably decreases until eventually a macroscopically phase separation occurs.

To further confirm this hypothesis, the association between CD and the TBA$^+$ cation was studied by ^{1}H NMR. The stoichiometry of association and binding constants were determined by the continuous variation, CVM, (or Job's plots) and titration methods.

Figure 3.30 shows representative ^{1}H NMR spectra of TBAH (a), β-CD (b) and a mixed β-CD:TBAH (c) solution, at a pH of 12.08. The obtained ^{1}H NMR spectra for β-CD and TBAH are similar to those previously reported [224-226]. Briefly, the ^{1}H NMR spectrum of β-CD in D$_2$O (figure 3.30a) presents (from upfield to downfield) a triplet (assigned to the H$_4$ protons) at δH$_4$ = 3.534 ppm and a doublet of doublets assigned to H$_2$ protons at δH$_2$ = 3.596 ppm. These protons are located outside the cavity of CD, near the narrow and wide sides, respectively. The H$_5$ and H$_6$ (including the anomeric H$_{6'}$) protons overlap at the chemical shift around 3.83 ppm. The H$_3$ protons, located inside the cavity, at the wide side, show a triplet at δH$_3$ = 3.920 ppm. The doublet located at δ = 5.025 ppm is assigned to H$_1$ protons, which are located outside of CD cavity and in between H$_4$ and H$_2$ protons. These chemical shifts show a slight downfield displacement when compared with those ones obtained for non-buffered CD solutions [227].

The ^{1}H NMR spectrum of TBAH (figure 3.30b) shows a triplet assigned to the methyl group (H$_\delta$) at 0.955 ppm, and the ^{1}H NMR assigned to methylene groups shows resonances at 1.370, 1.660 and 3.206 ppm for H$_\gamma$, H$_\beta$ and H$_\alpha$, respectively.

The ^{1}H NMR spectrum of a β-CD:TBAH mixed solution, with a molar ratio r=[TBAH]/[β-CD]=1.01, and with [β-CD]=0.506 mM, is given in figure 3.30c. It can be seen that resonances of CD and TBAH do not overlap; besides, and as can be seen below, upfield shifts ($\Delta\delta=\delta$(mixture)-δ(free)) for tetrabutylammonium protons are observed, whereas for the case of β-CD ^{1}H the presence of TBA$^+$ leads to downfield shifts.
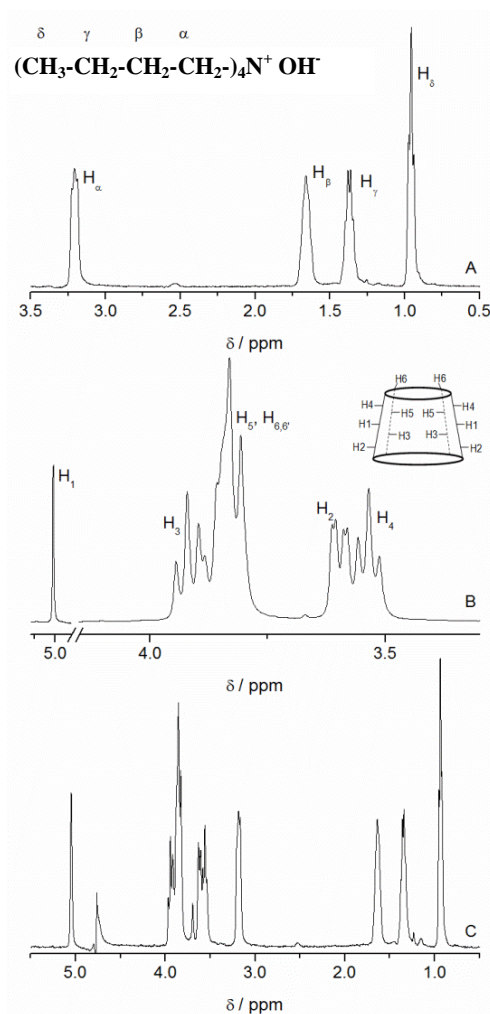
Figure 3.30: ^{1}H NMR spectra of solutions of a) TBAH, 1.02 mM; b) β-CD, 1.01 mM; and c) TBAH and β-CD, $x_{CD} = 0.5$ [228].

To evaluate the possible interaction between TBA$^+$ and β-CD, the stoichiometry and the corresponding binding constants were determined using the continuous variation, CVM, (or Job's plots) and titration methods, respectively [229]. The CVM is based on the

analysis of ^{1}H NMR spectra for a series of β-CD:TBAH mixtures, in which the total concentration of the two species is kept constant (ca.1.0 mM). The stoichiometries are determined by plotting $\Delta\delta$.[β-CD] or $\Delta\delta$.[TBAH] against x_i (where i = TBAH or CD) and finding the x_i values corresponding to the maximum (or minimum) of these distributions [230]. In figure 3.31 the Job's plots are represented. As can be observed, the CD protons, in particular the inner cavity proton H_3, suffer a downfield shift in the presence of TBAH. This may indicate the incorporation of the alkyl chains of TBA$^+$ in the CD cavity and the formation of inclusion complexes as previously suggested. Additionally, the downfield shift is probably a consequence of such supramolecular interaction where the ammonium group of the TBA$^+$ becomes closer to the CD inner cavity protons affecting their chemical environment. It is noted, however, that no significant differences between the different protons of either CD or TBAH, in terms of chemical shift displacements, are observed. On the other hand, an upfield shift is present in all protons of tetrabutylammonium, probably indicating that the presence of CD is inducing an anisotropic magnetic field on those protons.
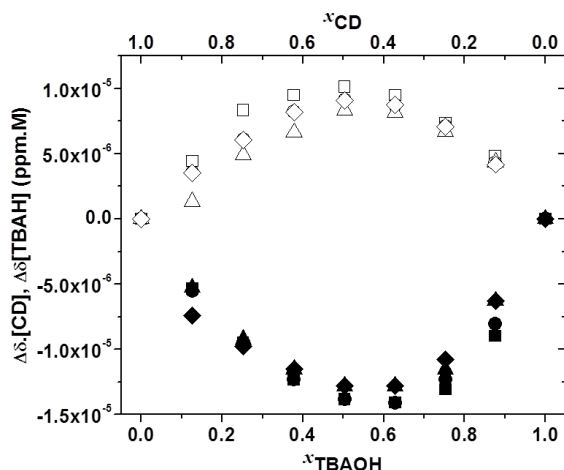
Figure 3.31: Job's plots for TBAH and β-CD protons for mixed TBAH:β-CD solutions. [1]H TBAH: (■) H_α, (●) H_β, (▲) H_γ, (♦) H_δ. [1]H β-CD: (□) H_4, (o) H_3, (Δ) H_1, (◊) H_5. The sum of the concentrations of TBAH and β-CD is kept constant at 1.0 mM [228].

An interesting point that comes out from the analysis of figure 3.31 is that the molar fraction of CD at which a maximum occurs (i.e. x around 0.5) does not perfectly match with the molar fraction of CD at which the minimum is observed (i.e. x $ca.$ 0.6).

In order to have an accurate determination of the inflexion points, a Gauss peak function analysis has been performed and the data are reviewed in table 3.5.

Table 3.5: Molar fractions and corresponding stoichiometry of association between TBAH (m) and β-CD (n) obtained from the CVM [228].

	H_4	H_3	H_1	H_5
x_{CD}	0.499 (0.007)	0.463 (0.004)	0.454 (0.004)	0.463 (0.004)
m:n	1.03 (0.01)	1.16 (0.01)	1.20 (0.01)	1.16 (0.01)
1	H_α	H_β	H_γ	H_δ
x_{TBAH}	0.616 (0.006)	0.590 (0.006)	0.607 (0.008)	0.537 (0.006)
m:n	1.61 (0.02)	1.44 (0.01)	1.55 (0.02)	1.16 (0.01)

Some inconsistency is observed when comparing the stoichiometries of association, as seen by CD or TBAH protons. This may be due to supramolecular interactions not involving exclusively the formation of inclusion complexes. Alternatively, it may be hypothesized that the ammonium group is also playing an important role by interacting electrostatically with hydroxyl groups located in the outside of CD cavity. It should be emphasized that not only hydrophobic interactions lead to an association between CD and a guest molecules; for instance, it has been reported that non-associated inorganic salts can be involved in the formation of "host-guest" complexes although with moderate association constants [231, 232].

Taking into account the stoichiometry of association found by the CVM, the equilibrium formation of the complex can be written as:

$$K = \frac{[CD-G]}{[CD]_f [G]_f} \quad (3.1)$$

where $[CD]_f$ and $[G]_f$ represent the concentration of free (non-complexed) species, β-CD and TBAH, respectively, and $[CD\text{-}G]$ is the concentration of the 1:1 complex.

Considering the corresponding mass balance equations, equation 3.1 can be re-written as:

$$K = \frac{f}{(1-f)([CD]_T - f[G]_T)} \quad (3.2)$$

where f is the fraction of TBAH complexed with the β-CD, and $[CD]_T$ and $[G]_T$ correspond to total concentrations of β-CD and TBAH, respectively.

Assuming fast exchange conditions, the observed chemical shift for a guest species is expressed as:

$$\delta_{exp} = (1-f)\delta_G + f\delta_{CD-G} \quad (3.3)$$

where δ_G and $\delta_{CD\text{-}G}$, represent the chemical shift of a given nucleus when free and complexed, respectively.

The chemical shift displacement of a given nucleus of the TBAH, can be expressed as:

$$\Delta\delta_{exp} = \frac{\Delta\delta_{CD-G}}{[G]_T}[CD-G] \tag{3.4}$$

where $[G]_T$ and $[CD\text{-}G]$ are the initial concentration of TBAH and of complex, respectively; for the 1:1 complex, after some algebraic manipulation and simplification results in

$$\Delta\delta_{exp} = \frac{\Delta\delta_{CD-G}}{2[G]_T}\left\{[G]_T + [CD]_T + \frac{1}{K} - \left(\left([G]_T + [CD]_T + \frac{1}{K}\right)^2 - 4\left([G]_T + [CD]_T\right)\right)^{0.5}\right\} \tag{3.5}$$

where $[CD]_T$ is the initial concentration of the β-CD.

The experimental data (see figure 3.32) can be perfectly fitted by equation 3.5, using a non-linear least-squares algorithm, to obtain the fitting parameters K and $\Delta\delta_{CD\text{-}G}$ (table 3.6).
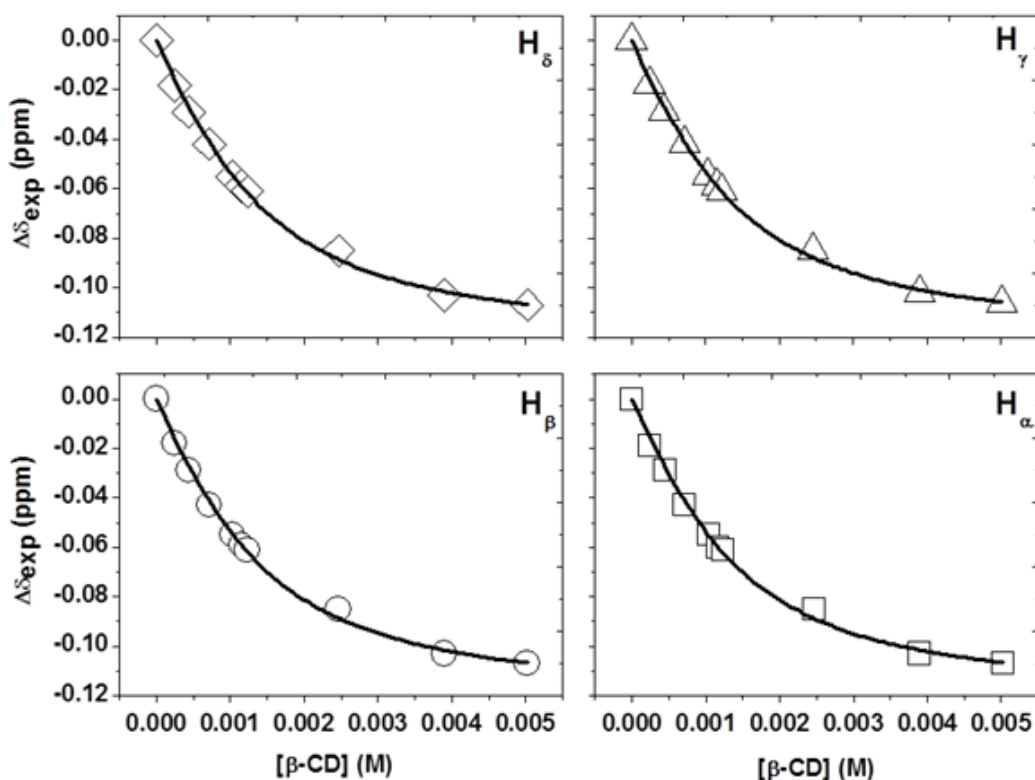
Figure 3.32: Experimental chemical shifts ($\Delta\delta_{exp}$) of TBAH (1.20 mM) protons as a function of β-CD concentration, at 25 ºC [228].

Table 3.6: Fitting parameters of equation 3.5 to experimental data (see figure 3.32) [228].

	CD	**[CD]/mM**	$\Delta\delta_{max}$/ppm	*K*	**R²**
H$_\delta$	β	1.20	−0.124 (±0.003)	1547 (±155)	0.99734
H$_\gamma$	β	1.20	−0.122 (±0.002)	1582 (±132)	0.99818
H$_\beta$	β	1.20	−0.124 (±0.003)	1573 (±166)	0.99704
H$_\alpha$	β	1.20	−0.123 (±0.003)	1616 (±189)	0.99639

R^2 is the correlation coefficient of the fitting of equation 3.5 to experimental data shown in figure 3.32.

The analysis of the data shows that equation 3.5 fits well to the $\Delta\delta$ experimental data. The ^{1}H NMR spectroscopy relies on direct measurements of the free and bound ligand in a solution containing a known amount of the CD and guest (in this case TBAH); consequently, it is possible to determine microscopic association constants [233] once the affinity of the different protons from the guest to the CD environment (or vice-versa) is different. In the present case, the estimated association constants for all protons are rather similar within the corresponding standard deviation (see table 3.6). Nevertheless, it is worth noticing that the *K* values decrease in the order $K(H_\alpha) > K(H_\gamma) > K(H_\beta) > K(H_\delta)$. This is in agreement with the previous discussion where it has been pointed out that, apart from the hydrophobic interactions, the ammonium group is also expected to play a relevant role in the supramolecular interaction.

Stability of cellulose solutions: role of surfactants

In figure 3.33, the viscoelastic properties are plotted as a function of temperature for a system of microcrystalline cellulose (MCC) dissolved in an NaOH aqueous based solvent with (figure 3.33*b*) and without (figure 3.33*a*) an amphiphilic cosolute (betaine derivative surfactant).
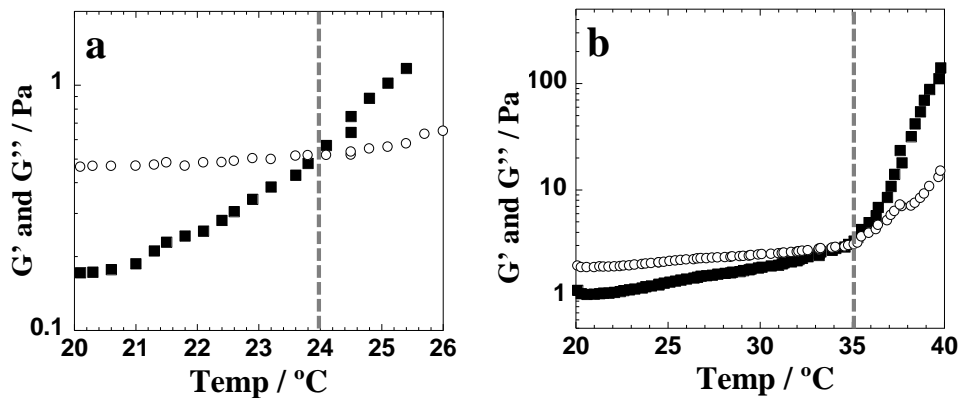
Figure 3.33: Elastic molulus, G' (■), and viscous modulus, G'' (○), versus temperature for 3.5 wt.% microcrystalline cellulose sample dissolved in the 10 wt.% NaOH/H_2O solvent system: (a), without betaine derivative and (b) with betaine derivative. Constant heating rate of 1 ºC/min. The temperature of gelation (G' = G'') is increased ca. 10 ºC in the presence of the amphiphilic additive. The vertical dashed grey line indicates the transition region (adapted from [206]).

Gelation occurs with the temperature increase for both NaOH based systems; however the gelation temperature, T_g, is shifted to higher temperatures, ca. 10 ºC, with the addition of an amphiphilic compound (estimated from the crossover of the storage modulus (G') and loss modulus (G'')). The vertical dashed lines demark the transition region from a liquid-like behavior (G''>G') to a solid-like behavior (G'>G'').

Identical effects are observed for acidic systems; in figure 3.34 is shown the effect of the addition of a surfactant in the gelation temperature of MCC dissolved in a highly concentrated zinc chloride aqueous solution at high temperature.
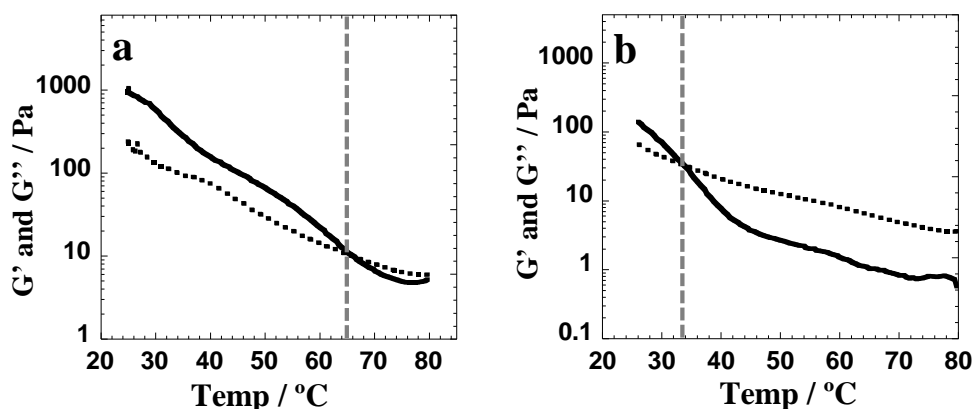
Figure 3.34: Elastic molulus, G', and viscous modulus, G'', versus temperature for 3.5 wt.% microcrystalline cellulose sample dissolved in 60 wt.% $ZnCl_2/H_2O$ solvent system: (a), without betaine derivative and (b) with betaine derivative. Constant cooling rate of 1 ºC/min. The

temperature of gelation, T$_g$, decreased more than 30 ºC in the presence of the amphiphilic additive. The vertical dashed grey line indicates the transition region (adapted from [206]).

For this system, gelation is observed at ca. 65 ºC in the absence of the amphiphilic compound. However, when the amphiphilic additive is present (figure 3.34b), the cellulose dope kept the liquid behavior (G'' > G') for a larger temperature range, shifting the gelation to temperatures below ca. 35 ºC. Even with the obvious differences among the different solvent systems presented and different dissolution procedures, it seems clear that the addition of certain amphiphilic additives leads to similar effects (i.e. an increase in the thermal stability of the cellulose dopes, allowing the solutions to preserve their liquid behavior). Gelation is believed to be due to self-aggregation of the cellulose chains in the solution, with time and/or induced by temperature changes. The increasing number of hydrophobic junction zones between the cellulose chains in the solution can be prevented by the presence of the amphiphilic specie. The obtained results suggest that the amphiphilic cosolute can reduce the hydrophobic interactions, preventing or delaying cellulose aggregation, resulting in an increased thermal and temporal stability.

Synopsis

Dope stability is found to be visibly influenced by the presence of amphiphilic or intermediate polarity species. The results suggest that certain cosolutes can prevent to some extent the hydrophobic association, here suggested to be the driving force for gelation of the solutions. As a consequence, the cellulose dopes increase their thermal and storage stability. For the aqueous TBAH system, a high performance solvent, the presence of an amphiphilic cation seems to be the key factor for the observed high dissolution power.

It has been demonstrated that the solvent capabilities can be controlled by adding β-cyclodextrin, which is suggested to decrease the amount of TBA$^+$ cations available in solution, thus considerably affecting the solubility of cellulose leading to gelation and turbidity of the solutions.

The formation of a host-guest complex is supported by the NMR experiments. The data does suggest the formation of 1:1 β-CD:TBA$^+$ complexes with association constants of

1580 M^{-1}. The worsening of the solvent with CD addition is also striking from the turbidimetry measurements.

3.6 - Regenerated materials: Solvent effect

It is expected that the way cellulose is dissolved and how it organizes in solution has a strong influence on the properties of the regenerated material [198].

A couple of examples can be mentioned. For instance, while in the viscose process (NaOH based solvent), cellulose chains apparently build up a loose network with gel particles, in the lyocell process (N-Methylmorpholine N-oxide (NMMO) based solvent) an entanglement network with highly swollen aggregates is observed [149]. Another study of the solution state of cellulose in NMMO shows the presence of a bimodal distribution of aggregates with up to 1000 chains [191, 234]. In all these cases, it is obvious that the regenerated material (in the form of films, fibers or other) behaves completely different, from a structural level up to mechanical properties, depending on the process used. The differences in mechanical properties of regenerated materials, such as Lyocell and viscose fibers, is mainly due to the differences in the applied regeneration process (i.e. air gap vs. wet spinning) and the associated differences in the draw ratios. However, parameters such as the polymer concentration and the dissolved state are also believed to markedly influence the properties of the regenerated materials and therefore this is an important motivation for a deeper characterization of the cellulose solutions. In this section we focus on acidic and alkaline aqueous solutions.

Here, by means of scanning electron microscopy (SEM) and X-ray powder diffraction (XRD) we report on the effect of distinct solvents, i.e. cold NaOH solutions versus aqueous solution of tetrabutylammonium hydroxide and also the effect of the addition of amphiphilic reagents on alkali based systems, but also acidic systems, on the degree of dissolution and the state of the regenerated cellulose. Additionally, the crystallinity index, estimated from XRD, is also reported for regenerated materials after dissolution in the different media.

Materials and methods

The materials and methods used are described in chapter 2.

Results

The regeneration step in cellulose processing, in order to produce fibers or films, occurs when dissolved cellulose in solution contacts with a coagulation solution, leading to a desolvation of the cellulose molecules and aggregation of the chains, in an arrangement which is influenced by the solution state of cellulose. Molecular aggregation during regeneration of cellulose typically is attributed to rearrangement of the hydrogen bonds (i.e. reformation of the intra- and intermolecular hydrogen bonds) [235]. A more recent view calls the attention to the role of hydrophobic interactions during the regeneration process; this analysis suggests that when the medium surrounding the cellulose molecules becomes energetically unfavorable for molecular dispersion, regeneration starts and the initial process would consist of the stacking of the hydrophobic glucopyranoside rings (driven by hydrophobic interactions), which then would line up by hydrogen bonding to form crystallites [100]. In what follows, the effect of the solvent system and the efficiency of dissolution on the properties of the regenerated materials are discussed.

Alkaline solvents

In figure 3.35 are presented SEM images of regenerated cellulose after dissolved in different alkali based solvent systems.
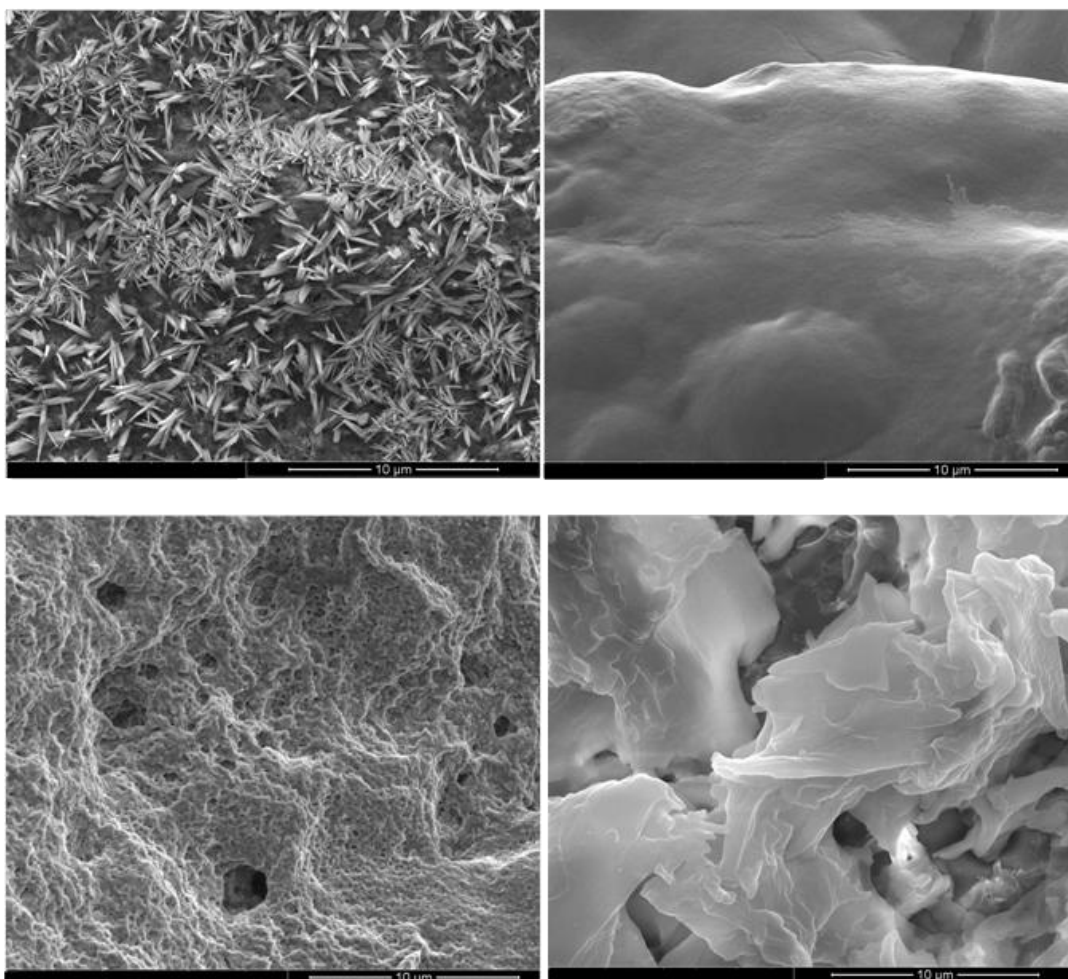
Figure 3.35: SEM images of the cellulosic materials regenerated in acidic medium. Cellulose has been previously dissolved in a NaOH aqueous solution (top left), NaOH/urea aqueous solution (top right), NaOH/thiourea aqueous solution (bottom left) and in TBAH aqueous solution (bottom right).

Needle-like crystallites are present in the material regenerated from sodium alkali solvent; the chains have a tendency to aggregate mainly side-by-side during precipitation, building up a complex crystalline structure. Also the incomplete dissolution observed for this system (discussed in section 3.3) should contribute to the crystalline structures formed. In acidic coagulation media, the H^+ assumes a key role in cellulose regeneration by neutralizing the alkaline content and, therefore, one can speculate that as cellulose becomes less charged, this leads to a hydrophobic aggregation of the cellulose chains. It is important to note that in SEM images of cellulose dissolved in aqueous NaOH (figure 3.11) crystallites are observed in solution; it is expected that these crystallites can also aggregate and thus a very crystalline material is obtained in the end. On the other hand, the solvents containing additives of

intermediate polarity, such as urea or thiourea, lead to "softer" morphologies after regeneration (no needle-like crystals are observed). Additionally, porous materials are also observed.

The SEM images of the regenerated materials dissolved in the TBAH-based solvent show also a much softer structure when compared with the resultant from the NaOH based solvent. The "continuous wrinkled-film type" morphology is still observed in some areas but, in most cases, the surface is flattened and seems to be constituted by aggregated sheets of cellulose molecules. This cellulose sheet-by-sheet stacking fits the proposed mechanism based on hydrophobic association. This rearrangement of cellulose chains that produces soft surface morphologies is obviously facilitated if the structure of the cellulose in solution is closer to a molecular dispersion state than to an aggregated state; the expected flexibility of the former is opposed to the rigidity of the latter. In other words, the flexibility of the film deduced by the flattening of the cellulose surface upon regeneration indicates a material with low crystallinity, i.e. highly crystalline samples would hardly adopt such flexible conformations and morphologies. As alluded to, such rigidity is expected to be correlated with the degree of crystallinity and this can be inferred from X-ray diffraction.

In figure 3.36 the X-ray diffraction patterns of the native cellulose and the regenerated materials from the alkali based systems are presented.
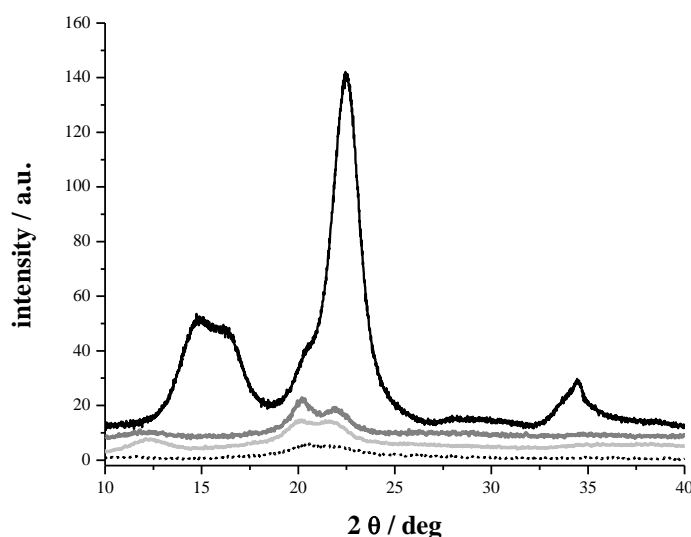
Figure 3.36: X-ray diffraction patterns for native MCC (full black curve), and regenerated materials from MCC dissolved in aqueous NaOH (dark grey curve), in aqueous NaOH/thiourea (light grey curve) and in aqueous TBAH (dotted curve).

The use of additives with amphiphilic properties such as urea, thiourea or alkyl-polyglucoside surfactant (APG) in the NaOH system or using a solvent with amphiphilic cations (TBAH) considerably reduces the crystallinity of the native MCC. Regarding the position of the diffraction peaks, the starting MCC material presents a major sharp diffraction centered at ca. 22.5º (002) with a side peak at 20.5° (021) typical for a cellulose I crystalline organization [165]. Other characteristic reflections of the cellulose I type structure can be found at 14.7º (101), 16.6º (10$\bar{1}$) and 34.7º (040). When cellulose is dissolved in the NaOH aqueous solution or in the NaOH/thiourea system, the regenerated structure changes to a cellulose II type arrangement with two main diffraction peaks centred at 20.1º (10$\bar{1}$) and 21.9º (002). A small bump at ca. 12.3º is indicative of a 101 lattice plane, also characteristic of a cellulose II crystal organization [165].

On the other hand, a more amorphous material with no detectable diffraction peaks is obtained when cellulose is regenerated from the TBAH aqueous system. The X-ray data are in good agreement with the NMR and SEM data.

The estimated crystallinity index of the materials, using the X-ray diffraction data (equation 2.1), shows CrI values of 85 and 82% for the native cellulose and that regenerated from NaOH solution, respectively; on the other hand, it was not possible to determine the CrI from the TBAH based solutions due to its amorphous nature [190]. It is important to keep in mind that although these values are not absolute, they provide good indications and correlate well with the SEM results.

Acidic solvents

Despite the chemical degradation of cellulose in most of the acidic systems studied, it is still possible to regenerate and precipitate cellulose using a non-solvent such as pure water or slightly alkaline solutions. In figure 3.37, electron micrographs of the regenerated cellulose from the acid solutions are presented. In some cases surfactants have been use to increase not only the dissolution efficiency but also to increase the stability of the dopes.
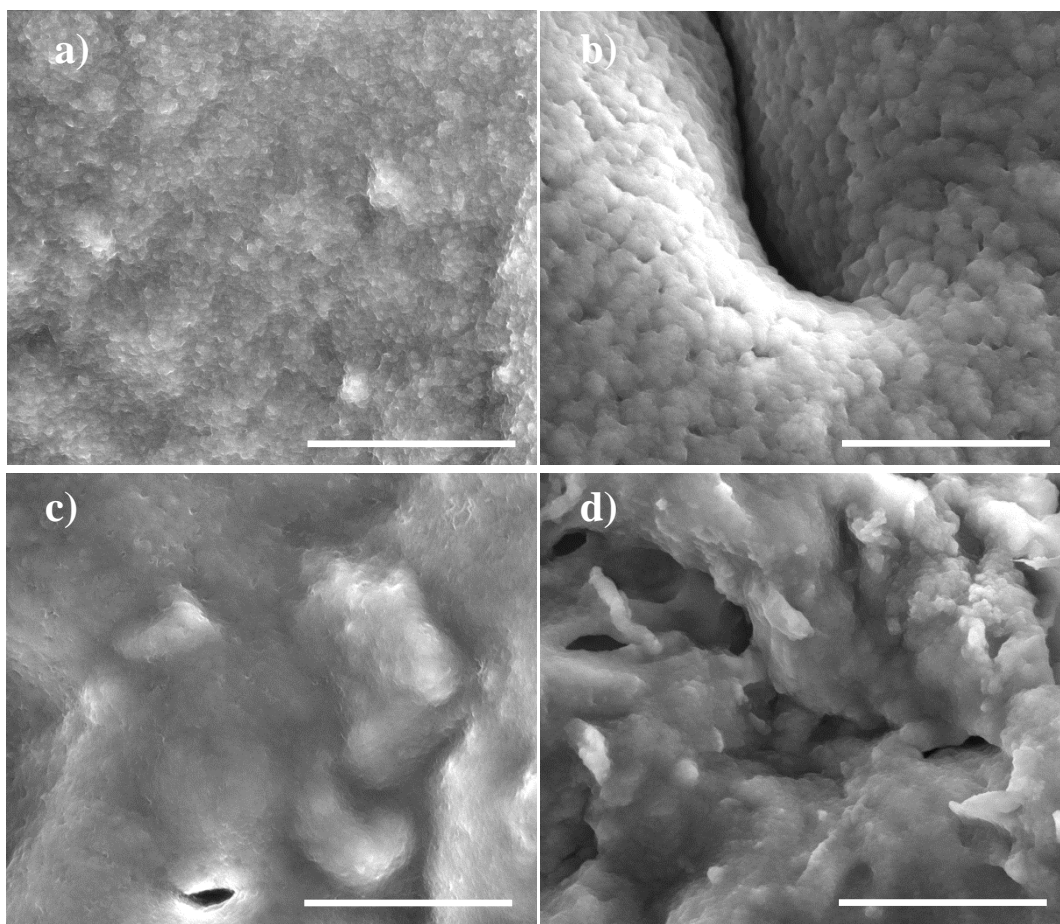
Figure 3.37: SEM images of regenerated materials in water. Cellulose has been previously dissolved in a) H_3PO_4 aqueous solution, b) in H_3PO_4/surfactant aqueous solution, c) in $ZnCl_2$ aqueous solution and d) in $ZnCl_2$/surfactant aqueous solution. The scale bars represent 10 µm.

As can be observed, all the regenerated samples present a smooth morphology, indicating the presence of low crystalline materials [190]. The considerable molecular weight decrease in the H_2SO_4/glycerol system makes the regeneration of any material unfeasible. Interestingly, the addition of surfactants to the acidic solvents results in what appears to be more porous materials when compared with the analogue systems without surfactant. The local increase of curvature in the cellulose reorganization induced by the surfactants may explain this behaviour but further work is being performed to understand the phenomenon.

The low crystallinity of the regenerated materials as being suggested by the SEM images is confirmed from the X-ray measurements.
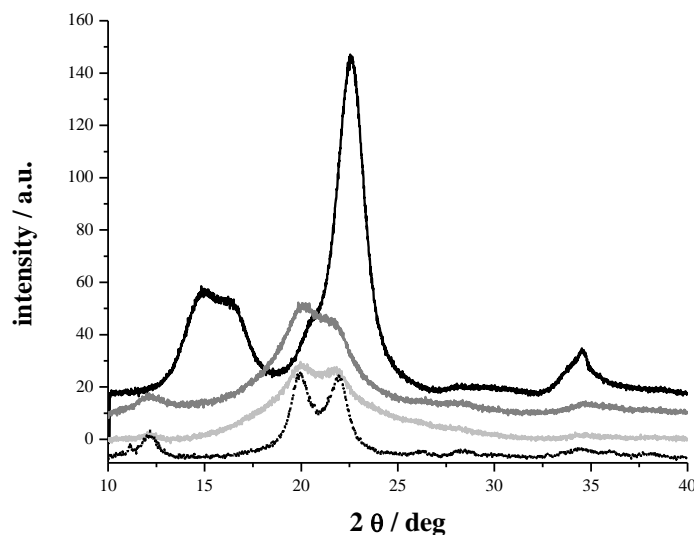
Figure 3.38: X-ray diffraction patterns for microcrystalline cellulose (black line), and regenerated materials from a solution of microcrystalline cellulose dissolved in H_3PO_4 aqueous (grey line), from a solution of microcrystalline cellulose dissolved in H_3PO_4/surfactant aqueous (light grey line) and from $ZnCl_2$ aqueous (dotted line).

Figure 3.38 clearly indicates a reduction in the crystallinity of the regenerated materials obtained from all the tested acidic solvent systems. Moreover, a change in the cellulose chain arrangement can be observed; while a typical cellulose I crystalline organization is obtained for the starting material, a cellulose II polymorph is obtained for the regenerated materials: for the H_3PO_4 and $ZnCl_2$ aqueous systems, the Bragg reflections are found at 12.2º ($1\bar{1}0$), 19.9º (110) and 22.0º (200) [109, 236]. The addition of a surfactant to the H_3PO_4 aqueous system, results in a change of the packing of the cellulose chains in the regenerated materials with reflections at 20.0 (110) and 21.8º (200), but without the reflection of the plane ($1\bar{1}0$) [236]. This might indicate a more amorphous material in comparison to the analogous surfactant-free system. Overall, the X-ray data are in good agreement with the SEM and PT ssNMR results.

Synopsis

In this section we have discussed the influence of the solvent system on the properties of regenerated cellulosic materials. There are significant differences in morphology and crystallinity of the precipitated materials depending on the solvent used. It is striking

that while the samples dissolved in NaOH exhibit a quite high crystallinity, with needle-like crystallites observed in SEM and higher CrI estimated from XRD, the cellulose samples obtained from NaOH/thiourea solution show a decrease in crystallinity while the materials from the TBAH solution lose considerably their crystallinity, presenting flexible continuous wrinkled-film type morphology; no CrI can be estimated from the XRD data. Similarly, materials regenerated from acidic solvents structurally tend to present smooth morphologies as expected for materials with low crystallinity.

The level of dissolution has implications for the properties of the regenerated materials; while for TBAH the lack of crystallinity and high flexibility of the regenerated materials indicate that dissolution progresses close to the molecular level, in the case of the NaOH dissolution is not complete and stable cellulose aggregates (crystallites) are still present in solution. The light scattering data indicates the presence of fairly small cellulose particles in the TBAH system (ca. 10–20 nm) while considerably larger cellulose particles (above 200 nm) are found for the NaOH system. The reduction in solvent polarity, obtained by addition of urea or thiourea results also in less crystalline materials, showing an improvement in solvent quality.

Smooth materials were obtained from solutions made in acidic solvents, which is indicative of the good dissolution level achieved when these solvents are used. The good performance of the acidic systems is clear, but the molecular weight decrease might be problematic for certain applications such as the fiber or film production. In these cases alternative strategies should be considered to prevent cellulose degradation such as the reduction of temperature or the addition of different additives or co-solvents.

<div align="right">

CHAPTER 4

</div>

Conclusions

      A wide range of solvents for cellulose were used during this study. In addition new methods were implemented to study cellulose in solution such as the polarization transfer solid state NMR (PT ssNMR). The technique is very useful; both solid and liquid fractions can be studied in one single experiment. Another interesting utility of this technique is the capability of detection of cellulose degradation products.

On the other hand, the successful extraction and characterization of CNCs from the cellulose derivatives (CMC and HPMC), that surprisingly were found to be significantly crystalline (cellulose II polymorph), allows the extraction of CNCs presenting a different crystal organization (cellulose I polymorph). This further suggests that there are specific parts of cellulose chains that remain insoluble during all the modification process. This is indicative of the major difficulty in obtaining molecular dispersed cellulose solutions.

During the studies, fundamental differences between the use of a small inorganic cation of high charge density and a large organic cation with amphiphilic character were found. Combining microscopic techniques, PT ssNMR and DLS it is possible to conclude that the use of an amphiphilic cation leads to cellulose dissolution down to the molecular level (or close to it) whereas this is not the case for the sodium ion. Furthermore, the addition of certain additives of intermediate polarity to NaOH based systems improves the dissolution efficiency. That dissolution into molecular solutions provides good support for the view that cellulose molecules have both polar and nonpolar regions and have a strong tendency to associate by hydrophobic interactions.

Dissolution and dope stability are found to be clearly influenced by the presence of amphiphilic species. Moreover, we have seen that combining cellulose ionization (either

achieved by extreme pH or adsorption of ionic species) with the weakening of the hydrophobic effect (for example by adding urea or thiourea) makes dissolution more efficient. For the TBAH system, a high performance solvent, the presence of an amphiphilic cation seems to be the key factor for an improved dissolution capacity; the solvent capabilities can be controlled and even reversed, thus decreasing the solvent capabilities, by the addition of salt (i.e. reducing the counterion entropy effect).

The dope stability of cellulose in aqueous TBAH can be reduced by adding β-cyclodextrin (suggested to trap the amphiphilic cations of the solvent) which decreases the concentration of free TBA$^+$ cations in solution and thus dramatically decreases the solubility of cellulose.

Acidic systems demonstrate good ability to dissolve cellulose, both in aqueous based systems and in non-aqueous ones. Although efficient, severe degradation might occur which can be a serious drawback for certain applications where a high degree of polymerization is required. In these cases, alternative strategies should be considered to prevent cellulose degradation such as the reduction of temperature or the addition of different additives or co-solvents.

Finally we have discussed the influence of the solvent system on the properties of the regenerated cellulosic materials. There are significant differences in morphology and crystallinity of the precipitated materials depending on the solvent used. It is striking that while the samples dissolved in NaOH exhibit a quite high crystallinity, with needle-like crystallites observed in SEM and higher CrI estimated from XRD, the cellulose samples obtained from NaOH/thiourea solutions show a decrease in crystallinity while the materials from the TBAH solution lose considerably their crystallinity, presenting flexible continuous wrinkled-film type morphology. Similarly, materials regenerated from acidic solvents structurally tend to present smooth morphologies as expected for materials with low crystallinity, which is indicative of the good dissolution level achieved when these solvents are used.

The level of dissolution is expected to have implications on the properties of the regenerated materials; while for TBAH the lack of crystallinity and high flexibility of the regenerated materials indicate that dissolution progresses close to the molecular level, in the case of the NaOH dissolution is not complete and stable cellulose aggregates (crystallites) are still present in solution.

<div align="right">

CHAPTER 5

</div>

References

[1] R.J. Moon, A. Martini, J. Nairn, J. Simonsen, J. Youngblood, Cellulose nanomaterials review: structure, properties and nanocomposites, Chemical Society Reviews, 40 (2011) 3941-3994.

[2] D. Klemm, B. Philipp, T. Heinze, U. Heinze, W. Wagenknecht, in: "Fundamentals and analytical methods. Comprehensive Cellulose Chemistry (vol 1)", Wiley - VCH, Weinheim, (1998).

[3] C. Chang, L. Zhang, Cellulose-based hydrogels: Present status and application prospects, Carbohydrate Polymers, 84 (2011) 40-53.

[4] X. Qiu, S. Hu, "Smart" Materials Based on Cellulose: A Review of the Preparations, Properties, and Applications, Materials, 6 (2013) 738.

[5] V.K. Varshney, S. Naithani, Chemical Functionalization of Cellulose Derived from Nonconventional Sources, in: S. Kalia, B.S. Kaith, I. Kaur (Eds.) Cellulose Fibers: Bio- and Nano-Polymer Composites, Springer Berlin Heidelberg, 2011, pp. 43-60.

[6] B. Medronho, B. Lindman, Competing forces during cellulose dissolution: From solvents to mechanisms, Curr. Opin. Colloid Interface Sci., 19 (2014) 32-40.

[7] J.T. Marsh, An introduction to the chemistry of cellulose, 2nd edn. Chapman & Hall, London, (1942).

[8] H. Krässig, J. Schurz, R.G. Steadman, K. Schliefer, W. Albrecht, M. Mohring, H. Schlosser, Cellulose, in: Ullmann's Encyclopedia of Industrial Chemistry, Wiley-VCH Verlag GmbH & Co. KGaA, 2000.

[9] D. Klemm, B. Heublein, H.P. Fink, A. Bohn, Cellulose: Fascinating biopolymer and sustainable raw material, Angewandte Chemie-International Edition, 44 (2005) 3358-3393.

[10] N.T. Thuong, C. Hélène, Sequence-Specific Recognition and Modification of Double-Helical DNA by Oligonucleotides, Angewandte Chemie International Edition in English, 32 (1993) 666-690.

[11] B. Lindman, R.S. Dias, M.G. Miguel, M.C. Morán, D. Costa, Manipulation of DNA by Surfactants, in: Highlights in Colloid Science, Wiley-VCH Verlag GmbH & Co. KGaA, 2008, pp. 179-202.

[12] B. Lindman, G. Karlström, L. Stigsson, On the mechanism of dissolution of cellulose, Journal of Molecular Liquids, 156 (2010) 76-81.

[13] B. Medronho, A. Romano, M.G. Miguel, L. Stigsson, B. Lindman, Rationalizing cellulose (in)solubility: reviewing basic physicochemical aspects and role of hydrophobic interactions, Cellulose, 19 (2012) 581-587.

[14] M. Bergenstråhle, J. Wohlert, M.E. Himmel, J.W. Brady, Simulation studies of the insolubility of cellulose, Carbohydrate Research, 345 (2010) 2060-2066.

[15] A. O'Sullivan, Cellulose: the structure slowly unravels, Cellulose, 4 (1997) 173-207.

[16] R.A. Festucci-Buselli, W.C. Otoni, C.P. Joshi, Structure, organization, and functions of cellulose synthase complexes in higher plants, Brazilian Journal of Plant Physiology, 19 (2007) 1-13.

[17] L. Tim, Cellulose Solvents ? Remarkable History, Bright Future, in: Cellulose Solvents: For Analysis, Shaping and Chemical Modification, American Chemical Society, 2010, pp. 3-54.

[18] D. Klemm, B. Heublein, H.-P. Fink, A. Bohn, Cellulose: Fascinating Biopolymer and Sustainable Raw Material, Angewandte Chemie International Edition, 44 (2005) 3358-3393.

[19] S. Sen, J.D. Martin, D.S. Argyropoulos, Review of Cellulose Non-Derivatizing Solvent Interactions with Emphasis on Activity in Inorganic Molten Salt Hydrates, ACS Sustainable Chemistry & Engineering, 1 (2013) 858-870.

[20] B. Medronho, B. Lindman, Competing forces during cellulose dissolution: From solvents to mechanisms, Current Opinion in Colloid & Interface Science, 19 (2014) 32-40.

[21] O. Biermann, E. Hädicke, S. Koltzenburg, F. Müller-Plathe, Hydrophilicity and Lipophilicity of Cellulose Crystal Surfaces, Angewandte Chemie International Edition, 40 (2001) 3822-3825.

[22] C. Yamane, T. Aoyagi, M. Ago, K. Sato, K. Okajima, T. Takahashi, Two Different Surface Properties of Regenerated Cellulose due to Structural Anisotropy, Polym. J, 38 (2006) 819-826.

[23] H. Miyamoto, M. Umemura, T. Aoyagi, C. Yamane, K. Ueda, K. Takahashi, Structural reorganization of molecular sheets derived from cellulose II by molecular dynamics simulations, Carbohyd Res, 344 (2009) 1085-1094.

[24] M. Bergenstrahle, K. Mazeau, L.A. Berglund, Molecular modeling of interfaces between cellulose crystals and surrounding molecules: Effects of caprolactone surface grafting, Eur Polym J, 44 (2008) 3662-3669.

[25] A.S. Gross, J.W. Chu, On the Molecular Origins of Biomass Recalcitrance: The Interaction Network and Solvation Structures of Cellulose Microfibrils, J Phys Chem B, 114 (2010) 13333-13341.

[26] H.M. Cho, A.S. Gross, J.-W. Chu, Dissecting Force Interactions in Cellulose Deconstruction Reveals the Required Solvent Versatility for Overcoming Biomass Recalcitrance, J Am Chem Soc, 133 (2011) 14033-14041.

[27] B. Medronho, B. Lindman, Brief overview on cellulose dissolution/regeneration interactions and mechanisms, Advances in Colloid and Interface Science.

[28] D. Klemm, B. Philipp, T. Heinze, U. Heinze, W. Wagenknecht, Fundamentals and Analytical Methods. Comprehensive Cellulose Chemistry, Wiley-VCH Verlag GmbH & Co. KGaA, 1998.

[29] F.J. Kolpak, J. Blackwell, The Structure of Regenerated Cellulose, Macromolecules, 8 (1975) 563-564.

[30] S. Raymond, A. Kvick, H. Chanzy, The Structure of Cellulose II: A Revisit, Macromolecules, 28 (1995) 8422-8425.

[31] M. Takai, J.R. Colvin, Mechanism of transition between cellulose I and cellulose II during mercerization, Journal of Polymer Science: Polymer Chemistry Edition, 16 (1978) 1335-1342.

[32] T. Okano, A. Sarko, Mercerization of cellulose. II. Alkali–cellulose intermediates and a possible mercerization mechanism, Journal of Applied Polymer Science, 30 (1985) 325-332.

[33] S. Bo, T. Vasily, W. James, Biopolymers, Processing, and Biodegradation, in: Renewable and Sustainable Polymers, American Chemical Society, 2011, pp. 117-132.

[34] M. Poletto, A.J. Zattera, V. Pistor, Structural Characteristics and Thermal Properties of Native Cellulose, 2013.

[35] J.T. Marsh, An Introduction to the Chemistry of Cellulose, 2nd ed., Chapman & Hall, London, 1942.

[36] S.M. Hudson, J.A. Cuculo, The Solubility of Unmodified Cellulose: A Critique of the Literature, Journal of Macromolecular Science, Part C, 18 (1980) 1-82.

[37] T. Heinze, A. Koschella, Solvents applied in the field of cellulose chemistry: a mini review, Polímeros, 15 (2005) 84-90.

[38] T. Huber, J. Müssig, O. Curnow, S. Pang, S. Bickerton, M. Staiger, A critical review of all-cellulose composites, J Mater Sci, 47 (2012) 1171-1186.

[39] F. Fu, Q. Yang, J. Zhou, H. Hu, B. Jia, L. Zhang, Structure and Properties of Regenerated Cellulose Filaments Prepared from Cellulose Carbamate–NaOH/ZnO Aqueous Solution, ACS Sustainable Chemistry & Engineering, 2 (2014) 2604-2612.

[40] E. Schweizer, Das Kupferoxyd-Ammoniak, ein Auflösungsmittel für die Pflanzenfaser, Journal für Praktische Chemie, 72 (1857) 109-111.

[41] I. ASTM, Standard Test Method for Viscosity of Cellulose by Cuprammonium Ball Fall, in, 2003, pp. 7 pages.

[42] K. Saalwächter, W. Burchard, P. Klüfers, G. Kettenbach, P. Mayer, D. Klemm, S. Dugarmaa, Cellulose Solutions in Water Containing Metal Complexes†, Macromolecules, 33 (2000) 4094-4107.

[43] W.B. Achwal, A.B. Gupta, Studies in a modified cadoxen solvent, Die Angewandte Makromolekulare Chemie, 2 (1968) 190-203.

[44] K. Kamide, K. Okajima, K. Kowsaka, Dissolution of Natural Cellulose into Aqueous Alkali Solution: Role of Super-Molecular Structure of Cellulose, Polym J, 24 (1992) 71-86.

[45] T. Yamashiki, T. Matsui, M. Saitoh, K. Okajima, K. Kamide, T. Sawada, Characterisation of cellulose treated by the steam explosion method. Part 1: Influence of cellulose resources on changes in morphology, degree of polymerisation, solubility and solid structure, British Polymer Journal, 22 (1990) 73-83.

[46] T. Yamashiki, K. Kamide, K. Okajima, K. Kowsaka, T. Matsui, H. Fukase, Some Characteristic Features of Dilute Aqueous Alkali Solutions of Specific Alkali Concentration (2.5 mol l-1) Which Possess Maximum Solubility Power against Cellulose, Polym J, 20 (1988) 447-457.

[47] L.H. Bock, Water-Soluble Cellulose Ethers, Industrial & Engineering Chemistry, 29 (1937) 985-987.

[48] L. Yan, Z. Gao, Dissolving of cellulose in PEG/NaOH aqueous solution, Cellulose, 15 (2008) 789-796.

[49] J. Cai, L. Zhang, Rapid Dissolution of Cellulose in LiOH/Urea and NaOH/Urea Aqueous Solutions, Macromolecular Bioscience, 5 (2005) 539-548.

[50] L. Zhang, D. Ruan, S. Gao, Dissolution and regeneration of cellulose in NaOH/thiourea aqueous solution, Journal of Polymer Science Part B: Polymer Physics, 40 (2002) 1521-1529.

[51] S. Fischer, H. Leipner, K. Thümmler, E. Brendler, J. Peters, Inorganic Molten Salts as Solvents for Cellulose, Cellulose, 10 (2003) 227-236.

[52] M. Hattori, Y. Shimaya, M. Saito, Solubility and Dissolved Cellulose in Aqueous Calcium- and Sodium-Thiocyanate Solution, Polym J, 30 (1998) 49-55.

[53] X. Lu, X. Shen, Solubility of bacteria cellulose in zinc chloride aqueous solutions, Carbohydrate Polymers, 86 (2011) 239-244.

[54] S. Kuga, The porous structure of cellulose gel regenerated from calcium thiocyanate solution, Journal of Colloid and Interface Science, 77 (1980) 413-417.

[55] H. Leipner, S. Fischer, E. Brendler, W. Voigt, Structural changes of cellulose dissolved in molten salt hydrates, Macromolecular Chemistry and Physics, 201 (2000) 2041-2049.

[56] O. El Seoud, T. Heinze, Organic Esters of Cellulose: New Perspectives for Old Polymers, in: T. Heinze (Ed.) Polysaccharides I, Springer Berlin Heidelberg, 2005, pp. 103-149.

[57] A. Isogai, A. Ishizu, J. Nakano, Dissolution mechanism of cellulose in SO2–amine–dimethylsulfoxide, Journal of Applied Polymer Science, 33 (1987) 1283-1290.

[58] T. Heinze, R. Dicke, A. Koschella, A.H. Kull, E.-A. Klohr, W. Koch, Effective preparation of cellulose derivatives in a new simple cellulose solvent, Macromolecular Chemistry and Physics, 201 (2000) 627-631.

[59] C.L. McCormick, D.K. Lichatowich, Homogeneous solution reactions of cellulose, chitin, and other polysaccharides to produce controlled-activity pesticide systems, Journal of Polymer Science: Polymer Letters Edition, 17 (1979) 479-484.

[60] K.E. Perepelkin, Lyocell fibres based on direct dissolution of cellulose in N-methylmorpholine N-oxide: Development and prospects, Fibre Chem, 39 (2007) 163-172.

[61] R.P. Swatloski, S.K. Spear, J.D. Holbrey, R.D. Rogers, Dissolution of Cellose with Ionic Liquids, Journal of the American Chemical Society, 124 (2002) 4974-4975.

[62] A. Pinkert, K.N. Marsh, S. Pang, M.P. Staiger, Ionic Liquids and Their Interaction with Cellulose, Chemical Reviews, 109 (2009) 6712-6728.

[63] H. Zhang, J. Wu, J. Zhang, J. He, 1-Allyl-3-methylimidazolium Chloride Room Temperature Ionic Liquid: A New and Powerful Nonderivatizing Solvent for Cellulose, Macromolecules, 38 (2005) 8272-8277.

[64] Y. Fukaya, K. Hayashi, M. Wada, H. Ohno, Cellulose dissolution with polar ionic liquids under mild conditions: required factors for anions, Green Chemistry, 10 (2008) 44-46.

[65] Y. Fukaya, A. Sugimoto, H. Ohno, Superior Solubility of Polysaccharides in Low Viscosity, Polar, and Halogen-Free 1,3-Dialkylimidazolium Formates, Biomacromolecules, 7 (2006) 3295-3297.

[66] N. Sun, M. Rahman, Y. Qin, M.L. Maxim, H. Rodriguez, R.D. Rogers, Complete dissolution and partial delignification of wood in the ionic liquid 1-ethyl-3-methylimidazolium acetate, Green Chemistry, 11 (2009) 646-655.

[67] D.M. Phillips, L.F. Drummy, D.G. Conrady, D.M. Fox, R.R. Naik, M.O. Stone, P.C. Trulove, H.C. De Long, R.A. Mantz, Dissolution and Regeneration of Bombyx mori Silk Fibroin Using Ionic Liquids, Journal of the American Chemical Society, 126 (2004) 14350-14351.

[68] Y. Zhao, X. Liu, J. Wang, S. Zhang, Effects of Cationic Structure on Cellulose Dissolution in Ionic Liquids: A Molecular Dynamics Study, ChemPhysChem, 13 (2012) 3126-3133.

[69] H. Garcia, R. Ferreira, M. Petkovic, J.L. Ferguson, M.C. Leitao, H.Q.N. Gunaratne, K.R. Seddon, L.P.N. Rebelo, C. Silva Pereira, Dissolution of cork biopolymers in biocompatible ionic liquids, Green Chemistry, 12 (2010) 367-369.

[70] F.P. Burns, P.-A. Themens, K. Ghandi, Assessment of phosphonium ionic liquid-dimethylformamide mixtures for dissolution of cellulose, Composite Interfaces, 21 (2013) 59-73.

[71] H. Sixta, A. Michud, L. Hauru, S. Asaadi, Y. Ma, A.W.T. King, I. Kilpeläinen, M. Hummel, Ioncell-F: A High-strength regenerated cellulose fibre, Nordic Pulp and Paper Research Journal, 30 (2015) 43-57.

[72] A. MICHUD, A. King, A. Parviainen, H. Sixta, L. HAURU, M. Hummel, I. KILPELÄINEN, Process for the production of shaped cellulose articles (WO 2014162062 A1), in, 2014.

[73] E. Gaidamauskas, E. Norkus, E. Butkus, D.C. Crans, G. Grincienė, Deprotonation of β-cyclodextrin in alkaline solutions, Carbohydrate Research, 344 (2009) 250-254.

[74] C. Yamane, H. Miyamoto, D. Hayakawa, K. Ueda, Folded-chain structure of cellulose II suggested by molecular dynamics simulation, Carbohydrate Research, 379 (2013) 30-37.

[75] D.L. Morgado, E. Frollini, Thermal decomposition of mercerized linter cellulose and its acetates obtained from a homogeneous reaction, Polímeros, 21 (2011) 111-117.

[76] B. Morgenstern, H.-W. Kammer, On the particulate structure of cellulose solutions, Polymer, 40 (1999) 1299-1304.

[77] D.M. Rein, R. Khalfin, N. Szekely, Y. Cohen, True molecular solutions of natural cellulose in the binary ionic liquid-containing solvent mixtures, Carbohydrate Polymers, 112 (2014) 125-133.

[78] K. Le, R. Sescousse, T. Budtova, Influence of water on cellulose-EMIMAc solution properties: a viscometric study, Cellulose, 19 (2012) 45-54.

[79] H. Liu, K.L. Sale, B.M. Holmes, B.A. Simmons, S. Singh, Understanding the Interactions of Cellulose with Ionic Liquids: A Molecular Dynamics Study, The Journal of Physical Chemistry B, 114 (2010) 4293-4301.

[80] E. Wernersson, B. Stenqvist, M. Lund, The mechanism of cellulose solubilization by urea studied by molecular simulation, Cellulose, (2015) 1-11.

[81] E.A. Grulke, Solubility parameter values. In: Brandrup J, Immergut EH, Grulke EA,, editors, 4th ed. Polymer handbook, vol. 7. New York, NY: Wiley, (1999).

[82] K. Holmberg, B. Jonsson, B. Kronberg, B. Lindman, Surfactants and polymers in aqueous solution. Wiley, Hoboken, (2002).

[83] J.B. Taylor, The water solubilities and heats of solution of short chain cellulosic oligosaccharides, Transactions of the Faraday Society, 53 (1957) 1198-1203.

[84] A. Brandt, J. Grasvik, J.P. Hallett, T. Welton, Deconstruction of lignocellulosic biomass with ionic liquids, Green Chem, 15 (2013) 550-583.

[85] M. Bergenstrahle, J. Wohlert, M.E. Himmel, J.W. Brady, Simulation studies of the insolubility of cellulose, Carbohyd Res, 345 (2010) 2060-2066.

[86] A.C. O'Sullivan, Cellulose: the structure slowly unravels, Cellulose, 4 (1997) 173-208.

[87] R.H. Atalla, D.L. Vanderhart, Native Cellulose - a Composite of 2 Distinct Crystalline Forms, Science, 223 (1984) 283-285.

[88] S.K. Cousins, R.M. Brown, Cellulose-I Microfibril Assembly - Computational Molecular Mechanics Energy Analysis Favors Bonding by Vanderwaals Forces as the Initial Step in Crystallization, Polymer, 36 (1995) 3885-3888.

[89] N. Isobe, K. Noguchi, Y. Nishiyama, S. Kimura, M. Wada, S. Kuga, Role of urea in alkaline dissolution of cellulose, Cellulose, 20 (2013) 97-103.

[90] C. Tanford, Isothermal Unfolding of Globular Proteins in Aqueous Urea Solutions, J Am Chem Soc, 86 (1964) 2050-&.

[91] M.C. Stumpe, H. Grubmüller, Polar or Apolar—The Role of Polarity for Urea-Induced Protein Denaturation, PLoS Computational Biology, 4 (2008) e1000221.

[92] H.J.Y. El-Aila, Effect of urea and salt on micelle formation of zwitterionic surfactants, J Surfact Deterg, 8 (2005) 165-168.

[93] T. Koishi, K. Yasuoka, X.C. Zeng, S. Fujikawa, Molecular dynamics simulations of urea-water binary droplets on flat and pillared hydrophobic surfaces, Faraday Discuss, 146 (2010) 185-193.

[94] P. Xiu, Z.X. Yang, B. Zhou, P. Das, H.P. Fang, R.H. Zhou, Urea-Induced Drying of Hydrophobic Nanotubes: Comparison of Different Urea Models, J Phys Chem B, 115 (2011) 2988-2994.

[95] B. Xiong, P. Zhao, K. Hu, L. Zhang, G. Cheng, Dissolution of cellulose in aqueous NaOH/urea solution: role of urea, Cellulose, in press. (2014) DOI: 10.1007/s10570-10014-10221-10577.

[96] M. Bergenstrahle-Wohlert, L.A. Berglund, J.W. Brady, P.T. Larsson, P.O. Westlund, J. Wohlert, Concentration enrichment of urea at cellulose surfaces: results from molecular dynamics simulations and NMR spectroscopy, Cellulose, 19 (2012) 1-12.

[97] A.J. Holding, M. Heikkilä, I. Kilpeläinen, A.W.T. King, Amphiphilic and Phase-Separable Ionic Liquids for Biomass Processing, ChemSusChem, 7 (2014) 1422-1434.

[98] C.-Z. Liu, F. Wang, A.R. Stiles, C. Guo, Ionic liquids for biofuel production: Opportunities and challenges, Applied Energy, 92 (2012) 406-414.

[99] B. Mostofian, J.C. Smith, X.L. Cheng, Simulation of a cellulose fiber in ionic liquid suggests a synergistic approach to dissolution, Cellulose, 21 (2014) 983-997.

[100] N. Isobe, S. Kimura, M. Wada, S. Kuga, Mechanism of cellulose gelation from aqueous alkali-urea solution, Carbohydrate Polymers, 89 (2012) 1298-1300.

[101] P.H. Hermans, Degree of Lateral Order in Various Rayons as Deduced from X-Ray Measurements, J Polym Sci, 4 (1949) 145-151.

[102] J. Hayashi, S. Masuda, S. Watanabe, Plane Lattice Structure in Amorphous Region of Cellulose Fibers, Nippon Kagaku Kaishi, (1974) 948-954.

[103] A. Ostlund, A. Idstrom, C. Olsson, P.T. Larsson, L. Nordstierna, Modification of crystallinity and pore size distribution in coagulated cellulose films, Cellulose, 20 (2013) 1657-1667.

[104] D.M. Rein, R. Khalfin, Y. Cohen, Cellulose as a novel amphiphilic coating for oil-in-water and water-in-oil dispersions, J Colloid Interf Sci, 386 (2012) 456-463.

[105] H. Nawaz, P.A.R. Pires, O.A. El Seoud, Kinetics and mechanism of imidazole-catalyzed acylation of cellulose in LiCl/N,N-dimethylacetamide, Carbohyd Polym, 92 (2013) 997-1005.

[106] L.K.J. Hauru, M. Hummel, A.W.T. King, I. Kilpelainen, H. Sixta, Role of Solvent Parameters in the Regeneration of Cellulose from Ionic Liquid Solutions, Biomacromolecules, 13 (2012) 2896-2905.

[107] R. Kargl, T. Mohan, M. Bracic, M. Kulterer, A. Doliska, K. Stana-Kleinschek, V. Ribitsch, Adsorption of Carboxymethyl Cellulose on Polymer Surfaces: Evidence of a Specific Interaction with Cellulose, Langmuir, 28 (2012) 11440-11447.

[108] J. Narewska, L. Lassila, P. Fardim, Preparation and characterization of new mouldable cellulose-AESO biocomposites, Cellulose, 21 (2014) 1769-1780.

[109] X. Hao, W. Shen, Z. Chen, J. Zhu, L. Feng, Z. Wu, P. Wang, X. Zeng, T. Wu, Self-assembled nanostructured cellulose prepared by a dissolution and regeneration process using phosphoric acid as a solvent, Carbohydrate Polymers, 123 (2015) 297-304.

[110] M. Ioelovich, Study of Cellulose Interaction with Concentrated Solutions of Sulfuric Acid, ISRN Chemical Engineering, 2012 (2012) 7.

[111] M. Martins, E. Teixeira, A. Corrêa, M. Ferreira, L.C. Mattoso, Extraction and characterization of cellulose whiskers from commercial cotton fibers, J Mater Sci, 46 (2011) 7858-7864.

[112] R. Carlton, Polarized Light Microscopy, in: Pharmaceutical Microscopy, Springer New York, 2011, pp. 7-64.

[113] J.R. Kuhn, Z. Wu, M. Poenie, Modulated polarization microscopy: a promising new approach to visualizing cytoskeletal dynamics in living cells, Biophysical Journal, 80 (2001) 972-985.

[114] R.J. Maude, W. Buapetch, K. Silamut, A Simplified, Low-Cost Method for Polarized Light Microscopy, The American Journal of Tropical Medicine and Hygiene, 81 (2009) 782-783.

[115] S. Sparenga, The Importance of Polarized Light Microscopy in the Analytical Setting, Microscopy and Microanalysis, 14 (2008) 1032-1033.

[116] R. Oldenbourg, Polarized Light Microscopy: Principles and Practice, Cold Spring Harbor Protocols, 2013 (2013) 1023-1036.

[117] Y. Lab, Basics of Polarizing Microscopy, in: Frontiers in Biophysical Imaging, University of California, Berkeley, 2012.

[118] R. Egerton, The Scanning Electron Microscope, in: Physical Principles of Electron Microscopy, Springer US, 2005, pp. 125-153.

[119] R. Egerton, An Introduction to Microscopy, in: Physical Principles of Electron Microscopy, Springer US, 2005, pp. 1-25.

[120] R.J. Beane, Using the Scanning Electron Microscope for Discovery Based Learning in Undergraduate Courses, Journal of Geoscience Education, 52 (2004) 250-253.

[121] R.E. Dinnebier, K. Friese, Modern XRD Methods in Mineralogy, in: P. Tropper (Ed.) Introduction to the Mineralogical Sciences, Eolss Publishers, Oxford, 2003.

[122] M. Birkholz, Principles of X-ray Diffraction, in: Thin Film Analysis by X-Ray Scattering, Wiley-VCH Verlag GmbH & Co. KGaA, 2006, pp. 1-40.

[123] L. Segal, J.J. Creely, A.E. Martin, C.M. Conrad, An Empirical Method for Estimating the Degree of Crystallinity of Native Cellulose Using the X-Ray Diffractometer, Textile Research Journal, 29 (1959) 786-794.

[124] R.T. O'Connor, Instrumental Analysis of Cotton Cellulose and Modified Cotton Cellulose, Marcel Dekker Incorporated, 1972.

[125] S.L. Upstone, Ultraviolet/Visible Light Absorption Spectrophotometry in Clinical Chemistry, in: Encyclopedia of Analytical Chemistry, John Wiley & Sons, Ltd, 2006.

[126] J.S.S.d. Melo, J. Pina, F.B. Dias, A.L. Maçanita, Experimental Techniques in Photochemistry (Characterisation of Singlet and Triplet Excited States), in: P. Douglas, H.D. Burrows, R. Evans (Eds.) Applied Photochemistry, Springer, London, 2013.

[127] B. Wardle, Principles and Applications of Photochemistry, John Wiley & Sons, Ltd., Manchester, 2009.

[128] J.W. Goodwin, R.W. Hughes, Chapter 1 Introduction, in: Rheology for Chemists: An Introduction (2), The Royal Society of Chemistry, 2008, pp. 1-13.

[129] A.L. Motyka, An Introduction to Rheology with an Emphasis on Application to Dispersions. , Journal of Chemical Education, 374-null (1996) 73 (74).

[130] K. Miyazaki, H.M. Wyss, D.A. Weitz, D.R. Reichman, Nonlinear viscoelasticity of metastable complex fluids, EPL (Europhysics Letters), 75 (2006) 915.

[131] H. Winter, M. Mours, Rheology of Polymers Near Liquid-Solid Transitions, in: Neutron Spin Echo Spectroscopy Viscoelasticity Rheology, Springer Berlin Heidelberg, 1997, pp. 165-234.

[132] B.H. Stuart, Introduction, in: Infrared Spectroscopy: Fundamentals and Applications, John Wiley & Sons, Ltd, 2005, pp. 1-13.

[133] T.N. Shaikh, S.A. Agrawal, Qualitative and Quantitative Characterization of Textile Material by Fourier Transform Infra-Red, International Journal of Innovative Research in Science, Engineering and Technology, 3 (2014) 8496-8502.

[134] B.H. Stuart, Experimental Methods, in: Infrared Spectroscopy: Fundamentals and Applications, John Wiley & Sons, Ltd, 2005, pp. 15-44.

[135] R.T. O'Connor, E.F. DuPré, D. Mitcham, Applications of Infrared Absorption Spectroscopy to Investigations of Cotton and Modified Cottons: Part I: Physical and Crystalline Modifications and Oxidation, Textile Research Journal, 28 (1958) 382-392.

[136] M.L. Nelson, R.T. O'Connor, Relation of certain infrared bands to cellulose crystallinity and crystal lattice type. Part II. A new infrared ratio for estimation of crystallinity in celluloses I and II, Journal of Applied Polymer Science, 8 (1964) 1325-1341.

[137] J. Široký, R. Blackburn, T. Bechtold, J. Taylor, P. White, Attenuated total reflectance Fourier-transform Infrared spectroscopy analysis of crystallinity changes in lyocell following continuous treatment with sodium hydroxide, Cellulose, 17 (2010) 103-115.

[138] M. Poletto, V. Pistor, R.M.C. Santana, A.J. Zattera, Materials produced from plant biomass: part II: evaluation of crystallinity and degradation kinetics of cellulose, Materials Research, 15 (2012) 421-427.

[139] F.G. Hurtubise, H. Krassig, Classification of Fine Structural Characteristics in Cellulose by Infared Spectroscopy. Use of Potassium Bromide Pellet Technique, Analytical Chemistry, 32 (1960) 177-181.

[140] H. Günther, Introduction, in: NMR Spectroscopy: Basic Principles, Concepts, and Applications in Chemistry, Wiley-VCH Verlag GmbH & Co. KGaA, 2013.

[141] C.S. Clendinen, B. Lee-McMullen, C.M. Williams, G.S. Stupp, K. Vandenborne, D.A. Hahn, G.A. Walter, A.S. Edison, 13C NMR Metabolomics: Applications at Natural Abundance, Analytical Chemistry, 86 (2014) 9242-9250.

[142] K. Kamide, K. Okajima, K. Kowsaka, T. Matsui, CP/MASS 13C NMR Spectra of Cellulose Solids: An Explanation by the Intramolecular Hydrogen Bond Concept, Polym J, 17 (1985) 701-706.

[143] A. Isogai, M. Usuda, T. Kato, T. Uryu, R.H. Atalla, Solid-state CP/MAS carbon-13 NMR study of cellulose polymorphs, Macromolecules, 22 (1989) 3168-3172.

[144] S. Gustavsson, L. Alves, B. Lindman, D. Topgaard, Polarization transfer solid-state NMR: a new method for studying cellulose dissolution, RSC Advances, 4 (2014) 31836-31839.

[145] W. Tscharnuter, Photon Correlation Spectroscopy in Particle Sizing, in: Encyclopedia of Analytical Chemistry, John Wiley & Sons, Ltd, 2006.

[146] B.J. Berne, R. Pecora, Dynamic Light Scattering: With Applications to Chemistry, Biology, and Physics, John Wiley & Sons, Inc., New York, 2000.

[147] R. Pecora, Dynamic Light Scattering Measurement of Nanometer Particles in Liquids, J Nanopart Res, 2 (2000) 123-131.

[148] I.O.f. Standardization, ISO 22412:2008 Particle size analysis -- Dynamic light scattering (DLS), in, 2008.

[149] L. Schulz, B. Seger, W. Burchard, Structures of cellulose in solution, Macromolecular Chemistry and Physics, 201 (2000) 2008-2022.

[150] K. Kamide, 2 - Characterization of Molecular Structure of Cellulose Derivatives, in: K. Kamide (Ed.) Cellulose and Cellulose Derivatives, Elsevier, Amsterdam, 2005, pp. 25-188.

[151] T. Heinze, A. Koschella, T. Liebert, V. Harabagiu, S. Coseri, Cellulose: Chemistry of Cellulose Derivatization, in: P. Navard (Ed.) The European Polysaccharide Network of Excellence (EPNOE), Springer Vienna, 2013, pp. 283-327.

[152] C.G. Lopez, S.E. Rogers, R.H. Colby, P. Graham, J.T. Cabral, Structure of sodium carboxymethyl cellulose aqueous solutions: A SANS and rheology study, Journal of Polymer Science Part B: Polymer Physics, 53 (2015) 492-501.

[153] L. Xiquan, Q. Tingzhu, Q. Shaoqui, Kinetics of the carboxymethylation of cellulose in the isopropyl alcohol system, Acta Polymerica, 41 (1990) 220-222.

[154] L. Alves, B. Medronho, F.E. Antunes, M.P. Fernández-García, J. Ventura, J.P. Araújo, A. Romano, B. Lindman, Unusual extraction and characterization of nanocrystalline cellulose from cellulose derivatives, Journal of Molecular Liquids.

[155] B.L. Peng, N. Dhar, H.L. Liu, K.C. Tam, Chemistry and applications of nanocrystalline cellulose and its derivatives: A nanotechnology perspective, The Canadian Journal of Chemical Engineering, 89 (2011) 1191-1206.

[156] J. Araki, S. Kuga, Effect of Trace Electrolyte on Liquid Crystal Type of Cellulose Microcrystals, Langmuir, 17 (2001) 4493-4496.

[157] V. Favier, H. Chanzy, J.Y. Cavaille, Polymer Nanocomposites Reinforced by Cellulose Whiskers, Macromolecules, 28 (1995) 6365-6367.

[158] M.A.S. Azizi Samir, F. Alloin, A. Dufresne, Review of Recent Research into Cellulosic Whiskers, Their Properties and Their Application in Nanocomposite Field, Biomacromolecules, 6 (2005) 612-626.

[159] M.S. Jahan, A. Saeed, Z. He, Y. Ni, Jute as raw material for the preparation of microcrystalline cellulose, Cellulose, 18 (2011) 451-459.

[160] F. Peng, J.-L. Ren, F. Xu, J. Bian, P. Peng, R.-C. Sun, Comparative Study of Hemicelluloses Obtained by Graded Ethanol Precipitation from Sugarcane Bagasse, Journal of Agricultural and Food Chemistry, 57 (2009) 6305-6317.

[161] R. Sun, X.F. Sun, G.Q. Liu, P. Fowler, J. Tomkinson, Structural and physicochemical characterization of hemicelluloses isolated by alkaline peroxide from barley straw, Polymer International, 51 (2002) 117-124.

[162] J.L. Ren, R.C. Sun, C.F. Liu, Z.Y. Chao, W. Luo, Two-step preparation and thermal characterization of cationic 2-hydroxypropyltrimethylammonium chloride hemicellulose polymers from sugarcane bagasse, Polymer Degradation and Stability, 91 (2006) 2579-2587.

[163] M. Kačuráková, A. Ebringerová, J. Hirsch, Z. Hromádková, Infrared study of arabinoxylans, Journal of the Science of Food and Agriculture, 66 (1994) 423-427.

[164] Z. Liu, Y. Ni, P. Fatehi, A. Saeed, Isolation and cationization of hemicelluloses from pre-hydrolysis liquor of kraft-based dissolving pulp production process, Biomass and Bioenergy, 35 (2011) 1789-1796.

[165] C.Y. Liang, Instrumental Analysis of Cotton Cellulose and Modified Cotton Cellulose, in: R.T. O'Connor (Ed.), Marcell Dekker Ink., New York, 1972, pp. 59.

[166] A. Isogai, R.H. Atalla, Dissolution of Cellulose in Aqueous NaOH Solutions, Cellulose, 5 (1998) 309-319.

[167] W. Wei, X. Wei, G. Gou, M. Jiang, X. Xu, Y. Wang, D. Hui, Z. Zhou, Improved dissolution of cellulose in quaternary ammonium hydroxide by adjusting temperature, RSC Advances, 5 (2015) 39080-39083.

[168] P. Langan, Y. Nishiyama, H. Chanzy, X-ray Structure of Mercerized Cellulose II at 1 Å Resolution, Biomacromolecules, 2 (2001) 410-416.

[169] C.J. Garvey, I.H. Parker, G.P. Simon, On the Interpretation of X-Ray Diffraction Powder Patterns in Terms of the Nanostructure of Cellulose I Fibres, Macromolecular Chemistry and Physics, 206 (2005) 1568-1575.

[170] N. Luo, Y. Lv, D. Wang, J. Zhang, J. Wu, J. He, J. Zhang, Direct visualization of solution morphology of cellulose in ionic liquids by conventional TEM at room temperature, Chemical Communications, 48 (2012) 6283-6285.

[171] M. Wada, Y. Nishiyama, G. Bellesia, T. Forsyth, S. Gnanakaran, P. Langan, Neutron crystallographic and molecular dynamics studies of the structure of ammonia-cellulose I: rearrangement of hydrogen bonding during the treatment of cellulose with ammonia, Cellulose, 18 (2011) 191-206.

[172] J. Keeler, Understanding NMR Spectroscopy, Wiley, 2005.

[173] M.J. Duer, Introduction to Solid-State NMR Spectroscopy, Blackwell Publishing Ltd, Oxford, 2004.

[174] K. Kamida, K. Okajima, T. Matsui, K. Kowsaka, Study on the Solubility of Cellulose in Aqueous Alkali Solution by Deuteration IR and 13C NMR, Polym J, 16 (1984) 857-866.

[175] J.C. Gast, R.H. Atalla, R.D. McKelvey, The 13c-n.m.r. spectra of the xylo- and cello-oligosaccharides, Carbohydrate Research, 84 (1980) 137-146.

[176] W.L. Earl, D.L. VanderHart, Observations by high-resolution carbon-13 nuclear magnetic resonance of cellulose I related to morphology and crystal structure, Macromolecules, 14 (1981) 570-574.

[177] A. Nowacka, P.C. Mohr, J. Norrman, R.W. Martin, D. Topgaard, Polarization Transfer Solid-State NMR for Studying Surfactant Phase Behavior, Langmuir, 26 (2010) 16848-16856.

[178] A. Nowacka, N.A. Bongartz, O.H.S. Ollila, T. Nylander, D. Topgaard, Signal intensities in 1H–13C CP and INEPT MAS NMR of liquid crystals, Journal of Magnetic Resonance, 230 (2013) 165-175.

[179] A. Nowacka, S. Douezan, L. Wadso, D. Topgaard, E. Sparr, Small polar molecules like glycerol and urea can preserve the fluidity of lipid bilayers under dry conditions, Soft Matter, 8 (2012) 1482-1491.

[180] E. Hellstrand, A. Nowacka, D. Topgaard, S. Linse, E. Sparr, Membrane Lipid Co-Aggregation with α-Synuclein Fibrils, PLoS ONE, 8 (2013) e77235.

[181] S. Björklund, T. Ruzgas, A. Nowacka, I. Dahi, D. Topgaard, E. Sparr, J. Engblom, Skin Membrane Electrical Impedance Properties under the Influence of a Varying Water Gradient, Biophysical Journal, 104 (2013) 2639-2650.

[182] J. Schaefer, E.O. Stejskal, R. Buchdahl, High-Resolution Carbon-13 Nuclear Magnetic Resonance Study of Some Solid, Glassy Polymers, Macromolecules, 8 (1975) 291-296.

[183] L. Alves, B. Medronho, F.E. Antunes, D. Topgaard, B. Lindman, The dissolution state of cellulose in aqueous based systems. 1. Alkaline solvents in: Manuscript in preparation, 2015.

[184] D.L. VanderHart, R.H. Atalla, Studies of microstructure in native celluloses using solid-state carbon-13 NMR, Macromolecules, 17 (1984) 1465-1472.

[185] H. Kono, T. Erata, M. Takai, Determination of the Through-Bond Carbon−Carbon and Carbon−Proton Connectivities of the Native Celluloses in the Solid State, Macromolecules, 36 (2003) 5131-5138.

[186] J. Kunze, H.-P. Fink, Structural Changes and Activation of Cellulose by Caustic Soda Solution with Urea, Macromolecular Symposia, 223 (2005) 175-188.

[187] M.E. Bos, Encyclopedia of Reagents for Organic Synthesis, Wiley, 2004.

[188] F. Porro, O. Bédué, H. Chanzy, L. Heux, Solid-State 13C NMR Study of Na−Cellulose Complexes, Biomacromolecules, 8 (2007) 2586-2593.

[189] B. Medronho, A. Romano, M. Miguel, L. Stigsson, B. Lindman, Rationalizing cellulose (in)solubility: reviewing basic physicochemical aspects and role of hydrophobic interactions, Cellulose, 19 (2012) 581-587.

[190] L. Alves, B.F. Medronho, F.E. Antunes, A. Romano, M.G. Miguel, B. Lindman, On the role of hydrophobic interactions in cellulose dissolution and regeneration: colloidal aggregates and molecular solutions, Colloids and Surfaces A: Physicochemical and Engineering Aspects.

[191] T. Röder, B. Morgenstern, The influence of activation on the solution state of cellulose dissolved in N-methylmorpholine-N-oxide-monohydrate, Polymer, 40 (1999) 4143-4147.

[192] K.-F. Arndt, B. Morgenstern, T. Röder, Scattering function of non-substituted cellulose dissolved in N-methylmorpholine-N-oxide-monohydrate, Macromolecular Symposia, 162 (2000) 109-120.

[193] U. Drechsler, S. Radosta, W. Vorwerg, Characterization of cellulose in solvent mixtures with N-methylmorpholine-N-oxide by static light scattering, Macromolecular Chemistry and Physics, 201 (2000) 2023-2030.

[194] G. Cheng, P. Varanasi, R. Arora, V. Stavila, B.A. Simmons, M.S. Kent, S. Singh, Impact of Ionic Liquid Pretreatment Conditions on Cellulose Crystalline Structure Using 1-Ethyl-3-methylimidazolium Acetate, The Journal of Physical Chemistry B, 116 (2012) 10049-10054.

[195] L. Kyllonen, A. Parviainen, S. Deb, M. Lawoko, M. Gorlov, I. Kilpelainen, A.W.T. King, On the solubility of wood in non-derivatising ionic liquids, Green Chemistry, 15 (2013) 2374-2378.

[196] R. Rinaldi, Instantaneous dissolution of cellulose in organic electrolyte solutions, Chemical Communications, 47 (2011) 511-513.

[197] M. Zavrel, D. Bross, M. Funke, J. Büchs, A.C. Spiess, High-throughput screening for ionic liquids dissolving (ligno-)cellulose, Bioresource Technology, 100 (2009) 2580-2587.

[198] O. Kuzmina, E. Sashina, D. Wawro, S.Troshenkowa, Dissolved State of Cellulose in Ionic Liquids - the Impact of Water, FIBRES & TEXTILES in Eastern Europe, 18 (2010) 32-37.

[199] X. Luo, L. Zhang, New solvents and functional materials prepared from cellulose solutions in alkali/urea aqueous system, Food Research International, 52 (2013) 387-400.

[200] S. Zhang, W.-C. Wang, F.-X. Li, J.-Y. Yu, Swelling and dissolution of cellulose in NaOH aqueous solvent systems, Cellulose chemistry and technology, 47 (2013) 671-679.

[201] M. Kihlman, B.F. Medronho, A.L. Romano, U. GermgÅrd, B. Lindman, Cellulose dissolution in an alkali based solvent: influence of additives and pretreatments, Journal of the Brazilian Chemical Society, 24 (2013) 295-303.

[202] B. Xiong, P. Zhao, K. Hu, L. Zhang, G. Cheng, Dissolution of cellulose in aqueous NaOH/urea solution: role of urea, Cellulose, 21 (2014) 1183-1192.

[203] M. Bergenståhle-Wohlert, L. Berglund, J. Brady, P.T. Larsson, P.-O. Westlund, J. Wohlert, Concentration enrichment of urea at cellulose surfaces: results from molecular dynamics simulations and NMR spectroscopy, Cellulose, 19 (2012) 1-12.

[204] A. Pinkert, K.N. Marsh, S. Pang, Reflections on the Solubility of Cellulose, Industrial & Engineering Chemistry Research, 49 (2010) 11121-11130.

[205] J. Cai, L. Zhang, S.L. Liu, Y.T. Liu, X.J. Xu, X.M. Chen, B. Chu, X.L. Guo, J. Xu, H. Cheng, C.C. Han, S. Kuga, Dynamic Self-Assembly Induced Rapid Dissolution of Cellulose at Low Temperatures, Macromolecules, 41 (2008) 9345-9351.

[206] B. Medronho, H. Duarte, L. Alves, F. Antunes, A. Romano, B. Lindman, Probing cellulose amphiphilicity, Nordic Pulp and Paper Research Journal, 30 (2015) 058-066.

[207] T. Ema, T. Komiyama, S. Sunami, T. Sakai, Synergistic effect of quaternary ammonium hydroxide and crown ether on the rapid and clear dissolution of cellulose at room temperature, RSC Advances, 4 (2014) 2523-2525.

[208] R. Zangi, R.H. Zhou, B.J. Berne, Urea's Action on Hydrophobic Interactions, J Am Chem Soc, 131 (2009) 1535-1541.

[209] Y.H.P. Zhang, J. Cui, L.R. Lynd, L.R. Kuang, A Transition from Cellulose Swelling to Cellulose Dissolution by o-Phosphoric Acid: Evidence from Enzymatic Hydrolysis and Supramolecular Structure, Biomacromolecules, 7 (2006) 644-648.

[210] T.F. Libert, T. Heinze, K. Edgar, Cellulose Solvents: For Analysis, Shaping and Chemical Modification, 1st edition ed., American Chemical Society, 2010.

[211] A. Sannino, C. Demitri, M. Madaghiele, Biodegradable Cellulose-based Hydrogels: Design and Applications, Materials, 2 (2009) 353-373.

[212] R. Xiong, F. Li, J. Yu, P. Hu, Z. Liu, Y.-L. Hsieh, Investigations on solution of cellulose in complex phosphoric acid solvent and its stability, Cellulose Chemistry and Technology, 47 (2013) 153-163.

[213] H. Boerstoel, H. Maatman, J.B. Westerink, B.M. Koenders, Liquid crystalline solutions of cellulose in phosphoric acid, Polymer, 42 (2001) 7371-7379.

[214] L. Alves, B. Medronho, F.E. Antunes, D. Topgaard, B. Lindman, The dissolution state of cellulose in aqueous based systems. 2. Acidic solvents   in: Manuscript in preparation, 2015.

[215] J.S. Moulthrop, R.P. Swatloski, G. Moyna, R.D. Rogers, High-resolution 13C NMR studies of cellulose and cellulose oligomers in ionic liquid solutions, Chemical Communications, (2005) 1557-1559.

[216] N.J. Cao, Q. Xu, L.F. Chen, Acid hydrolysis of cellulose in zinc chloride solution, Appl Biochem Biotechnol, 51-52 (1995) 21-28.

[217] L. Tim, Cellulose Solvents - Remarkable History, Bright Future, in: Cellulose Solvents: For Analysis, Shaping and Chemical Modification, American Chemical Society, 2010, pp. 3-54.

[218] M.L. Ramos, M.M. Caldeira, V.M.S. Gil, NMR spectroscopy study of the complexation of d-gluconic acid with tungsten(VI) and molybdenum(VI), Carbohydrate Research, 304 (1997) 97-109.

[219] J. Song, H. Fan, J. Ma, B. Han, Conversion of glucose and cellulose into value-added products in water and ionic liquids, Green Chemistry, 15 (2013) 2619-2635.

[220] Å. Östlund, D. Lundberg, L. Nordstierna, K. Holmberg, M. Nydén, Dissolution and Gelation of Cellulose in TBAF/DMSO Solutions: The Roles of Fluoride Ions and Water, Biomacromolecules, 10 (2009) 2401-2407.

[221] H. Liu, K.L. Sale, B.A. Simmons, S. Singh, Molecular Dynamics Study of Polysaccharides in Binary Solvent Mixtures of an Ionic Liquid and Water, The Journal of Physical Chemistry B, 115 (2011) 10251-10258.

[222] R. Li, L. Zhang, M. Xu, Novel regenerated cellulose films prepared by coagulating with water: Structure and properties, Carbohydrate Polymers, 87 (2012) 95-100.

[223] S. Zhang, F.-X. Li, J.-Y. Yu, Kinetics of cellulose regeneration from cellulose-NaOH-NaOH/Thiourea/Urea/H_2O System, Cellulose Chem. Technol., 45 (2011) 593-604.

[224] H.J. Schneider, F. Hacket, V. Rudiger, H. Ikeda, NMR studies of cyclodextrins and cyclodextrin complexes, Chem Rev, 98 (1998) 1755-1785.

[225] R.A. Carvalho, H.A. Correia, A.J.M. Valente, O. Soderman, M. Nilsson, The effect of the head-group spacer length of 12-s-12 gemini surfactants in the host-guest association with beta-cyclodextrin, J Colloid Interf Sci, 354 (2011) 725-732.

[226] X.J. Wang, J. Messman, J.W. Mays, D. Baskaran, Polypeptide Grafted Hyaluronan: Synthesis and Characterization, Biomacromolecules, 11 (2010) 2313-2320.

[227] B. Medronho, A.J.M. Valente, P. Costa, A. Romano, Inclusion complexes of rosmarinic acid and cyclodextrins: stoichiometry, association constants, and antioxidant potential, Colloid Polym Sci, 292 (2014) 885-894.

[228] B. Medronho, H. Duarte, L. Alves, F.E. Antunes, A. Romano, A.J. Valente, Inclusion Complexes of Cyclodextrins and the Tetrabutylammnonium Cation:

Stoichiometry, Association Constants and Effect on Cellulose Dissolution, in: Manuscript in preparation, 2015.

[229] A.J.M. Valente, O. Soderman, The formation of host-guest complexes between surfactants and cyclodextrins, Adv Colloid Interfac, 205 (2014) 156-176.

[230] A. Al-Soufi, P.R. Cabrer, A. Jover, R.M. Budal, J.V. Tato, Determination of second-order association constants by global analysis of H-1 and C-13 NMR chemical shifts. Application to the complexation of sodium fusidate and potassium helvolate by beta- and gamma-cyclodextrin, Steroids, 68 (2003) 43-53.

[231] A. Buvari, L. Barcza, Complex-Formation of Inorganic Salts with Beta-Cyclodextrin, J Inclusion Phenom, 7 (1989) 379-389.

[232] A.C.F. Ribeiro, V.M.M. Lobo, A.J.M. Valente, S.M.N. Simoes, A.J.F.N. Sobral, M.L. Ramos, H.D. Burrows, Association between ammonium monovanadate and beta-cyclodextrin as seen by NMR and transport techniques, Polyhedron, 25 (2006) 3581-3587.

[233] K.A. Connors, D.D. Pendergast, Microscopic Binding Constants in Cyclodextrin Systems - Complexation of Alpha-Cyclodextrin with Sym-1,4-Disubstituted Benzenes, J Am Chem Soc, 106 (1984) 7607-7614.

[234] T. Röder, B. Morgenstern, N. Schelosky, O. Glatter, Solutions of cellulose in N,N-dimethylacetamide/lithium chloride studied by light scattering methods, Polymer, 42 (2001) 6765-6773.

[235] S. Zhang, C.-F. Fu, F. Li, J. Yu, L. Gu, Direct Preparation of a Novel Membrane from Unsubstituted Cellulose in NaOH Complex Solution, Iranian Polymer Journal, 18 (2009) 767-776.

[236] M. Adsul, S.K. Soni, S.K. Bhargava, V. Bansal, Facile Approach for the Dispersion of Regenerated Cellulose in Aqueous System in the Form of Nanoparticles, Biomacromolecules, 13 (2012) 2890-2895.